2016•2017
FACULTEIT INDUSTRIËLE INGENIEURSWETENSCHAPPEN
master in de industriële wetenschappen: bouwkunde

Masterproef
Research into the fire stability RF60 (according to Eurocode 3) of modular units

Promotor :
Prof. dr. Jose GOUVEIA HENRIQUES

Promotor :
ing. MARK BROUWERS

Gezamenlijke opleiding Universiteit Hasselt en KU Leuven

Simon De Bruycker , Ruben Vaes
Scriptie ingediend tot het behalen van de graad van master in de industriële wetenschappen: bouwkunde

2016•2017
Faculteit Industriële ingenieurswetenschappen
master in de industriële wetenschappen: bouwkunde

Masterproef
Research into the fire stability RF60 (according to Eurocode 3) of modular units

Promotor :
Prof. dr. Jose GOUVEIA HENRIQUES

Promotor :
ing. MARK BROUWERS

Simon De Bruycker , Ruben Vaes
Scriptie ingediend tot het behalen van de graad van master in de industriële wetenschappen: bouwkunde

universiteit
►►hasselt

KU LEUVEN

Preface

Before you lies the dissertation "Research to fire stability RF60 (according to Eurocode 3) of modular buildings", which is a master's thesis conducted by two civil engineering students. It has been written to fulfill the graduation requirements of the Engineering study at the University of Hasselt in Diepenbeek, Belgium.

First, we would like to thank all the people who helped us in order to create this master's thesis. We would especially like to thank our two promoters: José Gouveia Henriques and Mark Brouwers. They provided us with the necessary information and feedback. They helped us when problems occurred and grant us with a critical and objective opinion on our progress and results. Thank you for that.

During the research we have encountered some setbacks and problems, even in the final stages of the research, causing us to do a lot of work in a very short time. But in the end we have succeeded in finalising a master's thesis on which we are proud.

The entire writing process gave an interesting view on structural fire design, something the education does not provide a lot of information about. Therefore it was challenging, but also very interesting to learn about this subject.

Finally, we hope that this research will be helpful and that you will enjoy your reading.

Simon De Bruycker, Ruben Vaes

Hasselt, June 6, 2017

Table of Contents

Symbols

Latin Upper Case Letters

A — Steel cross-section area

A_d — Design value of indirect actions from fire

A_p — Appropriate area of fire protection material per unit length of member

A_{vz} — Steel area for design of shear resistance

C_i — Protection coefficient of member face i

E — Young's modulus

E_d — Design value of the relevant effects of actions

E_{dA} — Design value of the relevant effects of Actions at ambient temperature when fire protection is added

$E_{fi,d}$ — Design value of the relevant effects of actions in fire conditions

$E_{fi,d,t}$ — Design effect of actions for fire situation

G — Shear modulus

$G_{k,j}$ — Characteristic values of permanent actions j

I_t — Torsional moment of inertia

I_w — Vaulting constant

$I_{y,z}$ — Moment of inertia

L — Beam span

L_{cr} — Critical beam span

M_{cr} — Critical bending moment

M_{Ed} — Design bending moment for normal temperature design

$M_{fi,Ed}$ — Design bending moment for fire temperature design

$M_{pl,Rd}$ — Plastic resistance to bending moment for normal temperature design

N_{Ed} — Design axial load for normal temperature design

$N_{fi,Ed}$ — Design axial load in fire situation

P — Design value of a prestressing load

$Q_{k,j}$ — Characteristic values of variable actions j

V — Volume of the steel member per unit length

V_{Ed} — Design shear load

$V_{pl,Rd}$ — Shear resistance for normal temperature design

W_{el} — Bending elastic modulus

W_{pl} — Bending plastic modulus

Latin Lower Case Letters

d_p — Thickness of the fire protection material

f_y — Steel yield strength

$g_{k,j}$ — Characteristic value of permanent action j

k — Reduction factor for a strength or deformation property

$k_{E,\theta}$ — Reduction factor (relative to E_a) for the slope of the linear elastic range at the steel temperature θ_a reached at time t

k_{LT} — The interaction factor

k_w — The strength reduction factor for welds

$k_{y,\theta}$ — The reduction factor for the yield strength of steel at the steel temperature θ_a reached at time t

k_θ — Reduction factor for a strength or deformation property, dependent on the steel temperature

l — Beam span

$q_{k,j}$ — Characteristic values of variable

	actions j
t	Time
v_d	Design value of the load
v_k	Characteristic value of the load
z_g	Distance from the plastic neutral axis to the centroid of the elemental area A_g

Greek letters

α	The convective heat transfer coefficient
β_M	Equivalent uniform moment factors
γ_G	Partial safety factor for the permanent action
γ_{GA}	Partial safety factor for the permanent Action at ambient temperature for design with additional fire protection
γ_{M0}	Partial factor for resistance of cross section at normal temperature
$\gamma_{M,fi}$	Partial factor for the relevant material property, for the fire situation
γ_Q	Partial safety factor for leading variable action
δ	Deflection of the steel beam
ξ	Reduction factor for permanent unfavourable loads
η_{fi}	Reduction factor for the design load level for the fire situation
θ_a	Temperature of the steel beam reached at time t
$\theta_{a,cr}$	Critical temperature
κ_1	An adaptation factor for non-uniform temperature across the cross-section
κ_2	An adaptation factor for non-uniform temperature across the beam

$\bar{\lambda}$	Non-dimensional slenderness for normal temperature design
λ_a	The relative slenderness at ambient temperature
$\overline{\lambda_{LT}}$	Non-dimensional slenderness for lateral torsional buckling
$\overline{\lambda_{LT,\theta}}$	Non-dimensional slenderness for lateral-torsional buckling in fire situation
$\overline{\lambda_\theta}$	Non-dimensional slenderness for the temperature q
λ_p	Thermal conductivity of the fire protection material
μ_0	Degree of utilization
μ_{LT}	Degree of utilization
μ_y	Degree of utilization
χ_{fi}	The reduction factor for flexural buckling in the fire design situation
$\chi_{LT,fi}$	The reduction factor for lateral-torsional buckling in the fire design situation
$\chi_{min,fi}$	The minimum value of $\chi_{y,fi}$ and $\chi_{z,fi}$
$\chi_{y,fi}$	The reduction factor for flexural buckling about the y-axis in the fire design situation
$\chi_{z,fi}$	The reduction factor for flexural buckling about the z-axis in the fire design situation
ψ	The combination factor for frequent values, given either by $\psi_{1,1}$ or $\psi_{2,1}$

List of figures

List of tables

Abstract

In this research an analysis of the fire stability R60 of modular buildings was performed. The objective is the study of the structural stability of modular construction, using the CBZ modular units, in fire situation. The parameters influencing the strength of the structures in a fire situation are investigated in order to provide a safe solution. The analysis of the fire stability was done using the 3D finite element analysis software RFEM. Different arrangements of units where tested to simulate the different modular building configurations. Hence, different structural configurations and loadings of the modular units were considered. Based on the results of the numerical solutions, the fire stability is analysed. Possible solutions are proposed for the identified problems. In addition this thesis provides guidance for the fire design of steel structures using the software RFEM.

1   Introduction

The popularity of steel as a material, used in the construction of large buildings, is rising due to its high strength and ductility. Therefore the need to improve the safety in steel constructions has increased significantly. Many engineers have made extensive progress over several decades considering this increase in safety. In addition, research for fire safety has had one of the most significant improvements due to major structural failures resulting from fire accidents, thus giving new insight on the behaviour of steel structures under fire conditions. This allowed steel beams to be designed according to accidental fire conditions in such a way that major structural failures do not occur during a certain period of time, which significantly reduces the risk of injury to people.

The main objective of this document is to provide the reader with a better understanding of the current methods used in fire design, for steel modular units according, to the European Standard Eurocode. Furthermore, this information is used to gain more insight in the proper use of the software RFEM for the fire stability calculations. This objective is realised by carefully analysing the background of a fire situation and its conditions. On top of that, a parametric study is done to elaborately explain all influencing factors for the fire resistance of steel members. This leads to an opportunity to validate the accuracy of the current methods of fire design used by the software RFEM, which is used by many engineers. Once the software is validated, various models can be designed in fire situation R60, giving the company CBZ in Zutendaal-Belgium the option to do so for all modular units they construct. One of these basic modular units used by CBZ can finally be analysed in this document in order to provide CBZ with the calculation methods and results. By doing so, this document serves as a guide for engineers that use RFEM.

In chapter one of this document, the background of a fire situation is examined and the parametric study is covered, leading to a better understanding of fire design in general. In chapter two this information is then used to validate the software RFEM in multiple validation examples. Finally, chapter three covers the evaluation of basic modular units in fire design for R60 and presents the results that were achieved.

2 Fire design of steel structures

2.1 Development of a fire

In order to design a model for a fire situation, a better understanding of the development of the fire itself and the thermal loads is required. Therefore, this chapter covers the requirements for the development of a fire and the most recent models used in fire design.

There are three ingredients needed to create a fire: fuel, oxygen and heat. When one of these ingredients is not present, no fire can develop. The fire reaction is maintained by a plentiful supply of oxygen. Secondly, there has to be a sufficient amount of heat or energy to increase the temperature of the materials to their ignition temperature. Lastly, there is need for a kind of fuel or a combustible material. A fire develops over three stages, as shown in Figure 1. During the first stage the temperature increases and the materials start to melt. When more fuel becomes available, in the form of heated gasses released by the materials, the materials start to ignite and this causes the fire to consume more and more energy. Only when all the fuel is burning, the second stage of the fire is reached. At this stage the fire is called a "fully developed fire". The stage is signalled by the phenomenon called "flashover". The fire keeps consuming fuel and materials and slowly starts to decay in the last stage. the fire ceases to exist, when no more fuel, material or oxygen is available.
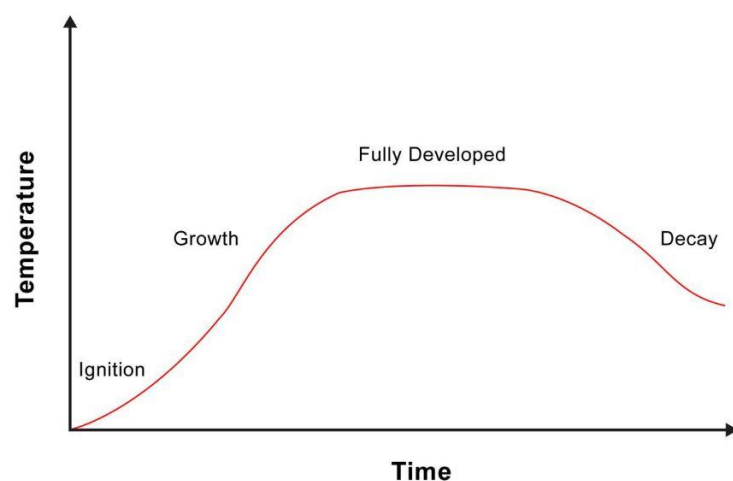
Figure 1: Fire development curve.[1]

15

2.2 Fire models

The development of a fire can be analysed using different models:

- – parametric models
- – zone models
- – field models

Parametric models are used to describe the fire development with a reduced amount of parameters. These models are not used to do specific calculations, but they are used to give a first insight in the situation. This is be done by using parametric fire models instead of nominal fire models. Only the most important parameters are taken into account to assess the situation, which are:

- - The geometry of the structure
- - The fire load
- - Windows and doors which create openings in the structure
- - The properties of the members which form the boundary of the structure.

Furthermore, an assumption is made in the parametric model that the temperature is uniform throughout the structure. Using this data, a more realistic nature of the fire is obtained in comparison to the usage of nominal fire models.

For the use of zone models, the room in which the fire is burning gets divided into a small number of zones. For each zone a uniform temperature distribution is assumed. The heat balance and energy balance are composed per sector, allowing a calculation of the effects of a developing fire.

Field models are similar to zone models. The space, which is influenced by the fire, are divided into an extensive amount of zones. Therefore, these models are interesting to calculate specific models, when the calculations with the basic methods are not encouraged. This can be the case when there is a high risk of damage or when the room has a complex geometrical shape.

Most of the time, the fire development is analysed using zone models. These models can be subdivided into one- and two-zone models, which are illustrated in Figure 2 and Figure 3. One-zone models assume a uniform temperature distribution over the entire zone. This type of model is used for the determination of the thermal load after the flashover; this means it is used to determine the thermal load for fully developed fires.
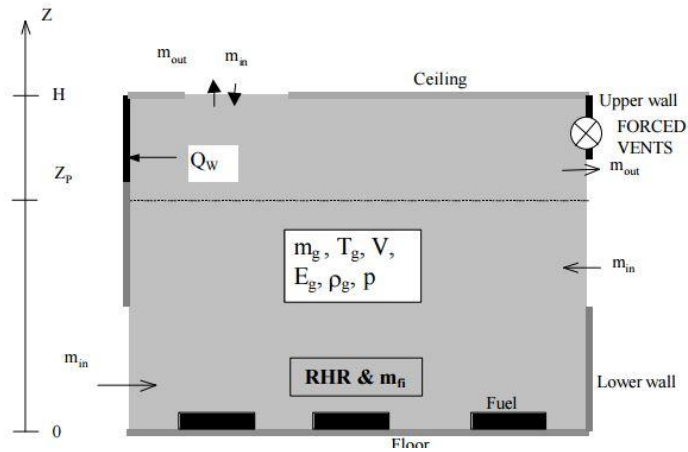
Figure 2: One-zone model.[2]

Two-zone models are used to observe the thermal load of a fire preceding the flashover. In this situation two zones are formed: a cold layer at the level of the floor and a warm layer appearing at the ceiling of the analysed space. This is the case before the fire is fully developed. For each zone, the mass and energy equilibriums can be calculated. The mass equilibrium takes into account that the total mass of gasses created by the fire, entered in the room and evacuated out of the room remains constant over time. The ability for gasses to enter or exit the room is established by the ventilation openings. The energy equilibrium states that there is a balance between the energy used by the combustion and the energy produced by the fire. The loss of energy can be explained by the need for energy to heat the gasses, the loss of heated gasses throughout the ventilation openings, the loss of heat by radiation and the heating of the building materials in the ceiling, the walls and the floor. The combustion reaction itself produces energy in the form of heat.
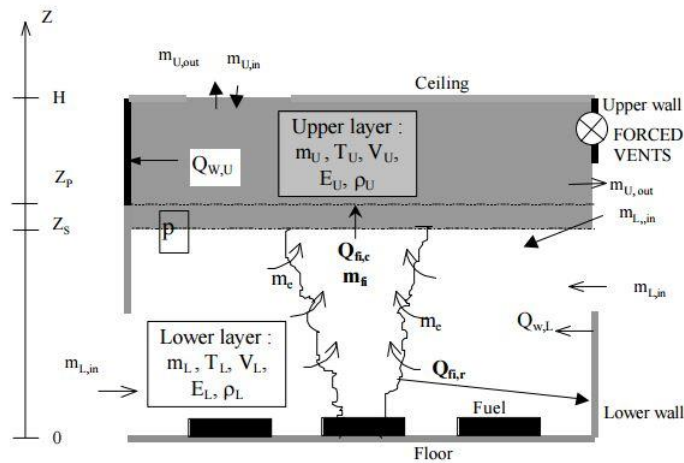
Figure 3: Two-zone model.[2]

2.3 The Design Fire

When the determination of the fire load is completed, the amount of available energy is known. However, this available energy does not lead to an estimation of the gas temperature in the compartment. Because a fire load can burn at a fast pace in one situation, while it can smoulder in another. This leads to very differing gas temperatures within the compartment. Another parameter thus needs to be considered in the design of a fire. This is done by calculating the "Rate of Heat Release" (RHR). As shown in Figure 4, a higher RHR leads to a smaller period of time in which the fire burns. However, the gas temperatures are significantly higher.
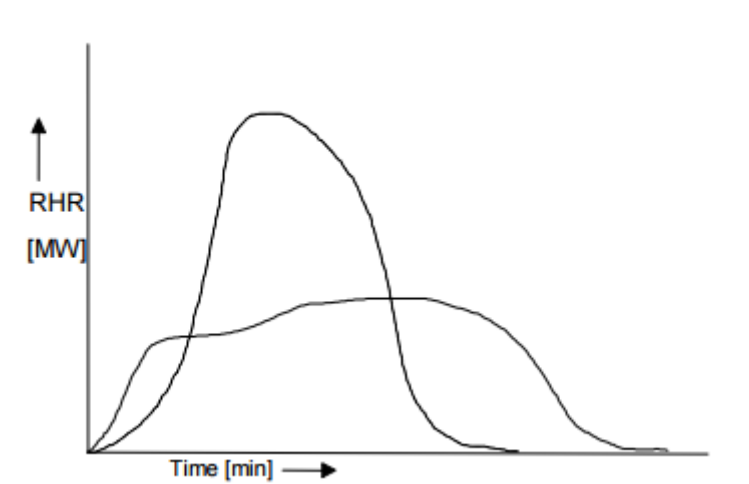
Figure 4: Influence of the RHR on the fire load. [3]

Depending on the amount of oxygen available in the room, fires can be divided into two categories:

- Fuel-controlled fire: In this case, the amount of oxygen is limitless. The limiting factor of the fire is the amount of flammable material present in the area, which serves as fuel, hence the name.
- Ventilation controlled fire: There is a limited amount of oxygen entering the area, causing oxygen to be the limiting factor. This is often the case for structures with little or no windows.

The RHR depends on the type of fire and the time within which the fire load burns and is therefore dependent on this fire classification. This is shown in Figure 5.

$$RHR = A_{fi} \cdot RHR_f \begin{cases} \text{For stacked wood pallets of height 0.5 m} & RHR_f = 1250 \text{ kW}/m^2 \\ \text{For stacked wood pallets of height 3.0 m} & RHR_f = 6000 \text{ kW}/m^2 \\ \text{For plastic bottles in cartons, stacked of 4.6 m} & RHR_f = 4320 \text{ kW}/m^2 \\ \text{For PS insulation board, rigid foam, stacked of 4.3 m} & RHR_f = 2900 \text{ kW}/m^2 \\ \text{Building use is theatres, cinemas, and libraries} & RHR_f = 500 \text{ kW}/m^2 \\ \text{Building use is offices, dwellings, shopping centres, transport public spaces} & RHR_f = 250 \text{ kW}/m^2 \\ \text{, hospital-, hotel- and school class-rooms} \end{cases}$$

RHR [W]

Fuel bed controlled

70% of the fire load has already burnt

$$RHR \div A_w \cdot \sqrt{h_a} \quad \text{(EN 1991-1-2)}$$

Ventilation controlled

Decrease phase

Flashover

$\theta_g \geq 500°C$

Rising phase

$t_{fi,end}$

Time

$$RHR = \left(\frac{t}{t_\alpha}\right)^2 [MW]$$

$$\int_0^{t_\alpha} RHR \, dt = A_{fi} \, q_f$$

Fire growth rate	Typical equivalent materials	t_α: Time [s] for RHR = 1 MW	Occupancy
Slow	no uniform fire load	600	Transport (Public Space)
Medium	Cotton/polyester sprung mattress	300	Dwelling, Hotel- & Hospital-room, Office, Classroom of a school
Fast	Full mail bags, plastic foam, stacked timber pallets	150	Shopping centre, Theatre, Cinema
Ultra-fast	Methyl alcohol pool fire, faster burning upholstered furniture	75	

OCCUPANCY / ACTIVITY	Fire load (80% fractile) q_α [MJ/m²]
Dwelling	948
Hospital (room)	280
Hotel (room)	377
Library	1824
Office	511
Classroom of a school	347
Shopping centre	730
Theatre (cinema)	365
Transport (public space)	122

Figure 5: Calculation of the RHR based on the type of fire. [3]

2.4   Basis of the calculations

The calculations used for this research are based on the Eurocodes. The Eurocodes are a collection of ten European normative documents and they are used to design and calculate buildings, structures and their foundations.

For this research Eurocodes 0 to 3 were used. Eurocodes 0 and 1 treat the basics of construction design. The information found in Eurocode EN 1993-1-2[4] is used for fire design of steel structures. The calculations used in this research can be found in these chapters of the Eurocodes and they are specified on a national level in the National Annex. The fire safety of constructions is established by law, based on the principles described in these documents.

When a construction is exposed to a fire situation, the calculations need to be executed based on the method of the limit states. There are two types of limit states:

- Ultimate limit state (ULS): In this state the maximum loading capacity is reached. When the ultimate limit state of a construction is exceeded, the construction fails because the static balance is lost. This causes instability, failures, buckling or cracks. When such instabilities occur in the building, occupants can be in danger.[5]

- Serviceability limit state (SLS): This can limit the use of a construction in three ways. Firstly, the deformation and bending of a structure can cause the external structure to disfigure or it can damage non-structural elements. Secondly the vibrations, caused by the loads in the serviceability limit state, can create discomfort to users, damage constructive elements or make equipment limp. Lastly, the serviceability limit state can result in undesirable cracks.[5]

The calculations for the fire resistance of constructions are made in ultimate limit state (ULS) since structural failure complements the highest risk for people occupying the construction. However, since fire situation taken into account and thus accidental actions are applied, different partial safety factors are used.

On top of this, all calculations are based on the standard ISO834 fire curve found in Eurocode 3. This standard fire curve can be seen in Figure 6. As explained earlier, real fire situations never follow this curve as realistic fires have a cooling phase (Figure 7). However, for the theoretical calculations, this assumption can be made.
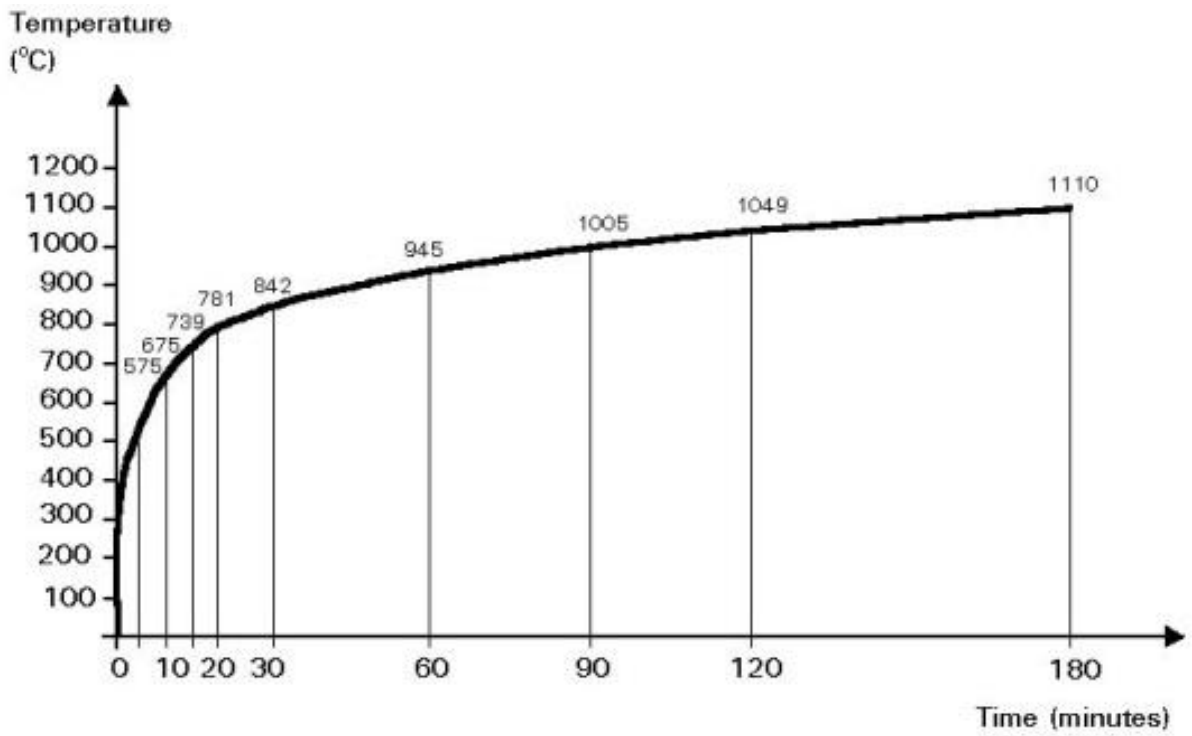
Figure 6: Standard ISO834 fire curve.[4]
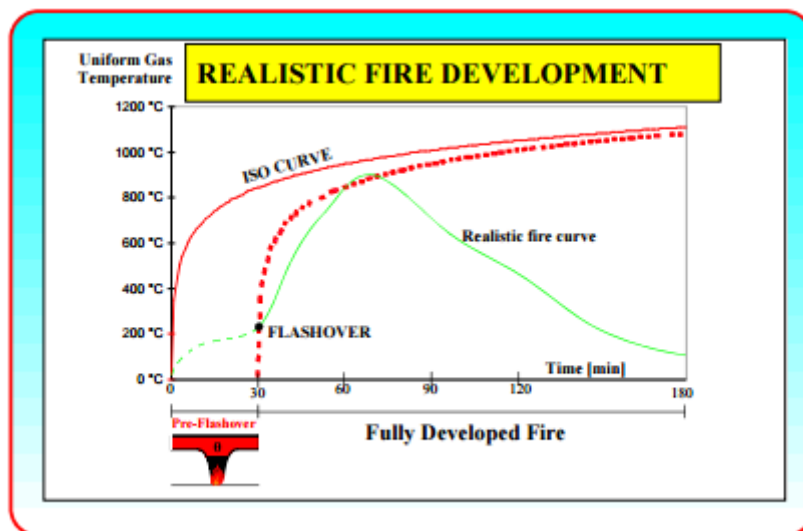
Figure 7: Comparison of the standard ISO 834 fire curve with a realistic fire curve. [3]

21

2.5 Definition of fire resistance

Fire resistance gives an indication of the capability of a construction to maintain its structural strength in a fire situation for a specific amount of time. The aspect "time" is very important since no structure is eternally resistant to fire. The indication of the fire resistance is done with three classifications which are defined as follows:

- R: "With this classification, the element will maintain its stability during the indicated time. This means that during the specified time, its load-bearing and self-load bearing capacity will be sufficient according to the Eurocode."[4]
- RE: "An element with this classification must be resistant to flames and inflammable gases, on top of conserving its stability properties mentioned in the R classification. The element must also be designed to prevent the spread of combustion gases and smoke on the side of the element that is not exposed to fire." [4]
- REI: "This is the strictest classification. The element must limit the temperature of the non-affected surface to 140°C (on average) and 180°C (maximum). The element must also prevent heat from spreading from the side that is not exposed to fire." [4]

These classifications are graphically presented in Figure 8.
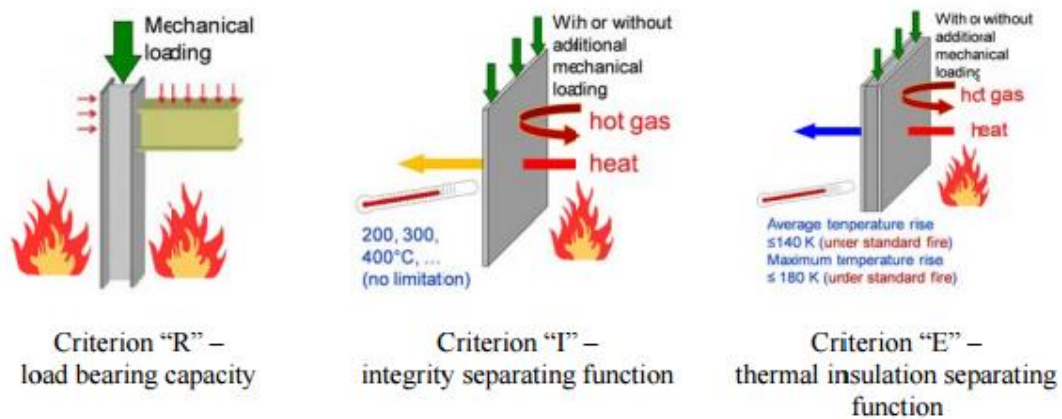
Figure 8: Fire resistance classifications of construction elements. [3]

For this research the focus lies on the R-classification. This fire resistance is defined by 3 "domains" as shown in Figure 9.

Eurocodes allow fire resistance to be established in any of 3 "domains":

Time: $t_{fi.d} \geq t_{fi.requ}$

Load resistance: $R_{fi.d.t} \geq E_{fi.d.t}$

Temperature: $\theta_{cr.d} \geq \theta_d$

$t_{fi.d}$: design fire resistance time
$t_{fi.requ}$: required fire resistance time

• Usually only directly feasible using advanced calculaton models.

• Feasible by hand calculation. Find reduced resistance at required resistance time.

• Most usual simple EC3 method. Find critical temperature for loading, compare with design temperature.

Figure 9: Domains used to define fire resistance. [3]

The determination of the fire resistance of structures can be done by following the step-by-step approach that is explained in the next chapter.

2.6   Step-by-step calculation of the fire resistance

2.6.1 Overview

1) Determination of the characteristic loads.
2) Transformation of the characteristic loads to design loads.
3) Classification of the examined elements as class 1, 2, 3 or 4 cross-section elements.
4) Calculation of the design resistance of the steel members.
5) Verification of the stability of the structure using the degree of utilization.
6) Extraction of the critical temperature of the steel members.
7) Evaluation of the temperature along the surface of the steel elements.
8) Comparison between the critical temperature and the thermal evaluation for both steel members without fire protection and steel members with fire protection.

During the determination of these responses, all influencing factors are elaborately explained to achieve a better understanding of the concept of fire resistance. Additionally, knowledge on these factors is essential to comprehend the guided calculations and results obtained later in the thesis.

2.6.2 Determination of the characteristic loads

For most cases the fire load is found in the tables from the Eurocode, where statistical averages of the fire load can be found depending on the occupancy. Table 1 represents the thermal loads on compartments based on the occupation.

Table 1: Average fire loads depending on the occupancy.[6]

Occupancy	Average	80% Fractile
Dwelling	780	948
Hospital (room)	230	280
Hotel (room)	310	377
Library	1 500	1 824
Office	420	511
Classroom of a school	285	347
Shopping centre	600	730
Theatre (cinema)	300	365
Transport (public space)	100	122
NOTE Gumbel distribution is assumed for the 80 % fractile.		

When the activity for the room is not described in the table, a detailed calculation can be done to determine the thermal loads. The characteristic thermal load is calculated while the amount of flammable material in the area is considered.

$$q_{fi,k} = \frac{\sum_i M_i H_{ui} \Psi_i}{A} \qquad (2.6.1)$$

With:

- M_i : the amount of flammable materials (kg) , further divided into two subdivisions

    A. Materials which are permanently present. These materials will stay in the space throughout the designed lifetime of the structure. To take these materials in to account an average value has to be *taken*.
    B. The non-permanent materials, those that can change over a course of time, are counted for 80% fractile.
- H_{ui}: the heat produced by the burning materials (MJ/kg)(values shown in Table 2), calculated by :

$$H_{ui} = H_{u,0}(1 - 0.01u) - 0.025u \qquad (2.6.2)$$

With:

         u : The amount of moisture in the materials (%)
         $H_{u,0}$: The combustion heat of the dry materials
- Ψ_i: The factor considering the protection against fire, the value can be found in Table 3. Note that $\Psi_i = 0$ for materials used to prevent and protect from fire.

Table 2: Values of H_{ui} derived from the Eurocode.[6]

Other products	
ABS (plastic)	35
Polyester (plastic)	30
Polyisocyanerat and polyurethane (plastics)	25
Polyvinylchloride, PVC (plastic)	20
Bitumen, asphalt	40
Leather	20
Linoleum	20
Rubber tyre	30
NOTE The values given in this table are not applicable for calculating energy content of fuels.	
Solids	
Wood	17,5
Other cellulosic materials • Clothes • Cork • Cotton • Paper, cardboard • Silk • Straw • Wool	20
Carbon • Anthracit • Charcoal • Coal	30
Chemicals	
Paraffin series • Methane • Ethane • Propane • Butane	50
Olefin series • Ethylene • Propylen • Butene	45
Aromatic series • Benzene • Toluene	40
Alcohols • Methanol • Ethanol • Ethyl alcohol	30
Fuels • Gasoline, petroleum • Diesel	45
Pure hydrocarbons plastics • Polyethylene • Polystyrene • Polypropylene	40

Table 3: Fire protection factors.[6]

Type of Protection	Ψ_i
Fireproof closet or rooms	0
Combustible packaging	1.0
Metal barrels (<450l) at atmospheric pressure	1.0
Liquids with flashpoint > 100°C , single reservoir	0.70
Liquid with flashpoint > 100°C, multiple barrels	1 for the biggest , 0 for the rest
Others	0.8 for the biggest, 0.55 for the rest

During a developing fire the materials start to disintegrate. When the probability of the occurrence of a fire and the disintegration of materials due to the fire are taken into account, the determinative fire load can be calculated.

$$q_{fi,d} = q_{fi,k} m \delta_{q1} \delta_{q2} \delta_n \qquad (2.6.3)$$

In this equation:

- m : The coefficient taking into account the loss of materials due to burning. When most materials in the area are cellulose-based materials, such as wood and paper, the coefficient can be assumed as m=0.8. In most cases this coefficient is set to m = 1.0.
- δ_{q1} : The probability factor that considers the chance a fire occurs based on the total area of the room. Standard values are shown in Table 4.
- δ_{q2} : The probability factor that considers the chance a fire occurs based on the activities of the room. Standard values are shown in Table 5.
- δ_n : Takes into account the different methods installed in the room to prevent a fire.

Table 4: Probability factor δ_{q1} based on the total room area.[6]

Compartment floor area A_f (m²)	Risk of fire δ_{q1}
25	1.10
250	1.50
2500	1.90
5000	2.00
10000	2.13

Table 5: Probability factor δ_{q2} based on the activities of the room.[6]

Risk of fire δ_{q2}	Occupancy of the area
0.78	Art gallery, museum, swimming pool
1.00	office, hotel, paper industry
1.22	manufactory of machines and engines
1.44	chemical laboratories
1.66	manufactory of fireworks and paint

Table 5: Probability factor δ_{q2} based on the activities of the room.[6]

2.6.3 Transformation of the characteristic loads to design loads

A load or an action is a force that is exerted onto a construction. Bending, caused by the temperature changes or differential consolidation, is a form of an indirect force exerted on a construction. The loads are divided into four groups which are defined by the Eurocode EN1990 as:

- Permanent action (G or g): The most common actions, that are listed as permanent action, are: self-weight or consolidation of the soil. These loads are working on a building and they stay there from the moment of construction until the building is demolished.
- Variable action (Q or q): These can be imposed loads, wind load or snow load. These loads will not be exerted permanently on a building. For example: The wind will not blow onto the construction all the time and there will be no snow on the roof during the summer.
- Accidental action (A): Fire, explosions or extraordinary impacts are accidental actions. In normal circumstances these actions will not occur. However, in this research these actions are observed for the calculations, because of the fact that fire is an accidental action.
- Seismic actions (A_E): these loads are caused by the seismic energy and movements.

When assessing the behaviour of construction in a fire situation, the design loads are calculated in the accidental design situation.

$$E_d = \sum_{j \geq 1} G_{k,j} + P + A_d + (\Psi_{1.1} \text{ or } \Psi_{2.1})Q_{k,1} + \sum_{i \geq i} \Psi_{2.i}Q_{k,i} \qquad (2.6.4)$$

In this case, it is unlikely that a high load combination is achieved. The main accidental action $Q_{k,1}$ has to be multiplied with the quasi-permanent combination factor $\Psi_{2,1}$ according to NBN 1991-1-2–ABN[6]. In case of fire there are some remarks that need to be taken into account. A fire produces a considerable amount of heat and this heat removes the possible present snow from the roof. Therefore snow loads has to be removed from the equation. Maintenance loads on the roof of a structure needs to be removed as well. The wind load can be reduced but not removed. For calculations in a fire situation only 20% of the wind load is taken into account. The only actions fully taken into account are self-weight and permanent actions, multiplied by safety factor $\gamma_g = 1.00$ and the wind load is combined with the factor $\Psi = 0.2$.

Since the design load in fire situation $E_{fi,d}$ is not the same as the load at ambient temperature E_d, a specific reduction factor has to be applied. The factor η_{fi} serves as that reduction factor. This gives the following equation:

$$E_{fi,d,t} = E_{fi,d} = \eta_{fi}E_d \qquad (2.6.5)$$

Where:

- E_d = the design value of the fundamental combination of loads on the structure. This is the most unfavourable of the following three equations:

   1. $E_d = \sum_{j\geq1} \gamma_{G,j} G_{k,j} + \gamma_p P + \gamma_{Q,1} Q_{k,1} + \sum_{i\geq i} \gamma_{Q,i} \Psi_{0.i} Q_{k,i}$ (2.6.6)
   2. $E_d = \sum_{j\geq1} \gamma_{G,j} G_{k,j} + \gamma_p P + \gamma_{Q,1} \Psi_{0.1} Q_{k,1} + \sum_{i\geq i} \gamma_{Q,i} \Psi_{0.i} Q_{k,i}$ (2.6.7)
   3. $E_d = \sum_{j\geq1} \xi_j \gamma_{G,j} G_{k,j} + \gamma_p P + \gamma_{Q,1} Q_{k,1} + \sum_{i\geq i} \gamma_{Q,i} \Psi_{0.i} Q_{k,i}$ (2.6.8)

- $E_{fi,d}$ = the design value of the combination of loads in fire situation.
- η_{fi} = reduction factor for fire situation, calculated for each of the previous equations as follows:

   1. $\eta_{fi} = \dfrac{G_k + \Psi_{fi} Q_{k,1}}{\gamma_G G_k + \gamma_{Q,1} Q_{k,1}}$ (2.6.9)

   2. $\eta_{fi} = \dfrac{G_k + \Psi_{fi} Q_{k,1}}{\gamma_G G_k + \gamma_{Q,1} \Psi_{0,1} Q_{k,1}}$

           (2.6.10)

   3. $\eta_{fi} = \dfrac{G_k + \Psi_{fi} Q_{k,1}}{\xi \gamma_G G_k + \gamma_{Q,1} Q_{k,1}}$

   (2.6.11)

In the last three equations Ψ_{fi}, the combination factor in fire situations equals $\Psi_{1,1}$ or $\Psi_{2,1}$. The reduction factor η_{fi} can be found when analysing the ratio between the permanent action G_k and the dominant variable action $Q_{k,1}$. The factors γ_G and γ_Q are the partial safety factors for permanent loads and variable loads respectively.

Table 6 gives the values of the combination factors ψ in relation to the different building types. As it can be seen, the factor $\Psi_{1,1}$ varies in function of the building type. This significantly influences the fire reduction factor η_{fi} as demonstrated in Figure 10.

Table 6: Recommended values of ψ factors for buildings.[5]

Action	ψ_0	ψ_1	ψ_2
Imposed loads in buildings, category (see EN 1991-1-1)			
Category A : domestic, residential areas	0,7	0,5	0,3
Category B : office areas	0,7	0,5	0,3
Category C : congregation areas	0,7	0,7	0,6
Category D : shopping areas	0,7	0,7	0,6
Category E : storage areas	1,0	0,9	0,8
Category F : traffic area, vehicle weight ≤ 30kN	0,7	0,7	0,6
Category G : traffic area, 30kN < vehicle weight ≤ 160kN	0,7	0,5	0,3
Category H : roofs	0	0	0
Snow loads on buildings (see EN 1991-1-3)*			
Finland, Iceland, Norway, Sweden	0,70	0,50	0,20
Remainder of CEN Member States, for sites located at altitude H > 1000 m a.s.l.	0,70	0,50	0,20
Remainder of CEN Member States, for sites located at altitude H ≤ 1000 m a.s.l.	0,50	0,20	0
Wind loads on buildings (see EN 1991-1-4)	0,6	0,2	0
Temperature (non-fire) in buildings (see EN 1991-1-5)	0,6	0,5	0
NOTE The ψ values may be set by the National annex. * For countries not mentioned below, see relevant local conditions.			
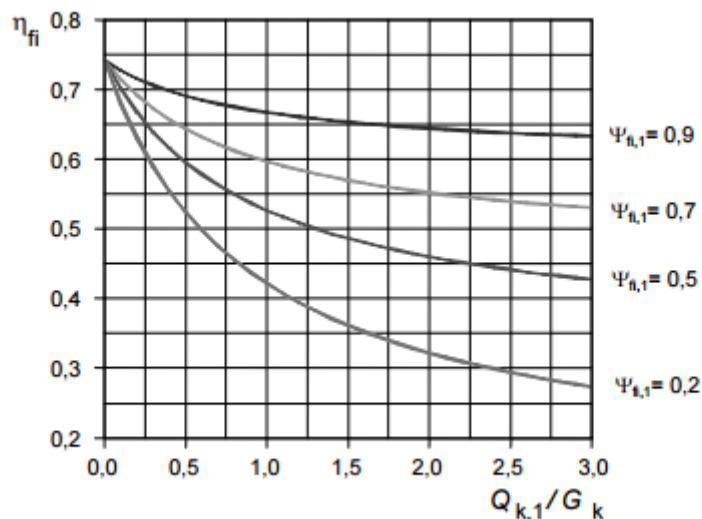
Figure 10: Influence of ψ factors on reduction factor η_fi. [3]

This reduction factor η_{fi} is often confused with the load level, which has the same symbol but has a different meaning. However, this load level is less important in our calculations and is therefore neglected.

2.6.4 Classification of the examined elements as class 1, 2, 3 or 4 cross-section elements

Before being able to calculate the fire resistance of a steel element, specific assumptions have to be made regarding instability phenomena. If instabilities are not critical for the element, a simplified calculation method can be used, though the assumption of neglecting instability phenomena should always be justified. However, this chapter takes these instabilities into consideration to achieve a more elaborate calculation. For the validation of the software, which is covered later in this document, some examples neglect instability phenomena to simplify the validation.

Because instability phenomena are taken into account, the slenderness of the steel cross-sections needs to be obtained. In order calculate the slenderness of each element, Eurocode 3 divides all steel elements into 4 classes. This division is done to simulate the possible local buckling of the steel cross-sections. These classes are based on the moment that the element can be subjected to:

- Class 1 cross-sections are called the "plastic design cross-sections" because the moment they are subjected to is equal to the plastic moment and additionally the cross-section is able to rotate locally, therefore creating a plastic hinge.
- Class 2 cross-sections are "compact cross-sections" as they are subjected to a bending moment equal to the plastic moment but cannot rotate.
- Class 3 cross-sections then are called the "non-compact cross-sections". These elements are only be subjected to a bending moment equal to the yield moment.
- Lastly the class 4 cross-section elements are called the "slender cross-sections" as they fail before being able to reach the yield moment.

In normal calculations, Table 7 would be used to evaluate the cross sections. However, in fire situation the mechanical properties of the steel cross-sections may vary and the risk for buckling can therefore be different, which leads to a reclassification of the cross-sections using different criteria. As seen in Figure 11, the influence of the elevated temperature has to be taken into account by using a reduction coefficient of 0.85 for the calculation ε.

Table 7: Maximum width-to-thickness ratios for compression parts. [7]

	Internal compression parts		
			Axis of bending
			Axis of bending
Class	Part subject to bending	Part subject to compression	Part subject to bending and compression
Stress distribution in parts (compression positive)			
1	$c/t \le 72\varepsilon$	$c/t \le 33\varepsilon$	when $\alpha > 0,5$: $c/t \le \dfrac{396\varepsilon}{13\alpha-1}$ when $\alpha \le 0,5$: $c/t \le \dfrac{36\varepsilon}{\alpha}$
2	$c/t \le 83\varepsilon$	$c/t \le 38\varepsilon$	when $\alpha > 0,5$: $c/t \le \dfrac{456\varepsilon}{13\alpha-1}$ when $\alpha \le 0,5$: $c/t \le \dfrac{41,5\varepsilon}{\alpha}$
Stress distribution in parts (compression positive)			
3	$c/t \le 124\varepsilon$	$c/t \le 42\varepsilon$	when $\psi > -1$: $c/t \le \dfrac{42\varepsilon}{0,67+0,33\psi}$ when $\psi \le -1^{*)}$: $c/t \le 62\varepsilon(1-\psi)\sqrt{(-\psi)}$

$\varepsilon = \sqrt{235/f_y}$	f_y	235	275	355	420	460
	ε	1,00	0,92	0,81	0,75	0,71

*) $\psi \le -1$ applies where either the compression stress $\sigma \le f_y$ or the tensile strain $\varepsilon_y > f_y/E$

$C1: M = M_{pl} \quad \phi > \phi_{req}$
$C2: M = M_{pl} \quad \phi < \phi_{req}$
$C3: M = M_{el}$
$C4: M = M_{eff,el}$

➤ classified as at ambient temperature

➤ however, different value of ε to take account of temperature influence

Temperature induced

$\varepsilon = 0.85\sqrt{\dfrac{235}{f_y}}$

Figure 11: Classification of cross-section of elements. [3]

2.6.5 Calculation of the design resistance of the steel members

2.6.5.1   Design conditions

Since instability phenomena are taken into account, the design load-bearing capacity cannot be derived directly from the design load-bearing capacity of the element at ultimate limit state. Thus, all stability verifications are integrated into the design. Additionally, due to elevated temperatures caused by the fire on the surface of the steel elements, the thermal and mechanical properties of steel decrease. Specific reduction factors are therefore included and taken into account this reduction in strength. These factors are explained further. Firstly there is a reduction due to the mechanical loads being calculated in accidental situation, then reduction factors for the thermal and mechanical properties of steel are considered. Lastly adaptation factors are necessary to take into account the fact that the temperature along the steel element is not always be uniform.

The resistance of the steel is calculated with the loads acting on an element during a fire situation. The calculation of the resistance is similar to the calculation in normal circumstances. The mechanical loads are calculated in accidental situation. Therefore, the properties of the steel need to be reduced as explained in Figure 11 earlier.

Additionally, the thermal and mechanical properties of steel are reduced when the surface of these elements is exposed to elevated temperatures due to the fire. In order to consider these reductions in strength, specific reduction factors $k_{E,\theta}$ and $k_{y,\theta}$ are regarded. The thermal properties of steel are: thermal conductivity, specific heat and density. The mechanical properties are the elastic modulus and the yield strength. The influence of fire on these properties is shown in Figure 12 and Figure 13.

Density of steel: 7850 kg/m³
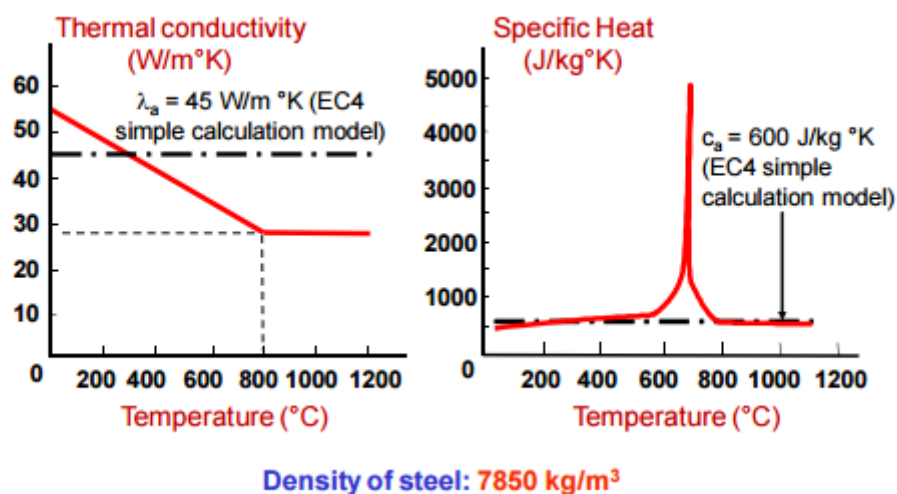
Figure 12: Thermal properties of steel at elevated temperatures. [3]
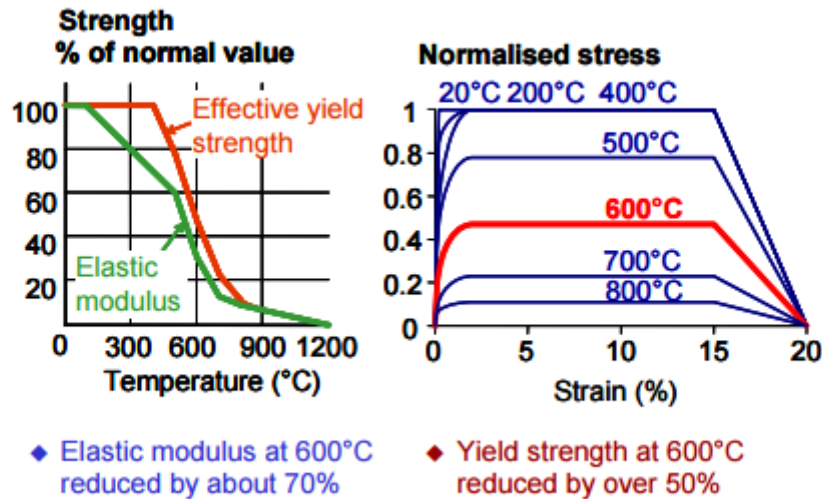
Figure 13: Mechanical properties of steel at elevated temperatures. [3]

The reduction of the steel elastic modulus and the yield strength is defined by the reduction factors $k_{E,\theta}$ and $k_{y,\theta}$. The correlation of the reduction of these properties due to elevated temperatures is shown in Table 8.

Table 8: Reduction factors at temperature θ_a relative to the value of f_y or E_a at 20°C. [3]

Steel temperature θ_a	Reduction factors at temperature θ_a relative to the value of f_y or E_a at 20 °C		
	Reduction factor (relative to f_y) for effective yield strength $k_{y,\theta} = f_{y,\theta}/f_y$	Reduction factor (relative to f_y) for proportional limit $k_{p,\theta} = f_{p,\theta}/f_y$	Reduction factor (relative to E_a) for the slope of the linear elastic range $k_{E,\theta} = E_{a,\theta}/E_a$
20 °C	1,000	1,000	1,000
100 °C	1,000	1,000	1,000
200 °C	1,000	0,807	0,900
300 °C	1,000	0,613	0,800
400 °C	1,000	0,420	0,700
500 °C	0,780	0,360	0,600
600 °C	0,470	0,180	0,310
700 °C	0,230	0,075	0,130
800 °C	0,110	0,050	0,090
900 °C	0,060	0,0375	0,0675
1000 °C	0,040	0,0250	0,0450
1100 °C	0,020	0,0125	0,0225
1200 °C	0,000	0,0000	0,0000

NOTE: For intermediate values of the steel temperature, linear interpolation may be used.

Lastly, temperature in steel is uniform at ambient temperature. In fire situation, this might not be the case. To take this difference into account in the calculations, two adaption factors are used.

κ_1 is the adaptation factor for non-uniform temperature across the cross section whereas κ_2 is the adaptation factor for non-uniform temperature along the beam. The values of these adaptation factors are defined as:

- $\kappa_1 = 0.70$ for unprotected beams with an exposure to fire on three sides.
  $\kappa_1 = 0.85$ for protected beams with an exposure to fire on three sides.
  $\kappa_1 = 1.00$ for beams with an exposure to fire on all four sides.
- $\kappa_2 = 0.85$ for statically indefinite beams that are simply supported.
  $\kappa_2 = 1.00$ for all other cases.

The structural performance of the steel members and connections is retained for a given amount of time during a fire. The profiles buckle under the loads applied on the construction during the fire. This happens when the loads exceed the resistance of the structure in fire conditions:

$$E_{fi,d} > R_{fi,d,t} \qquad (2.6.12)$$

These are the basics for the calculations that are shown next.

2.6.5.2 Resistance to tension

When an element is subjected to tension, the mechanical resistance is calculated for a uniform temperature division:

$$N_{fi,\theta,Rd} = k_{y,\theta} N_{Rd} \left(\frac{\gamma_{M,0}}{\gamma_{M,fi}} \right) \qquad (2.6.13)$$

For this equation:

- $k_{y,\theta}$: The reduction factor for yield stress at a temperature θ at time t
- N_{Rd} : The resistance of the steel-section at normal temperatures
- $\gamma_{M,0}$: The partial safety factor for the material properties in ambient temperature design.
- $\gamma_{M,fi}$: The partial safety factor for the material properties in fire design.

The values of these partial safety factors is shown in Table 9.

Table 9: Partial safety factors for materialistic properties of steel. [3]

Type of members	Ambient temperature design	Fire design
Cross-sections	$\gamma_{M0} = 1,0$	$\gamma_{M,fi} = 1,0$
Members with instability	$\gamma_{M1} = 1,0$	$\gamma_{M,fi} = 1,0$
Tension members to fracture	$\gamma_{M2} = 1,25$	$\gamma_{M,fi} = 1,0$
Joints	$\gamma_{M2} = 1,25$	$\gamma_{M,fi} = 1,0$

When an element is subjected to tension, the mechanical resistance can be calculated for a non-uniform temperature division:

$$N_{fi,\theta,Rd} = \sum_{i=1}^{n} A_i k_{y,\theta,i} \frac{f_y}{\gamma_{M,fi}} \tag{2.6.14}$$

With:

- A_i : The surface area with a temperature of θ_i
- $k_{y,\theta,i}$: The reduction factor for the yield strength
- f_y : The yield strength of steel

2.6.5.3   Resistance to compression

When the steel element is subjected to compression another formula is used to determine the mechanical resistance of the element.

$$N_{fi,\theta,Rd} = \chi_{fi} k_{y,\theta} N_{Rd} \left(\frac{\gamma_{M,0}}{\gamma_{M,fi}} \right) = \chi_{fi} A k_{y,\theta} \frac{f_y}{\gamma_{M,fi}} \tag{2.6.15}$$

Where:

- χ_{fi} : The reduction factor for buckling of a steel element in a fire situation, which can be calculated as shown next.
- $k_{y,\theta}$: The reduction factor for the yield strength of steel at a specific temperature

2.6.5.4   Resistance to buckling

The reduction factor for buckling can be determined using:

$$\chi_{fi} = \frac{1}{\varphi_\theta + \sqrt{\varphi_\theta{}^2 - \overline{\lambda_\theta}^2}} \tag{2.6.16}$$

And:

$$\varphi_\theta = \frac{1}{2} \left[1 + \alpha \overline{\lambda_\theta} + \overline{\lambda_\theta}^2 \right] \tag{2.6.17}$$

$$\alpha = 0.65 \sqrt{\frac{235}{f_y}} \tag{2.6.18}$$

To calculate the slenderness of the steel element, the slenderness of the element at normal temperature is corrected using reduction factors.

$$\overline{\lambda_\theta} = \bar{\lambda} \sqrt{\frac{k_{y,\theta}}{k_{E,\theta}}} \tag{2.6.19}$$

- $k_{y,\theta}$: Reduction factor for the yield strength at temperature θ.
- $k_{E,\theta}$: Reduction factor for the elastic modulus at a specific temperature θ at a specific time t.

In which:

$$\bar{\lambda} = \frac{\lambda}{\lambda_1}$$ (2.6.20)

$$\lambda = \frac{L_b}{i_z}$$ (2.6.21)

$$\lambda_1 = 93.9\varepsilon$$ (2.6.22)

$$\varepsilon = 0.85 * \sqrt{\frac{235}{f_y}}$$ (2.6.23)

Where

- L_b is the buckling length
- i_z is the gyration radius

In normal circumstances the buckling length of steel columns is determined by following simple rules. For a building with one floor, the column is fixed on one end and the buckling length is 0.7L. In multiple stories all columns are fixed on both ends, except for the top column, which is fixed at one end. The columns that are fixed at both ends have a buckling length of 0.5L and for the top floor the buckling length is 0.7L. This is illustrated in Figure 14.
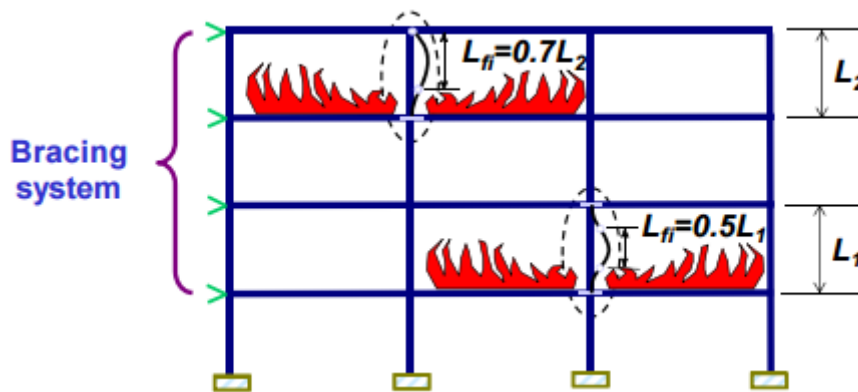
Figure 14: Buckling lengths in normal circumstances. [3]

2.6.5.5 Resistance to bending

The resistance of an element against the bending moment for class 1 and two with a uniform temperature can be determined:

$$M_{fi,\theta,Rd} = k_{y,\theta} M_{Rd} \left(\frac{\gamma_{M,0}}{\gamma_{M,fi}}\right)$$ (2.6.24)

- $k_{y,\theta}$: reduction factor for the yield strength at temperature θ
- M_{Rd} : the resistance to the bending moment at normal temperature or the reduced resistance to the bending moment when shear has been taken into account

Note that for class 3 sections $M_{Rd} = M_{el,Rd}$.

However, adaptation factors need to be considered to take into account the non-uniform division of the temperature along the cross-section of along the element, as explained earlier. The bending moment resistance of the element can thus be calculated with equation (2.6.25) and as shown in Figure 15:

$$M_{b,fi,t,Rd} = k_{y,\theta,max} M_{Rd} \left(\frac{\gamma_{M,0}}{\gamma_{M,fi}}\right) / (\kappa_1 \kappa_2) \tag{2.6.25}$$
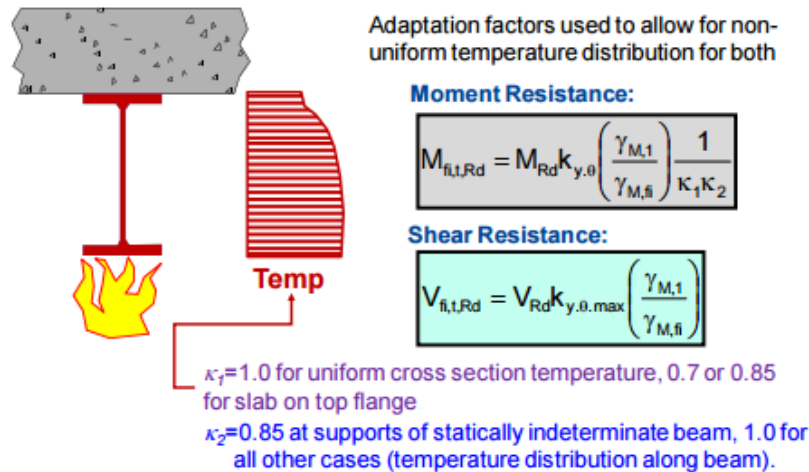
Figure 15: Adaptation factors due to non-uniform temperature along the element. [3]

2.6.5.6   Resistance to lateral torsional buckling

The non-dimensional slenderness of steel beams subjected to lateral torsional buckling is calculated as follows:

- For steel beams with class 1 or 2 cross-sections $\overline{\lambda_{fι,0}} = \overline{\lambda_{LT,20}} = \sqrt{\frac{W_{pl}*f_y}{M_{cr}}}$

$$\tag{2.6.26}$$

- For steel beams with class 3 cross-sections $\overline{\lambda_{fι,0}} = \overline{\lambda_{LT,20}} = \sqrt{\frac{W_{el}*f_y}{M_{cr}}}$

$$\tag{2.6.27}$$

With

M_{cr}: The elastic critical moment for lateral-torsional buckling of the element at 20°C

W_{pl} and W_{el}: The plastic and elastic section moduli at 20°C

This can be used together with the degree of utilization to determine further the critical temperature of the steel member. This is further explained in chapter 2.6.7.

The design resistance moment for Class 3 cross-sections is found by using this equation:

$$M_{b,fi,t,Rd} = \chi_{LT,fi} W_{el,y} k_{y,\theta,com} \left(\frac{f_y}{\gamma_{M,fi}} \right) \tag{2.6.28}$$

Where:

- $\chi_{LT,fi}$: the reduction factor for buckling as Eq. 2.6.16

2.6.5.7   Resistance to shear

The resistance to shear for columns is determined using the formula seen in Figure 15:

$$V_{fi,\theta,Rd} = k_{y,\theta,max} V_{Rd} \left(\frac{\gamma_{M,0}}{\gamma_{M,fi}} \right) \tag{2.6.29}$$

In which

- V_{Rd} : the resistance to shear for the section at normal temperature θ
- $k_{y,\theta,max}$: reduction factor of the yield strength of steel at the temperature of steel at time t

2.6.5.8   Resistance to combined bending and axial force

To determine the design value of the resistance to combined bending, shear and axial force the following formula is to be used respectively for elements with a cross section class 1,2 or 3 :

$$\frac{N_{fi,Ed}}{\chi_{min,fi} A k_{y,\theta} \frac{f_y}{\gamma_{M,fi}}} + \frac{k_y M_{y,fi,Ed}}{W_{pl,y} k_{y,\theta} \frac{f_y}{\gamma_{M,fi}}} + \frac{k_z M_{z,fi,Ed}}{W_{pl,z} k_{y,\theta} \frac{f_y}{\gamma_{M,fi}}} \leq 1 \tag{2.6.30a}$$

$$\frac{N_{fi,Ed}}{\chi_{z,fi} A k_{y,\theta} \frac{f_y}{\gamma_{M,fi}}} + \frac{k_{LT} M_{y,fi,Ed}}{\chi_{LT,fi} W_{pl,y} k_{y,\theta} \frac{f_y}{\gamma_{M,fi}}} + \frac{k_z M_{z,fi,Ed}}{W_{pl,z} k_{y,\theta} \frac{f_y}{\gamma_{M,fi}}} \leq 1 \tag{2.6.30b}$$

$$\frac{N_{fi,Ed}}{\chi_{min,fi} A k_{y,\theta} \frac{f_y}{\gamma_{M,fi}}} + \frac{k_y M_{y,fi,Ed}}{W_{el,y} k_{y,\theta} \frac{f_y}{\gamma_{M,fi}}} + \frac{k_z M_{z,fi,Ed}}{W_{el,z} k_{y,\theta} \frac{f_y}{\gamma_{M,fi}}} \leq 1 \tag{2.6.30c}$$

With:

- $N_{fi,Ed}$: is the design normal force in a fire situation.
- $M_{y,fi,Ed}$: is the design moment in fire situation.
- $\chi_{LT,fi}$: is the reduction factor for buckling as in Eq. 2.6.16

And k: the reduction factor of the elastic range at the maximum steel temperature in the compressed zone of the element at time t:

$$k_{LT} = 1 - \frac{\mu_{LT} N_{fi,Ed}}{\chi_{z,fi} A k_{y,\theta} \frac{f_y}{\gamma_{M,fi}}} \leq 1 \tag{2.6.31}$$

- where : $\mu_{LT} = 0{,}15\, \overline{\lambda_{y,\theta}}\, \beta_{M,LT} - 0{,}15 \leq 0{,}9$

$$k_y = 1 - \frac{\mu_y N_{fi,Ed}}{\chi_{y,fi} A k_{y,\theta} \frac{f_y}{\gamma_{M,fi}}} \leq 1 \tag{2.6.32}$$

- where : $\mu_y = (2\beta_{M,y} - 5)\overline{\lambda_{y,\theta}} + 0{,}44\beta_{M,LT} + 0{,}29 \leq 0{,}8$

$$k_z = 1 - \frac{\mu_z N_{fi,Ed}}{\chi_{z,fi} A k_{y,\theta} \frac{f_y}{\gamma_{M,fi}}} \leq 1 \tag{2.6.33}$$

- where : $\mu_z = (1{,}2\beta_{M,y} - 5)\overline{\lambda_{y,\theta}} + 0{,}44\beta_{M,LT} + 0{,}29 \leq 0{,}8$

2.6.6 Verification of the stability of the structure using the degree of utilization.

The degree of utilization is a non-dimensional factor that gives the relation between the acting fire load and the fire resistance of the element at t = 0.

$$\mu_0 = \frac{X_{Ed,fi}}{X_{Rd,fi,0}} \tag{2.6.34}$$

As illustrated in the Figure 16, the degree of utilization is often utilised to determine the boundary between a stable structure and a designed collapse. This degree of utilization can also be used to determine the critical temperature, which is used to define the fire resistance.
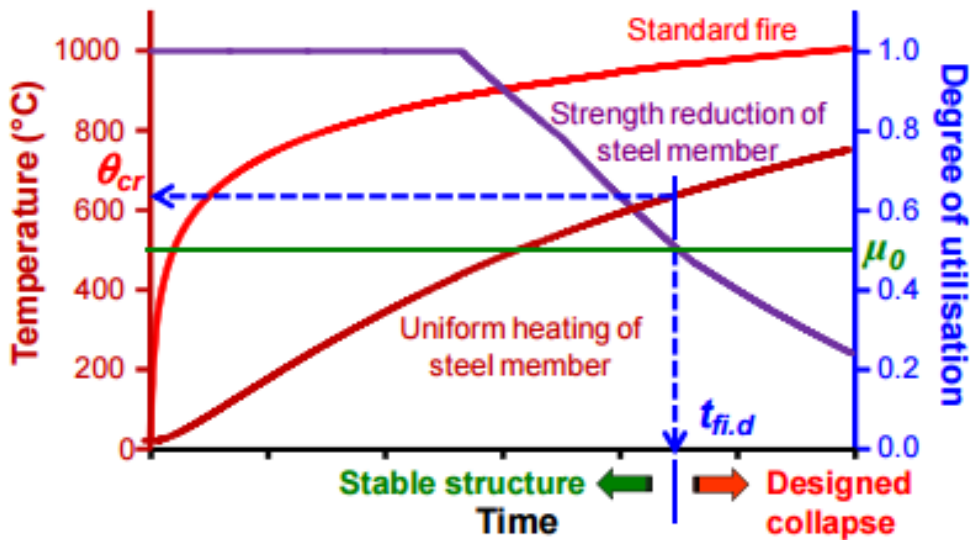
Figure 16: Relation between the degree of utilization and the critical temperature. [3]

A simple calculation of the degree of utilization is alternatively possible if no buckling can occur:

$$\mu_0 = \eta_{fi} * \left(\frac{\gamma_{M,fi}}{\gamma_{M0}} \right) \qquad (2.6.35)$$

However this is not applied in the calculations done in this thesis, since buckling is considered to be possible. Other suggestions for the calculation of this factor are made for that reason. These are defined as follows:

- For beams that are subjected to bending with lateral torsional buckling the design bending moment and the moment resistances of the cross-section are used:

$$\mu_0 = \frac{M_{fi}}{M_{pl,fi,0}} \; for \; class \; 1 \; or \; 2 \; cross - sections \qquad (2.6.36)$$

$$\mu_0 = \frac{M_{fi}}{M_{el,fi,0}} \; for \; class \; 3 \; cross - sections \qquad (2.6.37)$$

With

M_{fi}: The design bending moment of the element in fire situation
$M_{pl,fi,0}$: The plastic moment resistance of the element in fire situation, this however at t=0, which means the fire has not developed yet.
$M_{el,fi,0}$ The moment elastic resistance of the element in fire situation at t=0

- For columns subjected to an axial compressive force with flexural buckling:

$$\mu_0 = \frac{N_{fi}}{N_{pl,fi,0}} \qquad (2.6.38)$$

With

N_{fi} The design axial compressive force of the element in fire situation
$N_{pl,fi,0}$ the plastic axial resistance of the cross-section in fire situation at t=0

2.6.7 Extraction of the critical temperature of the steel members

The critical temperature is the temperature at which a steel element is about to fail. Once the degree of utilization is obtained, the critical temperature can be easily determined. However, a distinction has to be made between structures with instability phenomena and structures without instability phenomena.

The use of the critical temperature method is the direct method only used when there is no need to take the influence of the change in stability into account. The bearing strength of the element can be easily found by using the bearing strength at normal temperatures and taking into account the reduction factor for the yield strength $k_{y,\theta}$. The element does not fail until the loads applied onto the element exceed the bearing strength. For calculations where instability phenomena are neglected, the following relation shown in Figure 17 can be assumed between the critical temperature and the degree of utilization:
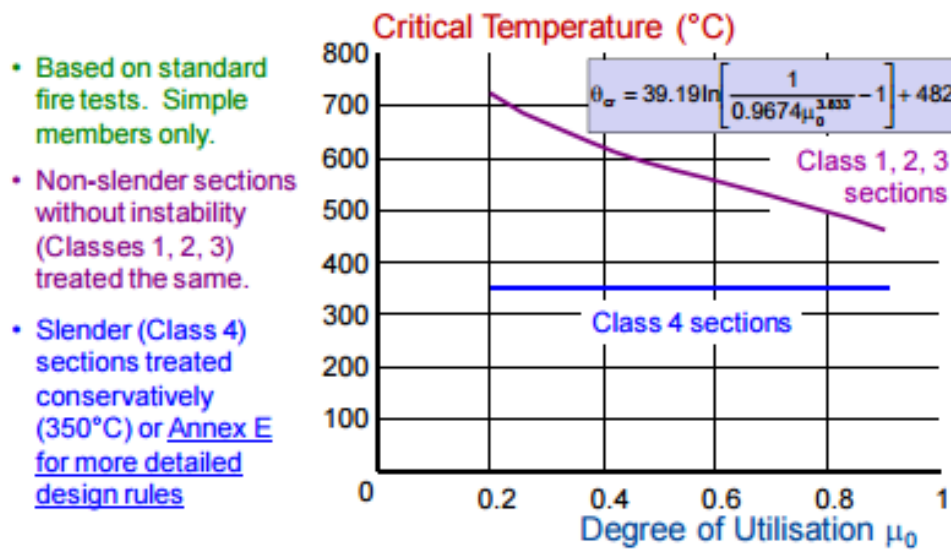
Figure 17: Critical temperature for calculations where instability phenomena are neglected. [3]

However, since instability phenomena are taken into account in the calculations in this thesis, in Table 10 the critical temperatures θ_{cr} are given , based on the non-dimensional slenderness of the element $\overline{\lambda_{fi,0}}$.

Table 10: Critical temperatures for steel elements, steel grade S235, based on the non-dimensional slenderness and the degree of utilization. [3]

$\bar{\lambda}_{\theta,0}$	0,0	0,2	0,4	0,6	0,8	1,0	1,2	1,4	1,6	1,8	2,0
μ_0											
0,04	1000	975	945	906	875	832	783	736	694	677	657
0,06	900	884	863	832	791	751	698	677	654	627	599
0,08	860	837	806	781	743	695	671	644	613	586	561
0,10	820	796	777	747	699	674	645	611	582	554	524
0,12	792	775	752	713	682	653	618	585	555	522	464
0,14	775	755	726	692	665	631	594	563	529	476	357
0,16	758	735	701	678	648	610	576	541	502	394	
0,18	742	714	689	665	631	593	559	520	440		
0,20	725	697	678	651	615	578	541	495	364		
0,22	708	688	667	638	598	564	523	443			
0,24	696	678	655	624	587	549	505	387			
0,26	688	668	644	610	575	535	472				
0,28	679	659	633	598	563	521	432				
0,30	671	649	622	588	552	506	385				
0,32	663	640	610	578	540	483					
0,34	654	630	599	568	528	452					
0,36	646	620	591	559	516	422					
0,38	638	611	583	549	505	382					
0,40	629	601	574	539	486						
0,42	621	593	566	529	464						
0,44	613	586	558	520	441						
0,46	604	579	549	510	418						
0,48	597	571	541	500	387						
0,50	590	564	532	483							
0,52	584	557	524	466							
0,54	577	550	516	449							
0,56	571	542	507	432							
0,58	565	535	498	415							
0,60	558	528	485	391							
0,62	552	520	472								
0,64	545	513	459								
0,66	539	506	445								
0,68	532	497	432								
0,70	526	487	419								

This table only shows the values obtained when working with a steel grade of S235. However, the tables when using other steel grades are also shown in Annex A

In fire situation the buckling length of an element is determined with the standard reduction factors based on the support conditions. The non-dimensional slenderness is calculated as explained previously with equation (5.7.1) and (5.7.2).

2.6.8 Evaluation of the temperature along the surface of the steel members

2.6.8.1   Generalities

When materials are subjected to the heat from the fire and the heated gasses created by the fire, their temperature increases as well. The temperature from the environment, the heated gasses and the fire, is transferred to the materials by convection and radiation. Heat transfer between materials that are in contact with each other, conduction, also influences the temperature of the materials.

The heat transfer can be described by Fourier's differential equation:

$$\frac{\partial (\rho c \theta)}{\partial t} + \frac{\partial \left(\lambda \left(\frac{\partial \theta}{\partial x} \right) \right)}{\partial x} + \frac{\partial \left(\lambda \left(\frac{\partial \theta}{\partial y} \right) \right)}{\partial y} + \frac{\partial \left(\lambda \left(\frac{\partial \theta}{\partial z} \right) \right)}{\partial z} = 0 \tag{2.6.39}$$

With:

- x,y,z : are the coordinates (m)
- θ : the temperature in the coordinates x,y,z (°C)
- ρ : the density (kg/m³)
- c : specific heat (J/kg)
- λ : heat transmission coefficient (W/mK)

The strength and stiffness of steel decreases when the temperature of the steel increases. This relation is shown in Figure 18, where each different curve represents a different temperature. This is also explained earlier, where additional reduction factors are considered in the calculations to take into account these decreasing properties of the steel element.
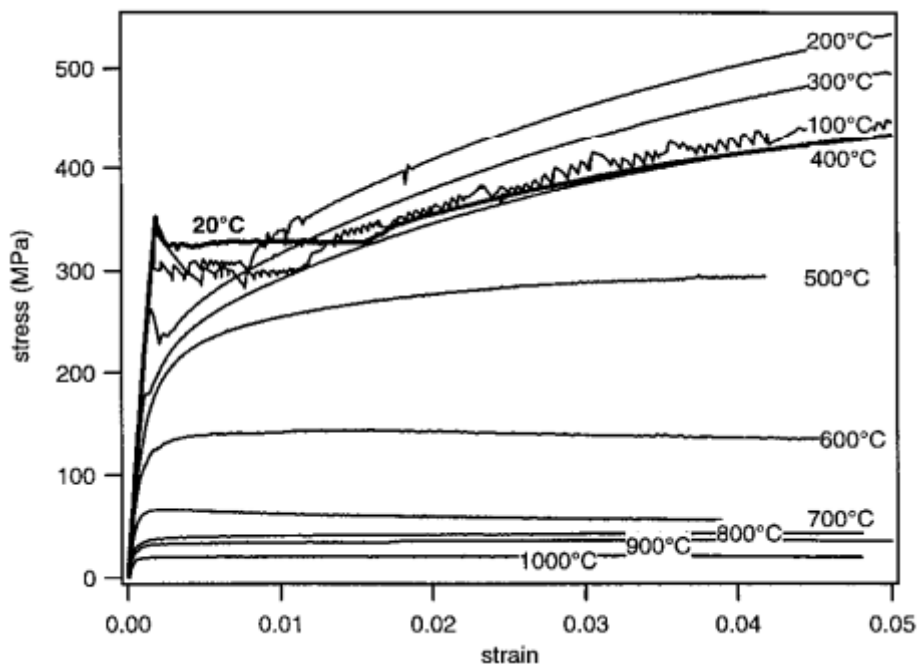
Figure 18: Stress-strain diagrams for different temperatures.[8]

The heat transmission of steel decreases until the temperature of the steel member reaches 800°C. This is illustrated in Figure 12.

2.6.8.2   Evaluation of the temperature of steel members without fire protection

Once the critical temperature is known, the heating of the element has to be evaluated, so these two values can be compared in order to check the fire resistance of the element.

The heating of this element is influenced by the section factor and the shadow factor of this element. The steel perimeter is defined as the ratio between the perimeter through which heat is transferred to steel and the steel volume. As can be seen in Figure 19, this section factor can change under specific conditions. For steel elements under a slab, the heat exchange between the connected surface of the steel element and the slab is neglected. For steel elements with fire protection, the perimeter is assumed equal to the perimeter of the fire protection.

bare steel members   **insulated steel members**
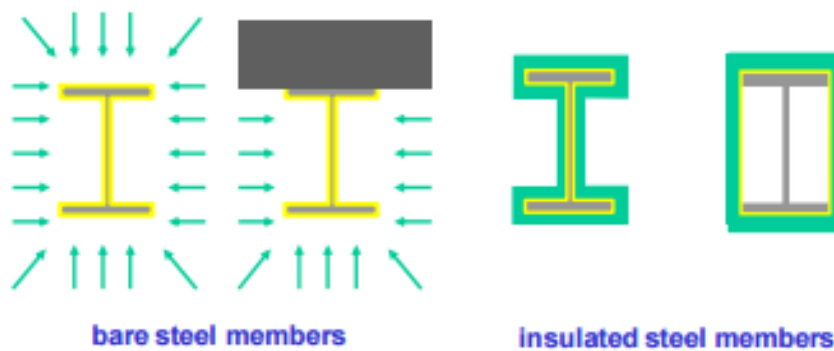
Figure 19: Perimeter of unprotected steel cross-sections. [3]

For unprotected steel elements with a constant cross-section, this section factor can be defined as the ratio between the perimeter of the element that is exposed to the fire and the cross-section area of this element, as shown in Figure 20.

perimeter   exposed perimeter   2(b+h)
c/s area   c/s area   c/s area
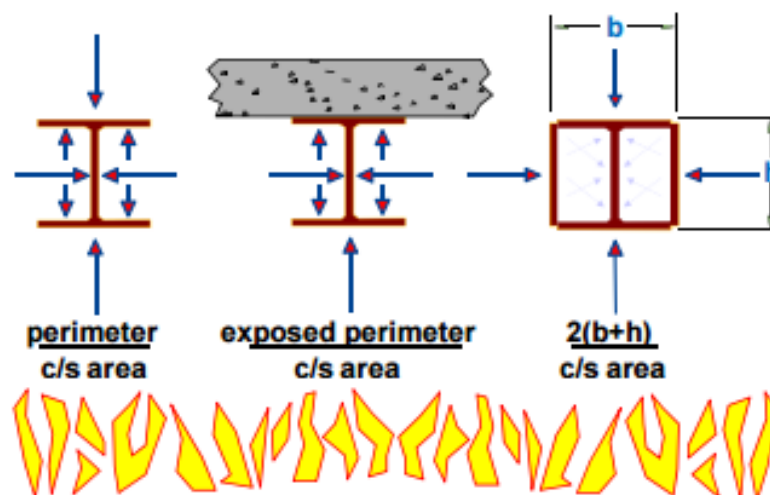
Figure 20: Section factor for unprotected steel cross-sections. [3]

For unprotected steel elements, a correctional factor is used to take into account the reduced radiation as shown in Figure 21. This is called the shadow factor k_{sh}.
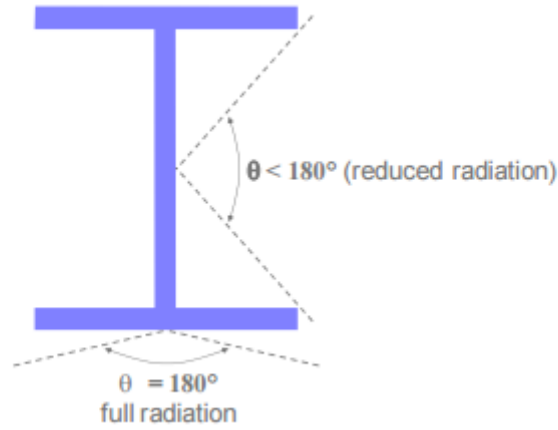
Figure 21: Shadow factor for unprotected steel cross-sections. [3]

The calculation of this shadow factor for I-shaped sections can be done by the following formula:

$$k_{sh} = 0.9 * \frac{\left(\frac{A_m}{V}\right)_b}{\frac{A_m}{V}} \qquad (2.6.35)$$

In which $\frac{A_m}{V}$ is the section factor and $\left(\frac{A_m}{V}\right)_b$ is the box value of the section factor. In all other cases the value of this shadow factor is calculated with the following formula:

$$k_{sh} = \frac{\left(\frac{A_m}{V}\right)_b}{\frac{A_m}{V}} \qquad (2.6.36)$$

With these factors, the heating of the element can be evaluated as follows:

$$\Delta\theta_a = k_{sh} \frac{1}{\rho_a c_a} \frac{A_m}{V} h_{net} \Delta t \qquad (2.6.37)$$

The materials are heated by radiation and convection, therefore the total heat transfer is computed as the sum of the heat transfer by conduction and the heat transfer by radiation.

$$h_{net,tot} = h_{net,c} + h_{net,r} \qquad (2.6.38)$$

The heat transfer due to radiation can be calculated as such:

$$h_{net,r} = \phi \epsilon_m \sigma \left(\left(\theta_g + 273\right)^4 - (\theta_m + 273)^4 \right) \qquad (2.6.39)$$

This is the radiation law of Stephan Bolzmann which states that "the maximum radiation temperature of the fire environment determines the maximum radiation to the steel element."

In this equation the Stephan Bolzmann constant σ is a physical constant that is equal to $5,67*10^{-8}$ W/m²K⁴. ϵ_m represents the emissivity of the element and is in every case equal to 0.7. The configuration factor ϕ is considered to be 1 for standard fire tests. θ_g then is the temperature of the gas and θ_m is the surface temperature of the material.

The heat transfer due to convection on the other hand can be calculated using the temperature difference:

$$h_{net,c} = \alpha_c\left(\theta_g - \theta_m\right) \tag{2.6.40}$$

Depending on the fire curve used to analyse the fire α_c can change.

- α_c = 25 W/m²K for standard fire curves
- α_c = 35 W/m²K for natural fire curves
- α_c = 50 W/m²K for hydrocarbon fire curves

As shown in Figure 22, unprotected elements can easily reach a fire resistance of R15. However, when tested for R30, the temperature elevates significantly, meaning that an unprotected element does not achieve a fire resistance of R30 without any design changes or fire protection.
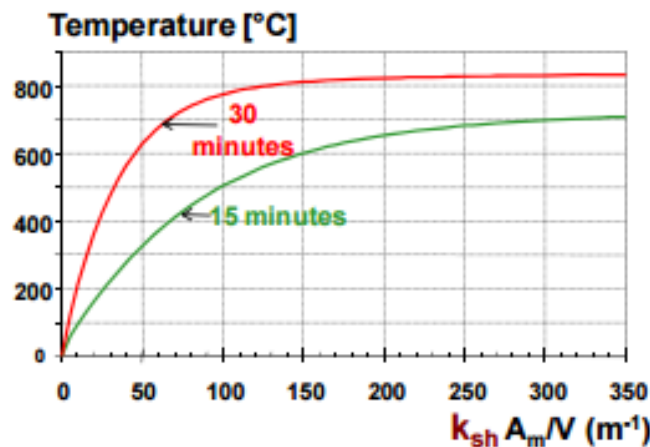
Figure 22: Fire resistance of steel elements in relation to their modified section factor. [3]

2.6.8.3   Evaluation of the temperature of steel members with fire protection

The evaluation of elements with fire protection follows the same principle as the evaluation of steel elements without fire protection. However, the effect of the insulation now needs to be taken into account when calculating the heat flux of the element. The thermal properties of the protected steel elements are directly derived from the fire tests, which means the shadow factor previously used to reduce radiation on the steel element is already taken into account. Therefore, the formulas used to evaluate the temperature in unprotected elements can now be written as follows:

$$\Delta\theta_a = K_{ins}\frac{1}{\rho_a c_a}\frac{A_a}{V}\left(\theta_g - \theta_a\right)\Delta t \tag{2.6.41}$$

Where

$$K_{ins} = k_{ins}\left(\frac{\lambda}{d}, \rho_c, c_p, \rho_a, c_a\right) \tag{2.6.42}$$

48

Which means that this factor is dependent on the thermal properties of the insulation and the steel element. In addition, when the thermal capacity of the insulation is small in comparison to the thermal properties of the steel element, a linear distribution of the temperature drop over the insulation can be assumed ($K_{ins} = \frac{\lambda}{d}$).

When applying the right type of insulation, the heat flow through the system (steel element and insulation) decreases significantly as seen in Figure 23.
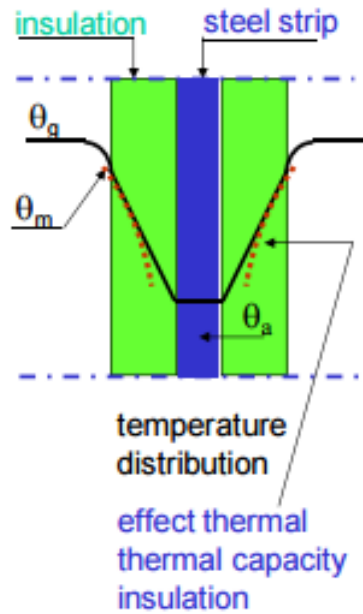
Figure 23: Temperature distribution with usage of insulation. [3]

Note that the goal of the insulation is to decrease the heat flux reaching the steel element considerably. Therefore, the temperature drop between the insulation and the steel element has to be large. This means that the temperature of the gas θ_g is not greater than that the surface temperature of the insulation θ_m. Corresponding with Figure 23, this gives:

$$\left(\theta_g - \theta_m\right) <<<< \left(\theta_m - \theta_a\right) \tag{2.6.43}$$

The section factor $\frac{A_a}{V}$ is now based on the perimeter of the fire protection instead of the cross-section. This is shown in Figure 24.
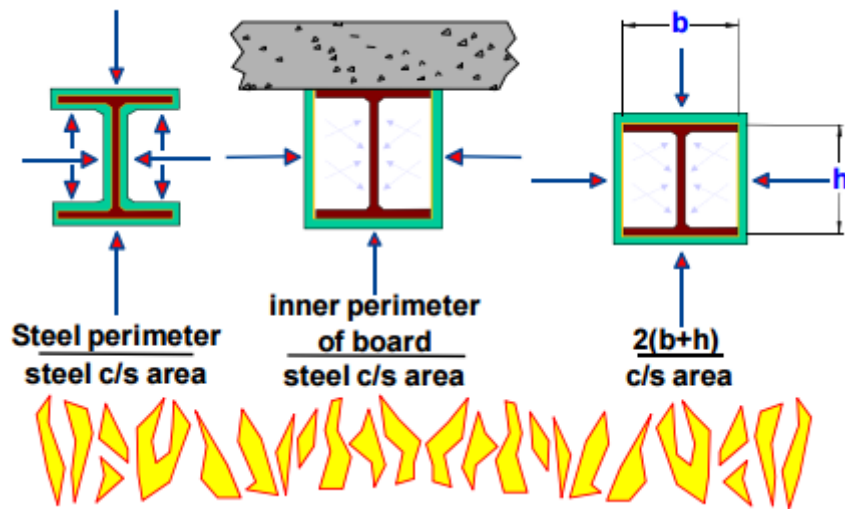
The thermal response of a steel profile can finally be determined with the following equation:

$$\Delta\theta_a = \frac{\lambda_p}{d_p}\frac{1}{\rho_a c_a}\frac{A_p}{V}\left(\frac{1}{1+\frac{\phi}{3}}\right)(\theta_g - \theta_a)\Delta t - \left(e^{\phi/10} - 1\right)\Delta\theta_g \tag{2.6.44}$$

With the thermal capacity of the steel profile:

$$\phi = \frac{c_p \rho_p}{c_a \rho_a} d_p A_p / V \tag{2.6.45}$$

When this equation is applied in an Excel sheet, the temperature of steel at the required time can be easily obtained.

2.6.9 Comparison of the critical temperature and the heating evaluation of the steel element

When the heating of the steel element is evaluated, the results are compared to the critical temperature obtained earlier to check the fire resistance of the steel element. The fire resistance of the element is met once the heating of the steel element does not exceed the critical temperature.

These eight steps are summarized in Figure 25 and Figure 26 to give a quick overview of the calculation.
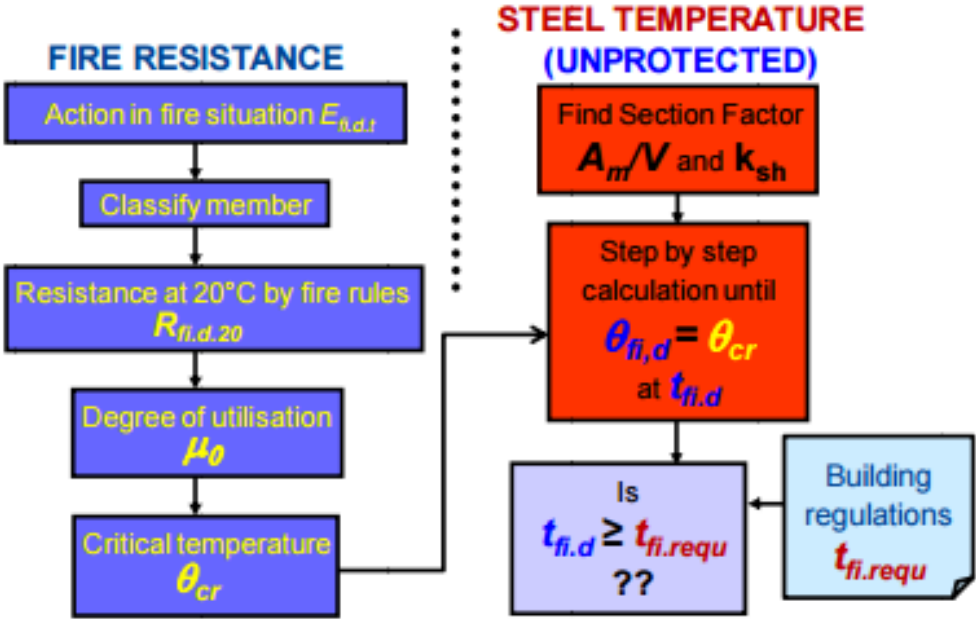
Figure 25: Step-by-step approach of the fire resistance calculation for unprotected elements. [3]
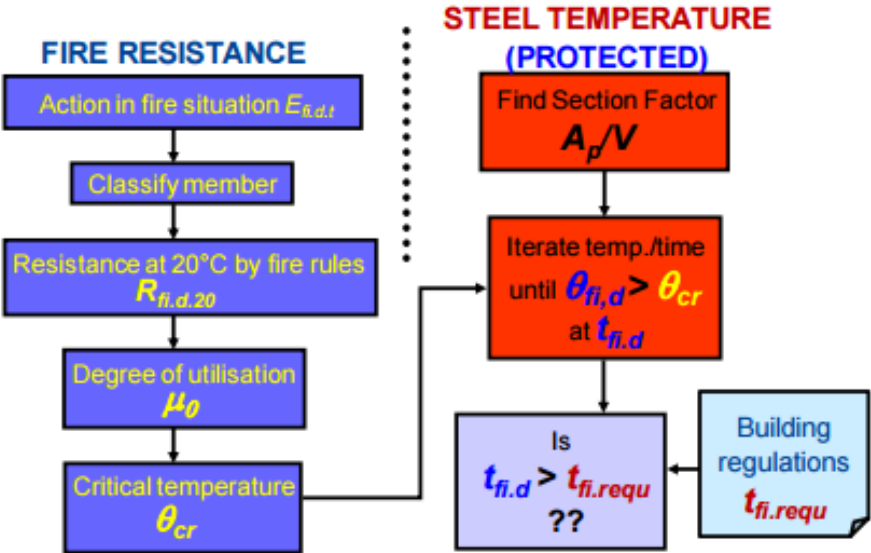
Figure 26: Step-by-step approach of the fire resistance calculation for protected elements. [3]

3 Structural fire design in RFEM

3.1 RFEM software

RFEM is a 3D finite element program in which the calculation of constructions made of steel, reinforced concrete, timber, glass or constructions using multiple materials is possible. RFEM is used to determine internal forces, deformations and support reactions using members, plates or walls, shells or a combination in one model. With a CAD-like graphical user interface, RFEM is easy to handle. RFEM has a modular structure:

- Model creation
- Load definition
- Computation of model
- Design of members and connections

There are several add-on modules available, which can be combined into a custom-tailored program package. In addition to structural analysis you can perform dynamic analysis of the add-on module RF dynam which handles vibration and seismic analysis. RFEM offers a great selection of integrated interfaces with other programs for a seamless project workflow. Data can be exchanged using direct interfaces with autoCAD Autodesk revit structure. Other exchange file formats such as dxf, ifc, stp and many more are available for BIM oriented planning.

In the following section, the validation of the RFEM fire design module is presented. Then, the model developed in RFEM to study the fire resistance of steel modular units is described.

3.2 Validation examples

For the validation of the software, multiple examples are worked out in order to determine RFEM's accuracy and reliability. Figure 27 shows a steel structure from which 3 elements are calculated in fire design. These elements are the tie BE, the secondary beam AB and the column GH.

Class 1 cross-sections are assumed and instability phenomena are neglected in the first two examples to simplify the manual calculations. The standard formula for the critical temperature can thus be used to check the fire resistance. In addition, the insulation used in protected elements is considered to be light-weight in the first two examples, which leads to $K_{ins} = \frac{\lambda}{d}$. The modified massivity factor can thus be simplified.
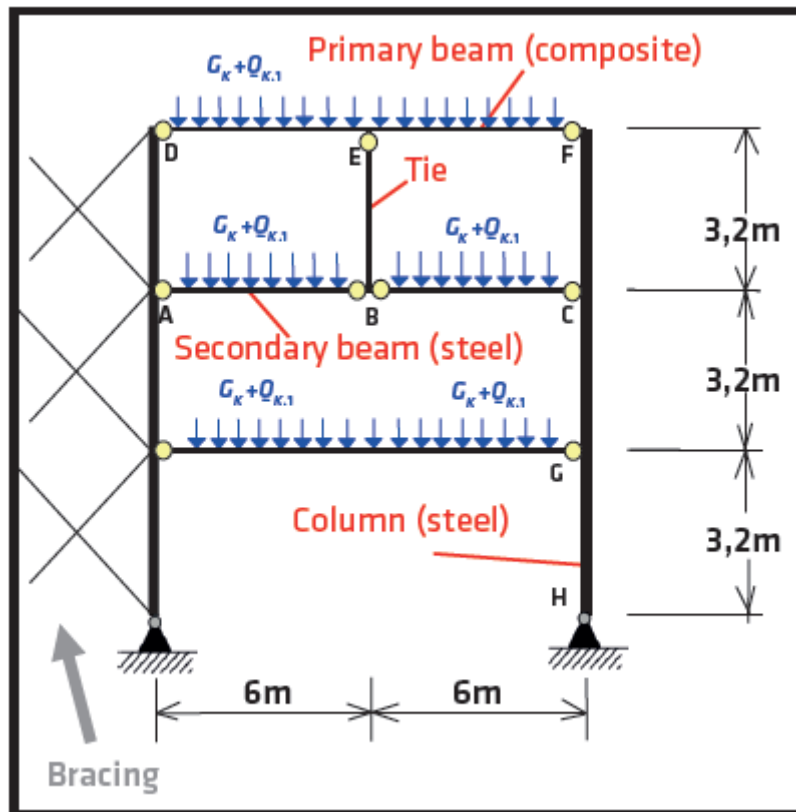
Figure 27: Validation structure. [9]

3.2.1 Tie element BE

The steel tie shown in Figure 28 has a length of 3.2 meters and has an IPE 120 profile. The force on the secondary beams create tension in the tie. For this example, an assumption was made for these forces. The total permanent action is assumed to be 24 kN/m while the total leading variable action is assumed to be 16.8 kN/m.
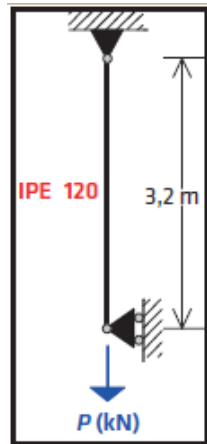
Figure 28: Steel tie, first example. [9]

With these actions, a total load of 345.60 kN is applied on the tie. When the self-weight of the tie is taken into account, a total force of 348.07 kN is applied on the tie. With the following steps a manual calculation has been made for this element. Table 11 shows all parameters used for this example. The calculation is made with Table 12. The calculation of the different parameters and design resistance was performed according to the EN 1993-1-2 [4], which was described is chapter 2.

Table 11: Parameters used for the calculation of the steel tie.

Parameters steel tie	Symbol	Value	Unit	Calculation method
Class cross-section	# 1-4	1	/	Table 7
Permanent load	g_k	24,00	kN/m	Assumed
Variable load	q_k	16,80	kN/m	Assumed
Axial force	F	0,00	kN	Assumed
Permanent safety factor	γ_g	1,35	/	EN1993-1-1
Variable safety factor	γ_q	1,50	/	EN1993-1-1
Height	h	0,12	m	IPE120
Width	b	0,06	m	IPE120
Length	l	3,20	m	IPE120
Buckling length	L_b	2.24	m	IPE120
Buckling length fire	$L_{b,fi}$	2,24	m	0.7*L
Reduction factor	ψ	0,50	/	EN1993-1-1
Thermal conductivity of the fire protection	λ_p	0,20	W/mK	Gypsum boards
Thickness of the fire protection	d_p	40,00	mm	Assumed
Section area	A_s	1320,00	mm²	IPE120
Effective shear area	A_{eff}	1320,00	mm²	IPE120
Steel perimeter	A	459,20	mm	IPE120
Steel perimeter exposed to fire	A_{fi}	459,20	mm	IPE120
Steel perimeter exposed to fire (BOX value)	$A_{fi,b}$	368,00	mm	IPE120
Steel perimeter of fire protection	A_p	368,00	mm	IPE120
Quality of steel	f_y	275,00	Mpa	S275
ULS Safety factor	γ_{M0}	1,00	/	EN1993-1-1
Safety factor in fire situation	$\gamma_{M,fi}$	1,00	/	EN1993-1-2
Self-weight of the beam	ρ	0,10	kN/m	IPE120

The fire resistance to axial load for this element is 363 kN as can be seen in Figure 31. Since the design fire load applied on the tie is equal to 195.79 kN, the degree of utilization can be calculated, which is then used to determine the critical temperature θ_{cr} of the steel tie. Note that for this example the tie is in tension, which means no buckling can occur. This is important as it leads to a simplified method for the determination of θ_{cr}, as explained in chapter 2.

<p style="text-align:center">Table 12: Calculation results for the steel tie.</p>

Calculation parameters	Symbol	Value	Unit	Calculation method
Fire reduction factor	η_{fi}	0,56	/	Equation (2.6.9)
Design loads				
Permanent load	g_d	/	kN	
Variable load	q_d	/	kN	
Total load	P	345,60	kN	Assumed
Axial force	N_{ed}	346,03	kN	P+ρ
Fire situation	$N_{ed,fi}$	194,64	kN	Equation (2.6.5)
Design resistance				
Ambient temperature	$N_{pl,Rd}$	363,00	kN	$\dfrac{A * f_y}{\gamma_{M0}}$
No Fire Protection				
Fire situation	$N_{fi,Rd}$	363,00	kN	Equation (2.6.13)
Degree of utilization	μ_0	0,54	/	Equation (2.6.29)
Critical temperature	θ_{cr}	573,28	°C	Figure 17
Shadow factor	k_{sh}	0,72	/	Equation (2.6.35)
Modified section factor		0,25	/	
With Fire Protection				
Modified massivity factor		1393,94	W/m³K	Equation (2.6.42)

When the critical temperature of the steel tie is obtained, a first evaluation of the R-value of the unprotected tie is possible. The modified section factor is determined after which Annex B is used as follows:

The critical temperature is equal to 572.31°C and the modified section factor is equal to 250m^{-1}. Interpolation in Figure 29 leads to an R-value of 9.8 minutes.

Temperature of unprotected Steel in °C, exposed to the ISO 834 fire curve for different values of $k_{sh}A_m/V$, [m^{-1}]
[Franssen and Vila Real, 2010]

Time [min.]	10 m^{-1}	15 m^{-1}	20 m^{-1}	25 m^{-1}	30 m^{-1}	40 m^{-1}	60 m^{-1}	100 m^{-1}	200 m^{-1}	300 m^{-1}	400 m^{-1}
0	20	20	20	20	20	20	20	20	20	20	20
1	21	22	23	24	24	26	29	34	48	61	73
2	25	27	29	31	33	38	46	62	100	133	162
3	29	33	37	41	45	53	68	97	161	214	259
4	33	40	46	52	59	71	94	136	226	296	351
5	39	48	57	65	74	90	122	178	291	373	430
6	45	57	68	79	90	111	151	221	354	441	494
7	51	66	80	94	108	133	181	265	413	498	545
8	58	76	93	110	126	156	213	308	466	545	584
9	65	86	106	126	144	180	245	351	512	583	615
10	73	97	120	142	164	204	277	392	552	614	640
11	80	108	134	159	183	229	309	432	587	640	660
12	88	119	149	177	204	253	340	469	616	662	678

Figure 29: Evaluation of the temperature of unprotected steel based on the section factor. [9]

This R-value of 9.8 minutes for the unprotected steel tie is much lower than the objective of 60 minutes. Therefore, fire protection needs to be added to the steel member. For this calculation, a fire protection of Gypsum boards is added to the element. This fire protection has a thickness d_p of 40 mm and a thermal conductivity λ_p of 0.2 W/mK. With these values, the modified massivity factor is calculated as shown in Table 12. Using this modified massivity factor of 1393.94 W/m³K, the R-value of the steel tie can again be obtained by using Figure 30, which is derived from the Euro-Nomograms in Annex B.

Note that this figure shows the relation between the R-value and the modified massivity factor of the steel tie, whereas Figure 29 shows the relation between the R-value and the section factor. This can be explained due to the fact that additional fire protection is used which leads to a lower thermal conductivity of the system, meaning that the normal section factor of the steel tie is no longer applicable.

Using the modified massivity factor of 1394 W/m³K and interpolation in Figure 30, an R-value of 60 minutes is obtained.

Temperature of protected steel in °C, exposed to the ISO 834 fire curve for different values of $\frac{A_p}{V}\frac{\lambda_p}{d_p}$, [W/m³K]
[Franssen and Vila Real, 2010]

Time [min.]	100 W/m³K	200 W/m³K	300 W/m³K	400 W/m³K	600 W/m³K	800 W/m³K	1000 W/m³K	1500 W/m³K	2000 W/m³K
0	20	20	20	20	20	20	20	20	20
5	24	27	31	35	41	48	55	71	86
10	29	38	46	54	70	85	100	133	164
15	35	49	62	75	100	123	145	194	237
20	41	61	79	97	130	160	189	251	305
25	47	72	96	118	159	197	231	305	366
30	54	84	113	140	188	232	271	354	421
35	60	97	130	161	216	266	309	400	470
40	67	109	147	181	244	298	346	442	514
45	74	121	163	202	270	329	380	481	554
50	80	133	179	222	296	359	413	516	589
55	87	145	196	241	321	387	443	549	621
60	94	156	211	261	345	414	472	578	650
65	100	168	227	279	368	440	499	606	676
70	107	180	242	298	391	465	525	631	699

Figure 30: Evaluation of the temperature of protected steel based on the modified massivity factor. [9]

These results are compared to the results that are extracted with the software, which leads to the conclusion whether the software is valid or not. The setup for the example made in RFEM is shown in the figures that follow. It is important that all support conditions are exactly the same as the conditions used for the manual calculations, as these can influence the results. A permanent load of 144kN (24kN/m*6m) and a variable load of 100.8kN (16.8kN/m*6m)are applied to simulate the exact forces used in the manual calculations.

Figure 31: RFEM graphic representation of the steel tie.

The unprotected steel tie is verified with RFEM for an R-value of 15 minutes. As can be seen in Table 13, the steel tie does not suffice ($\eta > 1$). This can be explained by looking at the temperature of the steel tie at the required time(Table 14).

Table 13: RFEM design results for the steel tie for R15.

Design results R15	Symbol	Value	Unit	Calculation (EN 1993-1-2)
Axial load	$N_{fi,Ed}$	194.85	kN	
Cross-section area	A	13.21	cm²	
Yield strength	f_y	27.50	kN/cm²	3.2.1
Partial material factor at ambient temperature	γ_{M0}	1.000		6.1
Plastic design resistance	$N_{pl,Rd}$	363.28	kN	(6.6)
Reduction factor for yield strength	$K_{y,\theta}$	0.229		Tab. 3.1
Partial material factor in fire situation	$\gamma_{M,fi}$	1.000		2.3(1)
Fire design resistance	$N_{fi,\theta,Rd}$	83.32	kN	eq. (4.3)
Design ratio	η	2.34		EN 1993-1-2, eq. (4.1)

Table 14: RFEM design parameters for the steel tie for R15.

Fire parameters R15	Symbol	Value	Unit	Calculation (EN1993-1-2)
Required fire resistance	t_{req}	15	min	
Time interval	Δt	5	s	
Fire curve		Standard		
Coefficient for heat flux due to convection	α_c	25.000	W/(m²K)	EN 1991-1-2, 3.2
Coefficient of haze	φ	1.000		
Area radiation of the element	ε_f	0.700		EN 1993-1-2, 2.2
Radiation of the fire	ε_m	1.000		EN 1991-1-2, 3.1(6)
Stefan-Boltzmann constant	σ	5.67×10^{-8}	W/(m²K⁴)	
Self-weight	ρ_a	7850	kg/m³	
Exposure to fire		All sides		
Partial factor for fire situation	$\gamma_{M,fi}$	1.000		
Unprotected section factor	A_m / V	363.361	m⁻¹	EN 1993-1-2, 4.2.5.1(1)
Shadow factor	k_{sh}	0.690		EN 1993-1-2, 4.2.5.1(2)
Gas temperature at required time	$\theta_{g(treq)}$	738.561	°C	EN 1991-1-2, eq. (3.4)
Steel temperature at required time	$\theta_{a(treq)}$	700.541	°C	EN 1993-1-2, eq. (4.25)

This temperature of 700.541°C is much higher than the critical temperature of 573.28°C, which is unacceptable. In addition, this elevated temperature leads to a reduction of the effective yield strength of the steel tie as explained in chapter 2. For this case $k_{y,\theta}$ is equal to 0.229, as shown in Table 13. This value from RFEM corresponds with the values shown in Table 8 in chapter 2. When taking into account this reduction factor, the fire resistance of the steel tie significantly reduces and R15 is not be obtained.

In conclusion, RFEM takes into account all parameters defined in chapter 2 and the manual calculations, leading to a valid result.

Fire protection is now added to the steel tie. Then the steel tie is calculated again, giving the results shown in Table 15 and Table 16.

Table 15: Design parameters for the steel tie for R60.

Fire parameters R60	Symbol	Value	Unit	Formula
Required fire resistance	t_{req}	60	min	
Time interval	Δt	30	s	
Fire curve		Standard		
Coefficient for heat flux due to convection	α_c	25.00	W/(m²K)	EN 1991-1-2, 3.2
Coefficient of haze	φ	1.00		
Area radiation of the element	ε_f	0.70		EN 1993-1-2, 2.2
Radiation of the fire	ε_m	1.00		EN 1991-1-2, 3.1(6)
Stefan-Boltzmann constant	σ	5.67×10^8	W/(m²K⁴)	
Self-weight	ρ_a	7850	kg/m³	
Exposure to fire		All sides		
Partial factor for fire situation	$\gamma_{M,fi}$	1.00		
Type of fire protection		Contour		
Self-weight	ρ_p	800.00	kg/m³	EN 1993-1-2, 4.2.5.2(1)
Heat conductivity	λ_p	0.20	W/K	
Specific heat	c_p	1700.00	J/(kgK)	EN 1993-1-2, 4.2.5.2(1)
Thickness	d_p	40.00	mm	
Protected section factor	A_p / V	363.36	m^{-1}	EN 1993-1-2, 4.2.5.2(1)
Gas temperature at required time	$\theta_{g(treq)}$	945.34	°C	EN 1991-1-2, eq. (3.4)
Steel temperature at required time	$\theta_{a(treq)}$	231.65	°C	EN 1993-1-2, eq. (4.27)

The steel temperature of the member is now 231.65°C at the required time, which means $k_{y,\theta}$ is equal to 1.00. In other words, no reduction of the effective yield strength is required, meaning the fire resistance of the steel tie is not affected by the fire. As a result, the steel tie does obtain an R-value of 60 minutes.

Table 16: RFEM design results for the steel tie for R60.

Design results R60	Symbol	Value	Unit	Calculation (EN1993-1-2)
Axial load	$N_{fi,Ed}$	194.85	kN	
Cross-section area	A	13.21	cm²	
Yield strength	f_y	27.50	kN/cm²	3.2.1
Partial material factor at ambient temperature	γ_{M0}	1.000		6.1
Plastic design resistance	$N_{pl,Rd}$	363.28	kN	(6.6)
Reduction factor for yield strength	$K_{y,\theta}$	1.000		Tab. 3.1
Partial material factor in fire situation	$\gamma_{M,fi}$	1.000		2.3(1)
Fire design resistance	$N_{fi,\theta,Rd}$	363.28	kN	eq. (4.3)
Design ratio	η	0.54		EN 1993-1-2, eq. (4.1)

A summary of all results is given in Table 17 in order to make a comparison between the manual calculations and the results obtained by RFEM. The steel temperature and reduction factor $k_{y,\theta}$ were not calculated in the manual calculations because this was unnecessary. However these values can easily be determined using the same principle applied in the manual calculations. For the unprotected steel tie, the Euro-nomograms from Annex B can be used to obtain the steel temperature. Using the section factor of 250 m^{-1} and a fire resistance of R15, the actual steel temperature is obtained by interpolation. A steel temperature of 695°C is reached. For the protected steel tie the same interpolation method is applied with both a fire resistance of R60 and a modified massivity factor of 1393.94W/m³K. A steel temperature of 555.74°C is obtained. Remarkably, this value is higher than the value obtained by RFEM (231.65°C). This can be explained with the assumptions that have been made in the beginning of this chapter. For the manual calculations, the insulation is considered lightweight, which means the modified massivity factor is simplified and the temperature distribution is assumed to be linear. In reality however, this is not the case. RFEM makes this distinction and a lower steel temperature can thus be obtained.

The reduction factor $k_{y,\theta}$ can then be calculated with Table 8. For the unprotected steel tie, $k_{y,\theta}$ is equal to 0.242. For the protected steel tie, a reduction factor of 1.00 is assumed even though the steel temperature exceeds 400°C. This is again due to the assumption that the insulation is lightweight and the steel temperature is therefore higher than in reality.

Table 17: Comparison of the results obtained by manual calculations and RFEM for the steel tie.

Summary	R15 (Manual)	R60 (Manual)	R15 (RFEM)	R60 (RFEM)
Fire load	346.03 kN	346.03 kN	346.05 kN	346.05 kN
Plastic resistance	363.00 kN	363.00 kN	363.28 kN	363.28 kN
Steel temperature	695.00 °C	555.74 °C	700.541 °C	231.65 °C
$k_{y,\theta}$	0.232	1.00	0.229	1.00
Fire resistance	84.216 kN	363.00 kN	83.32 kN	363.28 kN
Validation	NOK	OK	NOK	OK

3.2.2 Secondary beam AB

The steel member shown in Figure 32 has a length of 6 meters and has an IPE 360 profile. For this example, the same assumption has been made for the acting forces as in the steel tie. The total permanent action is assumed to be 24 kN/m while the total leading variable action is assumed to be 16.8 kN/m. The fire resistance R60 is validated for this example. An additional assumption was made to consider the reduction factor $k_{y,\theta}$ to show once again the influence of this reduction of the effective yield strength of a steel member.
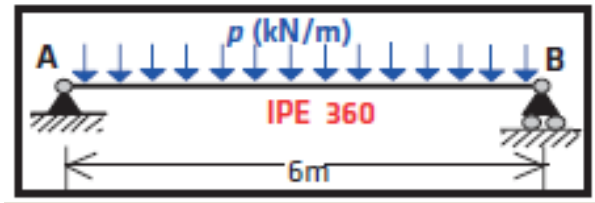
Figure 32: Steel beam, second example. [9]

The parameters used in the manual calculations are shown in Table 18. Due to these loads, a bending moment of 262.67 kNm and a shear load of 175.11 kN are applied on the steel beam.

Table 18: Parameters used for the calculation of the steel beam AB.

Parameters steel beam	Symbol	Value	Unit	Calculation
Class cross-section	# 1-4	1		Table 7
Permanent load	g_k	24,00	kN/m	Assumed
Variable load	q_k	16,80	kN/m	Assumed
Axial force	F	0,00	kN	Assumed
Permanent safety factor	γ_g	1,35		EN1993-1-1
Variable safety factor	γ_q	1,50		EN1993-1-1
Height	h	0,36	m	IPE360
Width	b	0,18	m	IPE360
Length	l	6,00	m	IPE360
Buckling length	L_b	6,00	m	IPE360
Buckling length fire	$L_{b,fi}$	4,00	m	0.7*L
Reduction factor	ψ	0,50		EN1993-1-1
Thermal conductivity of the fire protection	λ_p	0,20	W/mK	Gypsum boards
Thickness of the fire protection	d_p	15,00	mm	Assumed
Section area	A_s	7270,00	mm²	IPE360
Effective shear area	A_{eff}	3514,00	mm²	IPE360
Steel perimeter	A	1142,00	mm	IPE360
Steel perimeter exposed to fire	A_{fi}	1142,00	mm	IPE360
Steel perimeter exposed to fire (BOX value)	$A_{fi,b}$	888,00	mm	IPE360
Steel perimeter of fire protection	A_p	888,00	mm	IPE360
Quality of steel	f_y	275,00	Mpa	S275
ULS Safety factor	γ_{M0}	1,00		EN1993-1-1
Safety factor in fire situation	$\gamma_{M,fi}$	1,00		EN1993-1-2
Self-weight of the beam	ρ	0,57	kN/m	IPE360
Modulus of elasticity	E	210000,00	MPa	IPE360
Moment of inertia	$I_{y,z}$	162700000,00	mm⁴	IPE360
Radius of gyration	i_z	0,05	m	IPE360
Torsional moment of inertia	I_t	59,30		IPE360
Vaulting constant	I_w	17,00		IPE360
Plastic resistance moment	W_{pl}	1,02	m³	IPE360
Elastic resistance moment	W_{el}	0,09	m³	IPE360
Reduction factors for non-uniform temperature distribution	K_1	0,70	0,85	EN1993-1-2
	K_2	1,00		EN1993-1-2

The same principle as with the steel tie is applied in this example. The formulas used to calculate the bending moment resistance and the shear resistance of the steel beam are shown in Table 19. Note that for the shear resistance, the effective shear area of the cross-section is used instead of the full cross-section area. As a result, the shear resistance is reduced significantly to 557.92 kN. As explained in chapter 2, adaptation factors needs to be regarded when calculating the bending moment resistance in order to take into account the non-uniform distribution of the temperature along the cross-section and along the steel beam. This leads to a bending moment resistance of 400.71 kNm. The degree of utilization can then be found by dividing the design bending moment with the bending moment resistance, which gives a result of 0.37. Since instability phenomena are neglected for this example and the cross-section is of class 1, the standard formula can be used to determine the critical temperature. As can be seen, the critical temperature for the unprotected steel beam is equal to 632.34 °C, which is used to evaluate the fire resistance of the steel beam using again the Euro-monograms found in Annex B

Table 19: Calculation of the fire resistance for the steel beam without fire protection.

Calculation parameters	Symbol	Value	Unit	Calculation method
Design load				
Bendig moment	M_{ed}	262,66	kNm	$\left(P + \rho * \gamma_g\right) * \dfrac{l^2}{8}$
Shear load	V_{ed}	175,11	kN	$\left(P + \rho * \gamma_g\right) * \dfrac{l}{2}$
Fire situation	$M_{ed,fi}$	147,75	kNm	$\eta_{fi} * M_{Ed}$
	$V_{ed,fi}$	98,50	kN	$\eta_{fi} * V_{Ed}$
Cross section class control	c/t			
Bending resistance	$M_{pl,Rd}$	280,50	kNm	$\dfrac{W_{pl,y} * f_y}{\gamma_{M0}}$
Shear resistance	$V_{pl,Rd}$	557,92	kN	$\dfrac{A * \dfrac{f_y}{\sqrt{3}}}{\gamma_{M0}}$
No fire protection				
	$M_{fi,20,Rd}$	280,50	kNm	Equation (2.6.24)
	$M_{fi,0,Rd}$	400,71	kNm	Equation (2.6.25)
Degree of utilization	μ_0	0,37		Equation (2.6.29)
Critical temperature	θ_{cr}	632,34	°C	Figure 17
Shadow factor	k_{sh}	0,70		Equation (2.6.35)
Modified section factor		0,11		

A modified section factor of 110 m^{-1} and a critical temperature of 632.34 °C lead to a fire resistance of 17.5 minutes. This is illustrated in Figure 33.

Temperature of unprotected Steel In °C, exposed to the ISO 834 fire curve for different values of $k_{sh}A_m/V$, [m^{-1}] [Franssen and Vila Real, 2010]

Time [min.]	10 m^{-1}	15 m^{-1}	20 m^{-1}	25 m^{-1}	30 m^{-1}	40 m^{-1}	60 m^{-1}	100 m^{-1}	200 m^{-1}	300 m^{-1}	400 m^{-1}
0	20	20	20	20	20	20	20	20	20	20	20
1	21	22	23	24	24	26	29	34	48	61	73
2	25	27	29	31	33	38	46	62	100	133	162
3	29	33	37	41	45	53	68	97	161	214	259
4	33	40	46	52	59	71	94	136	226	296	351
5	39	48	57	65	74	90	122	178	291	373	430
6	45	57	68	79	90	111	151	221	354	441	494
7	51	66	80	94	108	133	181	265	413	498	545
8	58	76	93	110	126	156	213	308	466	545	584
9	65	86	106	126	144	180	245	351	512	583	615
10	73	97	120	142	164	204	277	392	552	614	640
11	80	108	134	159	183	229	309	432	587	640	660
12	88	119	149	177	204	253	340	469	616	662	678
13	97	131	164	195	224	278	372	503	641	680	693
14	105	143	179	213	244	303	402	535	663	695	705
15	114	155	194	231	265	328	432	565	682	708	716
16	122	167	210	249	286	353	460	591	697	718	725
17	131	180	225	268	307	377	487	615	710	727	732
18	140	193	241	286	328	401	513	638	721	733	736
19	150	206	257	305	348	425	538	658	729	737	743

Figure 33: Evaluation of the temperature of unprotected steel based on the section factor. [9]

To achieve a fire resistance of 60 minutes, additional fire protection is required. Since fire protection is used, the adaptation factor k_1 changes to 0.85 as well. This results in a reduction of the bending moment resistance to 329.68 kNm. Thus, the degree of utilization is equal to 0.45 which leads to a critical temperature of 602.07°C, as shown in Table 20. For fire protection, gypsum boards with a thickness of 15 mm and a thermal conductivity of 0.2 W/mK are used, which leads to a modified massivity factor of 1627.94W/m³K, as can be seen.

Table 20: Calculation of the fire resistance of the steel beam with fire protection.

Calculation parameters	Symbol	Value	Unit	Calculation method
With Fire Protection				
	$M_{fi,20,Rd}$	280,50	kNm	Equation (2.6.24)
	$M_{fi,0,Rd}$	330,00	kNm	Equation (2.6.25)
Degree of utilization	μ_0	0,45		Equation (2.6.29)
Critical temperature	θ_{cr}	602,23	°C	Figure 17
Shadow factor	k_{sh}	0,70		
Modified section factor		0,11		
Modified massivity factor		1628,61	W/m³K	Equation (2.6.42)

With this modified massivity factor of 1627.94W/m³K and the critical temperature of 602.07°C, Annex B can again be used to verify if R60 is met. This is illustrated in Figure 34. When interpolation is used, the steel temperature at 60 minutes is equal to 597°C, which is lower than the critical temperature. The requirement R60 is therefore achieved.

Temperature of protected steel in °C, exposed to the ISO 834 fire curve for different values of $\frac{A_p}{V}\frac{\lambda_p}{d_p}$, [W/m³K]
[Franssen and Vila Real, 2010]

Time [min.]	100 W/m³K	200 W/m³K	300 W/m³K	400 W/m³K	600 W/m³K	800 W/m³K	1000 W/m³K	1500 W/m³K	2000 W/m³K
0	20	20	20	20	20	20	20	20	20
5	24	27	31	35	41	48	55	71	86
10	29	38	46	54	70	85	100	133	164
15	35	49	62	75	100	123	145	194	237
20	41	61	79	97	130	160	189	251	305
25	47	72	96	118	159	197	231	305	366
30	54	84	113	140	188	232	271	354	421
35	60	97	130	161	216	266	309	400	470
40	67	109	147	181	244	298	346	442	514
45	74	121	163	202	270	329	380	481	554
50	80	133	179	222	296	359	413	516	589
55	87	145	196	241	321	387	443	549	621
60	94	156	211	261	345	414	472	578	650
65	100	168	227	279	368	440	499	606	676
70	107	180	242	298	391	465	525	631	699

Figure 34: Evaluation of the temperature of protected steel based on the modified massivity factor. [9]

Now this example is simulated in RFEM and the results are compared. The situation is shown in Figure 35.
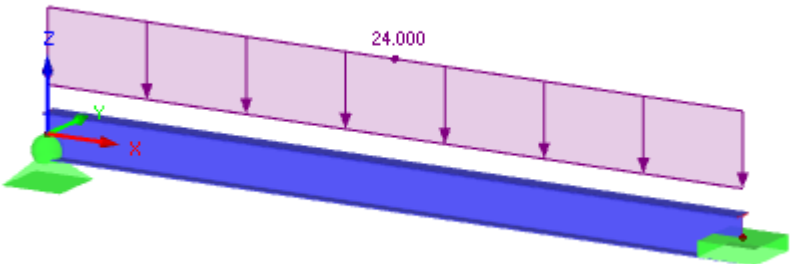
Figure 35: RFEM graphic representation of the second example.

The fire parameters obtained from RFEM are shown in Table 21. The temperature of the steel beam at 60 minutes is lower than the critical temperature of 602°C. Note that this was said to be sufficient in the manual calculations. However, as shown in Table 22, the steel beam does not attain a fire resistance of R60.

Table 21: RFEM design parameters for the steel beam for R60.

Fire parameter R60	Symbol	Value	Unit	Calculation method
Required fire resistance	t_{req}	60	min	
Time interval	Δt	30	s	
Fire curve		Standard		
Coefficient for heat flux due to convection	α_c	25.000	W/(m²K)	EN 1991-1-2, 3.2
Coefficient of haze	φ	1.000		
Area radiation of the element	ε_f	0.700		EN 1993-1-2, 2.2
Radiation of the fire	ε_m	1.000		EN 1991-1-2, 3.1(6)
Stefan-Boltzmann constant	σ	5.67×10^{-8}	W/(m²K⁴)	
Self-weight	ρ_a	7850	kg/m³	
Exposure to fire		All sides		
Partial factor for fire situation	$\gamma_{M,fi}$	1.000		
Type of fire protection		Casing		
Self-weight	ρ_p	800.000	kg/m³	EN 1993-1-2, 4.2.5.2(1)
Heat conductivity	λ_p	0.200	W/K	
Specific heat	c_p	1700.000	J/(kgK)	EN 1993-1-2, 4.2.5.2(1)
Thickness	d_p	15.000	mm	
Protected section factor	A_p / V	145.745	m⁻¹	EN 1993-1-2, 4.2.5.2(1)
Gas temperature at required time	$\theta_{g(treq)}$	945.340	°C	EN 1991-1-2, eq. (3.4)
Steel temperature at required time	$\theta_{a(treq)}$	584.068	°C	EN 1993-1-2, eq. (4.27)

Table 22: RFEM design results for the steel beam for R60.

Design results steel beam	Symbol	Value	Unit	Calculation (EN1993-1-2)
Design moment	$M_{fi,y,Ed}$	259.27	kNm	
Plastic moment resistance	$W_{pl,y}$	1019.00	cm³	
Yield strength	f_y	27.50	kN/cm²	3.2.1
Partial material factor at ambient temperature	γ_{M0}	1.00		6.1
Design resistance	$M_{pl,y,Rd}$	280.23	kNm	eq. (6.13)
Design shear load	$V_{fi,z,Ed}$	218.32	kN	
Effective shear area	$A_{v,z}$	35.14	cm²	6.2.6(3)
Design shear resistance	$V_{pl,z,Rd}$	557.89	kN	eq. (6.18)
Unity check $V_{fi,z,Ed} / V_{pl,z,Rd}$	$v_{fi,z}$	0.391		6.2.8(2)
Reduction factor	$k_{y,\theta}$	0.519		Tab. 3.1
Material factor	$\gamma_{M,fi}$	1.000		2.3(1)
Moment resistance	$M_{fi,y,\theta,Rd}$	145.55	kNm	eq. (4.8)
U.C.-waarde	η	1.78		EN 1993-1-2, eq. (4.1)

As explained in the beginning of this chapter, yield strength reduction and elastic modulus reduction, due to elevated temperatures, are not considered in this example. This shows the influence of these reduction factors. While the manual calculations resulted in a fire resistance of R60 for this element, it is shown in RFEM that due to the elevated temperatures, this value cannot be achieved because of the yield strength reduction $k_{y,\theta}$ which is equal to 0.454. The resistance moment decreases due to this reduction, which leads to an increase in degree of utilization μ_0. This in turn causes the critical temperature to drop dramatically. When evaluating the heating of the element, a significant increase in the design of the fire protection is necessary to lower the surface temperature of the element below the critical temperature. This is illustrated in example 3, where instability phenomena are also included in the analysis for a more elaborate result.

A summary for this example is given in Table 23.

Table 23: Comparison of the results obtained by manual calculations and RFEM for the steel beam AB.

Summary	R60 (Manual)	R60 (RFEM)
Bending moment	262 kN	259.27 kN
Shear load	175 kN	218.32 kN
Bending resistance	280.5 kNm	280.23 kNm
Shear resistance	557.92 kN	557.89 kN
Critical temperature	602°C	602°C
Steel temperature	597°C	584°C
Reduction factor $k_{y,\theta}$	1	0.454
Fire resistance	280.5 kNm	127.11 kNm
Validation	OK	NOK

When reductions in yield strength would be taken into account in the manual calculations, the following result was achieved:

Table 24: Results for the steel beam AB with yield strength reductions.

Summary	R60 (Manual)	R60 (RFEM)
Bending moment	262 kN	259.27 kN
Shear load	175 kN	218.32 kN
Bending resistance	280.5 kNm	280.23 kNm
Shear resistance	557.92 kN	557.89 kN
Critical temperature	602°C	602°C
Steel temperature	597°C	584°C
Reduction factor $k_{y,\theta}$	0.471	0.454
Fire resistance	132.116	127.11 kNm
Validation	NOK	NOK

This shows that RFEM provides valid results and takes into account all influencing factors for the design of steel members in fire situation.

3.2.3 Column GH

For the example shown in Figure 36, instability manifestations are included for a more elaborate fire resistance calculation. The cross section is still classified as class 1. In contrast to the first two examples, instability phenomena are taken into consideration. All design parameters for this example are shown in Table 25.
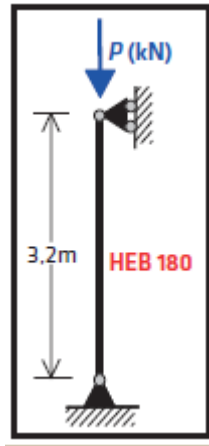
Figure 36: Steel column, third example. [9]
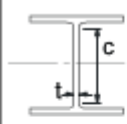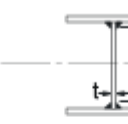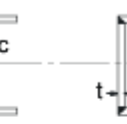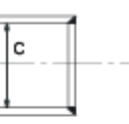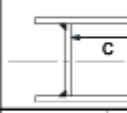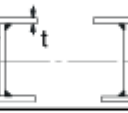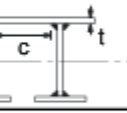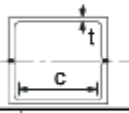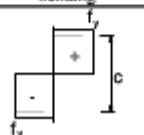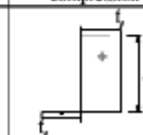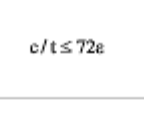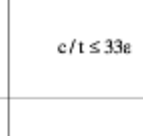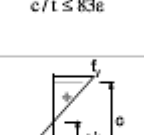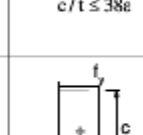
Table 25: Parameters used for the calculation of the steel column GH.

Parameters steel beam	Symbol	Value	Unit	Calculation
Class cross-section	# 1-4	1		Table 7
Permanent load	g_k	24,00	kN/m	Assumed
Variable load	q_k	16,80	kN/m	Assumed
Axial force	F	1057,50	kN	Assumed
Permanent safety factor	γ_g	1,35		EN1993-1-1
Variable safety factor	γ_q	1,50		EN1993-1-1
Height	h	0,18	m	HEB180
Width	b	0,18	m	HEB180
Length	l	3,20	m	HEB180
Buckling length	L_b	3,20	m	HEB180
Buckling length fire	$L_{b,fi}$	2,24	m	0.7*L
Reduction factor	ψ	0,50		EN1993-1-1
Thermal conductivity of the fire protection	λ_p	0,20	W/mK	Gypsum boards
Thickness of the fire protection	d_p	15,00	mm	Assumed
Section area	A_s	6530,00	mm²	HEB180
Effective shear area	A_{eff}	6530,00	mm²	HEB180
Steel perimeter	A	1015,00	mm	HEB180
Steel perimeter exposed to fire	A_{fi}	1015,00	mm	HEB180
Steel perimeter exposed to fire (BOX value)	$A_{fi,b}$	720,00	mm	HEB180
Steel perimeter of fire protection	A_p	720,00	mm	HEB180
Quality of steel	f_y	275,00	Mpa	S275
ULS Safety factor	γ_{M0}	1,00		EN1993-1-1
Safety factor in fire situation	$\gamma_{M,fi}$	1,00		EN1993-1-2
Self-weight of the beam	ρ	0,51	kN/m	HEB180
Modulus of elasticity	E	210000,00	MPa	HEB180
Moment of inertia	$I_{y,z}$	38130000,00	mm⁴	HEB180
Radius of gyration	iz	0.05	m	HEB180
Torsional moment of inertia	I_t	42,16		HEB180
Vaulting constant	I_w	93750,00		HEB180
Plastic resistance moment	W_{pl}	0,48	m³	HEB180
Elastic resistance moment	W_{el}	0,23	m³	HEB180
Reduction factors for non-uniform temperature distribution	K_1	0,70	0,85	EN1993-1-2
	K_2	1,00		EN1993-1-2

As mentioned earlier, the occurrence of instability is taken into account. On top of that, the standard formula for calculating the critical temperature is no longer applicable, as explained in chapter 2. The critical temperatures have to be obtained by using the figures from Annex A. Next, the manual calculation is made with an Excel sheet.

First the cross-section are classified using Table 26. Since c_f is equal to 70.8mm and t_f is equal to 14mm, the ratio c_f/t_f is equal to 5.057, which is lower than the required value of $33\varepsilon = 25.94$ for parts subject to compression. For the web, c_w and t_w are respectively equal to 122mm and 8.5mm which gives a ratio c_w/t_w of 14.35, which is also lower than 25.94. Thus, the flange and web are both classified as class 1 so the cross-section is class 1.

Table 26: Cross-section classification. [7]

		Internal compression parts		

Class	Part subject to bending	Part subject to compression	Part subject to bending and compression		
Stress distribution in parts (compression positive)					
1	$c/t \leq 72\varepsilon$	$c/t \leq 33\varepsilon$	when $\alpha > 0,5$: $c/t \leq \dfrac{396\varepsilon}{13\alpha-1}$ when $\alpha \leq 0,5$: $c/t \leq \dfrac{36\varepsilon}{\alpha}$		
2	$c/t \leq 83\varepsilon$	$c/t \leq 38\varepsilon$	when $\alpha > 0,5$: $c/t \leq \dfrac{456\varepsilon}{13\alpha-1}$ when $\alpha \leq 0,5$: $c/t \leq \dfrac{41,5\varepsilon}{\alpha}$		
Stress distribution in parts (compression positive)					
3	$c/t \leq 124\varepsilon$	$c/t \leq 42\varepsilon$	when $\psi > -1$: $c/t \leq \dfrac{42\varepsilon}{0,67 + 0,33\psi}$ when $\psi \leq -1^{*}$: $c/t \leq 62\varepsilon(1-\psi)\sqrt{(-\psi)}$		
$\varepsilon = \sqrt{235/f_y}$	f_y	235	275	355	420	460
	ε	1,00	0,92	0,81	0,75	0,71

*) $\psi \leq -1$ applies where either the compression stress $\sigma \leq f_y$ or the tensile strain $\varepsilon_y > f_y/E$

As displayed in Table 27, the axial force that is applied on the column is equal to 1059.71kN and the design resistance to axial loads is equal to 1795.75kN. The buckling resistance is be calculated by integrating the reduction factor χ. To find this reduction factor, the slenderness has to be calculated as shown in Figure 49. Note that ε is not yet reduced by a factor 0.85 due to fire because this buckling resistance is first calculated at ambient temperature. The buckling length equals 0.7*L for this case since one end of the column is fixed and one end is hinged. This length is thus equal to 0.7*3.2m = 2.24m. The relative slenderness is then equal to 0.56. Next, the buckling curve has to be determined in order to obtain an value for the imperfection factor α. This is done by following the instructions in Table 29. Since the height of the HEB profile is equal to the width of the profile, h/b is smaller than 1.2 and with t_f <100, buckling curve c is obtained for buckling around the weak axis z. The imperfection factor α is thus equal to 0.49, which leads to φ being equal to 0.75. χ can then be calculated and is equal to 0.81. The buckling resistance of the column is now equal to 1447.59kN. The column can resist to buckling at ambient temperature. However, fire design still needs to be checked.
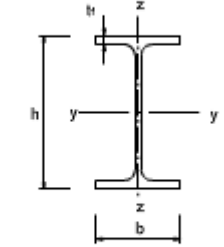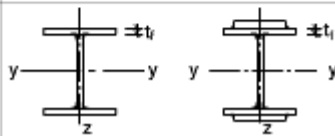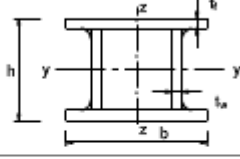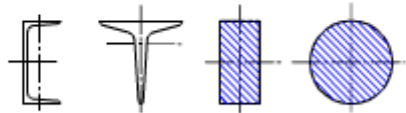
Table 27: Calculation of the design resistance of the steel column at ambient temperature.

Calculation parameters	Symbol	Value	Unit	Calculation method
Fire reduction factor	η_{fi}	0,56		
Design loads				
Permanent load	g_d	/	kN	
Variable load	q_d	/	kN	
Total load	P	1057,50	kN	Assumed
Axial force	N_{ed}	1059,70	kN	P+ρ
Fire situation	$N_{ed,fi}$	596,08	kN	$\eta_{fi} * N_{Ed}$
Design resistance				
Ambient temperature				
Design resistance	$N_{b,Rd}$	1795,75	kN	$\dfrac{A * f_y}{\gamma_{M0}}$

Calculation parameters	Symbol	Value	Unit	Calculation method
Buckling at ambient temperature				
Slenderness	λ	49,02		Equation (2.6.21)
	ε	0,92		Equation (2.6.23)
	λ_1	86,80		Equation (2.6.22)
Relative slenderness	$\bar{\lambda}$	0,56		Equation (2.6.20)
Choose Alfa	φ	0,75		$0.5[1 + \alpha(\bar{\lambda} - 0.2) + \bar{\lambda}^2]$
	χ	0,81		$\chi = \dfrac{1}{\phi + \sqrt{\phi^2 - \bar{\lambda}^2}}$
Buckling resistance	$N_{b,Rd}$	1447,59	kN	$N_{b,Rd} = \chi * N_{pl,Rd}$

Table 29: Selection of buckling curve for a cross-section. [7]

First, a fire resistance of R15 needs to be verified for the steel column. In fire situation, ε is reduced by a factor 0.85. As a result, the relative slenderness increases to 0.66. The imperfection factor α and the reduction factor φ is now also calculated differently, as can be seen in Table 30. These changes lead to a reduction of χ to 0.64, which in turn causes the resistance to buckling to decrease to 1153.29kN. The reduction factors for the effective yield strength and the elastic modulus of steel due to the fire now need to be taken into account. In order to do this, the steel temperature at t = 15 minutes has to be obtained. For R15, the calculations are simple since the steel temperature can be directly derived by using figures from Annex B and the corresponding section factor. The section factor for this steel column is equal to 99m^{-1}. The steel temperature, extracted from Annex B, is then equal to 565°C. This is illustrated in Figure 37. For a temperature of 565°C, a reduction factor $k_{y,\theta}$ of 0.578 is obtained from Table 8. Thus, the fire design resistance for the column is equal to 666 kN. This is higher than the fire load of 596 kN while the temperature of the steel column is lower than the critical temperature of 579.3°C. The column is therefore verified for R15.

Temperature of unprotected Steel in °C, exposed to the ISO 834 fire curve for different values of $k_{sh}A_m/V$, [m^{-1}]
[Franssen and Vila Real, 2010]

Time	10	15	20	25	30	40	60	100	200	300	400
[min.]	m^{-1}	m^{-1}	m^{-1}	m^{-1}	m^{-1}	m^{-1}	m^{-1}	m^{-1}	m^{-1}	m^{-1}	m^{-1}
0	20	20	20	20	20	20	20	20	20	20	20
1	21	22	23	24	24	26	29	34	48	61	73
2	25	27	29	31	33	38	46	72	100	133	162
3	29	33	37	41	45	53	68	107	161	214	259
4	33	40	46	52	59	71	94	146	226	296	351
5	39	48	57	65	74	90	122	188	291	373	430
6	45	57	68	79	90	111	151	231	354	441	494
7	51	66	80	94	108	133	181	275	413	498	545
8	58	76	93	110	126	156	213	318	466	545	584
9	65	86	106	126	144	180	245	361	512	583	615
10	73	97	120	142	164	204	277	402	552	614	640
11	80	108	134	159	183	229	309	442	587	640	660
12	88	119	149	177	204	253	340	479	616	662	678
13	97	131	164	195	224	278	372	513	641	680	693
14	105	143	179	213	244	303	402	545	663	695	705
15	114	155	194	231	265	328	432	565	682	708	716
16	122	167	210	249	286	353	460	591	697	718	725

Figure 37: Evaluation of the temperature of unprotected steel column based on the section factor. [9]

Calculation parameters	Symbol	Value	Unit	Calculation method
No Fire Protection				
Slenderness fire situation	λ	49,02		
	ε	0,79		
	λ_1	73,78		
Relative slenderness	$\bar{\lambda}$	0,66		
For t = 0 $$\sqrt{[\frac{k_{y,\theta}}{k_{E,\theta}}]} = \sqrt{\frac{1}{1}}$$	$\bar{\lambda}_\theta$	0,66		$\bar{\lambda}\sqrt{[\frac{k_{y,\theta}}{k_{E,\theta}}]}$
Imperfection factor	α	0,60		$0.65\sqrt{\frac{235}{f_y}}$
	φ	0,92		$0.5[1 + \alpha\bar{\lambda}_\theta + \bar{\lambda}_\theta{}^2]$
	X_{fi}	0,64		$\dfrac{1}{\phi_\theta + \sqrt{\phi_\theta{}^2 - \bar{\lambda}_\theta{}^2}}$
Fire design resistance	$N_{b,fi,0,Rd}$	1153,29	kN	$\chi_{fi}\dfrac{A * f_y}{\gamma_{M0}}$
Degree of utilization	μ_0	0,52		$\dfrac{N_{Ed,fi}}{N_{b,fi,0,Rd}}$
Critical temperature	θ_{cr}	579,30	°C	Figure 17

Next, R60 is verified for the column. Since the goal of this example is to have a more elaborate validation of the software, the modified massivity factor cannot simply be calculated with the protected section facto and the thermal properties of the insulation. This results in a modified massivity factor of 1470. Otherwise, the same problem as in example one would occur, where the temperature of the steel column would be much lower in RFEM than the temperature calculated manually. Therefore equations 5.8.11 and 5.8.12 from chapter 2 is used to evaluate the steel temperature of the column over time. In this evaluation, not only the thermal properties of the insulation are taken into account, but also the thermal properties of the steel column. As explained in chapter 2, this results in a much more realistic distribution of temperature through the insulation. When using Gypsum boards as a case protection with a thickness of 15mm while evaluating R60, a modified massivity factor of 1231.13 W/m³K is obtained. The steel temperature can then be extracted using the same principle as in the previous examples. A temperature of 521.9°C is obtained as illustrated in Figure 38.

Temperature of protected steel in °C, exposed to the ISO 834 fire curve for different values of $\frac{A_p}{V}\frac{\lambda_p}{d_p}$, [W/m²K]
[Franssen and Villa Real, 2010]

Time [min.]	100 W/m³K	200 W/m³K	300 W/m³K	400 W/m³K	600 W/m³K	800 W/m³K	1000 W/m³K	1500 W/m³K	2000 W/m³K
0	20	20	20	20	20	20	20	20	20
5	24	27	31	35	41	48	55	71	86
10	29	38	46	54	70	85	100	133	164
15	35	49	62	75	100	123	145	194	237
20	41	61	79	97	130	160	189	251	305
25	47	72	96	118	159	197	231	305	366
30	54	84	113	140	188	232	271	354	421
35	60	97	130	161	216	266	309	400	470
40	67	109	147	181	244	298	346	442	514
45	74	121	163	202	270	329	380	481	554
50	80	133	179	222	296	359	413	516	589
55	87	145	195	241	321	387	443	549	621
60	94	156	211	261	345	414	472	578	650
65	100	168	227	279	368	440	499	606	676

Figure 38: Evaluation of the temperature of protected steel based on the modified massivity factor. [9]

For this temperature, the reduction factors for the yield strength and the elastic modulus are respectively equal to 0.712 and 0.538, calculated by interpolation of Table 8. This is illustrated in Figure 39 .The resistance of the column is reduced further by these factors. The final buckling resistance in fire situation for this column is equal to 821.142kN while the surface temperature of the steel column is lower than the critical temperature. This means the column realises a fire resistance of R60.

Steel temperature θ_a	Reduction factors at temperature θ_a relative to the value of f_y or E_a at 20 °C		
	Reduction factor (relative to f_y) for effective yield strength $k_{y,\theta} = f_{y,\theta}/f_y$	Reduction factor (relative to f_y) for proportional limit $k_{p,\theta} = f_{p,\theta}/f_y$	Reduction factor (relative to E_a) for the slope of the linear elastic range $k_{E,\theta} = E_{a,\theta}/E_a$
20 °C	1,000	1,000	1,000
100 °C	1,000	1,000	1,000
200 °C	1,000	0,807	0,900
300 °C	1,000	0,613	0,800
400 °C	1,000	0,420	0,700
500 °C	0,780	0,360	0,600
600 °C	0,470	0,180	0,310
700 °C	0,230	0,075	0,130
800 °C	0,110	0,050	0,090
900 °C	0,060	0,0375	0,0675
1000 °C	0,040	0,0250	0,0450
1100 °C	0,020	0,0125	0,0225
1200 °C	0,000	0,0000	0,0000

NOTE: For intermediate values of the steel temperature, linear interpolation may be used.

Figure 39: Reduction factors at temperature θ_a to the yield strength and elastic modulus.

The validation of the column by the software RFEM is shown next. The setup for this example is shown in Figure 40.

Figure 40: RFEM graphic representation of the column GH.

First, fire stability R15 is again checked with RFEM. The parameters for this example are shown in Table 31. A section factor of 159.4m^{-1} is obtained. With a shadow factor of 0.623, this section factor is modified to 99.3m^{-1}. Additionally, the steel temperature at t=15 minutes is equal to 565.241°C.

Table 31: RFEM design parameters for the steel column GH for R15.

Fire parameters R15	Symbol	Value	Unit	Calculation method
Required fire resistance	t_{req}	15	min	
Time interval	Δt	5	s	
Fire curve		Standard		
Coefficient for heat flux due to convection	α_c	25.00	W/(m²K)	EN 1991-1-2, 3.2
Coefficient of haze	φ	1.00		
Area radiation of the element	ε_f	0.70		EN 1993-1-2, 2.2
Radiation of the fire	ε_m	1.00		EN 1991-1-2, 3.1(6)
Stefan-Boltzmann constant	σ	$5.67\text{x}10^{-8}$	W/(m²K⁴)	
Self-weight	ρ_a	7850	kg/m³	
Exposure to fire		All sides		
Partial factor for fire situation	$\gamma_{M,fi}$	1.00		
Unprotected section factor	A_m / V	159.387	m^{-1}	EN 1993-1-2, 4.2.5.1(1)
Shadow factor	k_{sh}	0.623		EN 1993-1-2, 4.2.5.1(2)
Gas temperature at required time	$\theta_{g(treq)}$	738.561	°C	EN 1991-1-2, eq. (3.4)
Steel temperature at required time	$\theta_{a(treq)}$	565.241	°C	EN 1993-1-2, eq. (4.25)

With this steel temperature, a reduction factor $k_{y,\theta}$ of 0.578 is obtained. This leads to a fire design resistance of 662.89 kN, as shown in Table 32. This is higher that the fire load of 596.21kN, while the temperature is again lower than the critical temperature. This means the column is verified for R15 by RFEM.

Table 32: RFEM design results for the steel column GH for R15.

Design results R15	Symbol	Value	Unit	Calculation (EN1993-1-2)
Modulus of elasticity	E	21000.0	kN/cm²	
Moment of inertia	I_z	1363.0	cm^4	
Buckling length	$L_{cr,z}$	2.240	m	
Critical load	$N_{cr,z}$	5630.14	kN	
Cross-section area	A	65.25	cm²	
Yield strength	f_y	27.50	kN/cm²	3.2.1
Slenderness	λ_z	0.565		
Reduction factor for the yield strength	$k_{y,\theta}$	0.578		Tab. 3.1
Reduction factor for the elastic modulus	$k_{E,\theta}$	0.411		EN 1993-1-2, Tab. 3.1
Slenderness in fire situation	$\lambda_{z,\theta}$	0.670		EN 1993-1-2, eq. (4.7)
Compression force	$N_{fi,Ed}$	596.21	kN	
Imperfection factor	α	0.601		EN 1993-1-2, 4.2.3.2(2)
Extra factor	$\varphi_{z,\theta}$	0.925		EN 1993-1-2, 4.2.3.2(2)
Reduction factor	$\chi_{z,fi}$	0.639		EN 1993-1-2, eq. (4.6)
Partial material factor	$\gamma_{M,fi}$	1.000		2.3(1)
Buckling resistance	$N_{b,fi,z,\theta,Rd}$	662.89	kN	EN 1993-1-2, eq. (4.5)
Design ratio	η	0.90		EN 1993-1-2, eq. (4.1)

Next, fire stability R60 is checked in RFEM. The fire parameters for this example are shown in Table 33. As can be seen, the steel temperature of the column reaches 521.946°C when gypsum board case insulation with a thickness of 15mm is used.

Table 33: RFEM design parameters for the steel column GH for R60.

Fire parameter R60	Symbol	Value	Unit	Calculation (EN1993-1-2)
Required fire resistance	t_{req}	60	min	
Time interval	Δt	30	s	
Fire curve		Standard		
Coefficient for heat flux due to convection	α_c	25.00	W/(m²K)	EN 1991-1-2, 3.2
Coefficient of haze	φ	1.00		
Area radiation of the element	ε_f	0.700		EN 1993-1-2, 2.2
Radiation of the fire	ε_m	1.000		EN 1991-1-2, 3.1(6)
Stefan-Boltzmann constant	σ	5.67×10^{-8}	W/(m²K^4)	
Self-weight	ρ_a	7850	kg/m³	
Exposure to fire		All sides		
Partial factor for fire situation	$\gamma_{M,fi}$	1.000		
Type of fire protection		Casing		
Self-weight	ρ_p	800.000	kg/m³	EN 1993-1-2, 4.2.5.2(1)
Heat conductivity	λ_p	0.200	W/K	
Specific heat	c_p	1700.000	J/(kgK)	EN 1993-1-2, 4.2.5.2(1)
Thickness	d_p	15.000	mm	
Protected section factor	A_p / V	110.345	m^{-1}	EN 1993-1-2, 4.2.5.2(1)
Gas temperature at required time	$\theta_{g(treq)}$	945.340	°C	EN 1991-1-2, eq. (3.4)
Steel temperature at required time	$\theta_{a(treq)}$	521.946	°C	EN 1993-1-2, eq. (4.27)

The design results provided by RFEM are then shown in Table 34. The buckling resistance in fire situation for the column is equal to 830.11kN, which is higher than 596.21kN. Therefore the column has obtained a fire resistance of R60.

Table 34: RFEM design results for the steel column GH for R60.

Design results R60	Symbol	Value	Unit	Calculation (EN1993-1-2)
Modulus of elasticity	E	21000.0	kN/cm²	
Moment of inertia	I_z	1363.0	cm^4	
Buckling length	$L_{cr,z}$	2.240	m	
Critical load	$N_{cr,z}$	5630.14	kN	
Cross-section area	A	65.25	cm²	
Yield strength	f_y	27.50	kN/cm²	3.2.1
Slenderness	λ_z	0.565		
Reduction factor for the yield strength	$k_{y,\theta}$	0.712		Tab. 3.1
Reduction factor for the elastic modulus	$k_{E,\theta}$	0.536		EN 1993-1-2, Tab. 3.1
Slenderness in fire situation	$\lambda_{z,\theta}$	0.650		EN 1993-1-2, verg. (4.7)
Compression force	$N_{fi,Ed}$	596.21	kN	
Imperfection factor	α	0.601		EN 1993-1-2, 4.2.3.2(2)
Extra factor	$\varphi_{z,\theta}$	0.907		EN 1993-1-2, 4.2.3.2(2)
Reduction factor	$\chi_{z,fi}$	0.650		EN 1993-1-2, verg. (4.6)
Partial material factor	$\gamma_{M,fi}$	1.000		2.3(1)
Buckling resistance	$N_{b,fi,z,\theta,Rd}$	830.11	kN	EN 1993-1-2, verg. (4.5)
Design ratio	η	0.72		EN 1993-1-2, verg. (4.1)

A summary of the results is shown in Table 35 and Table 36.

Table 35: Comparison of the results for R15 obtained by manual calculations and RFEM for the steel column GH.

Summary	R15 (Manual)	R15 (RFEM)
Fire load	596.08 kN	596.21 kN
Buckling length	2.24 m	2.24 m
Relative slenderness at ambient temperature	0.56	0.565
Steel temperature at 15 minutes	565°C	565.241°C
Reduction factor $k_{y,\theta}$	0.578	0.578
Reduction factor $k_{E,\theta}$	0.411	0.411
Relative slenderness at 15 minutes	0.67	0.67
Imperfection factor α	0.60	0.601
Reduction factor φ	0.92	0.925
Reduction factor χ	0.64	0.639
Fire design resistance	666 kN	662.89 kN
Validation	OK	OK

Table 36: Comparison of the results for R60 obtained by manual calculations and RFEM for the steel column GH.

Summary	R60 (Manual)	R60 (RFEM)
Fire load	596.08 kN	596.21 kN
Buckling length	2.24 m	2.24 m
Relative slenderness at ambient temperature	0.56	0.565
Steel temperature at 60 minutes	521.9°C	521.946°C
Reduction factor $k_{y,\theta}$	0.712	0.712
Reduction factor $k_{E,\theta}$	0.538	0.536
Relative slenderness at 60 minutes	0.66	0.65
Imperfection factor α	0.60	0.601
Reduction factor φ	0.92	0.907
Reduction factor χ	0.64	0.65
Fire design resistance	821.142 kN	830.11 kN
Validation	OK	OK

From the comparison of these three manual calculations with their respective calculations in RFEM can be concluded that the software is valid. Even the reduction factors for the yield strength and the elastic modulus, due to elevated temperatures, are taken into account by RFEM, which again guarantees a safe calculation for the fire resistance of steel elements. This means that various models can now be calculated with the software.

3.3 The RFEM Model of modular units
3.3.1 CBZ modular units

For the present research, one single unit was modelled in the 3D finite element analysis software RFEM. The calculations executed for the study are all preformed on this single unit shown in Figure 41. The unit is constructed out of twelve essential steel elements. These form the main structural components of the unit.
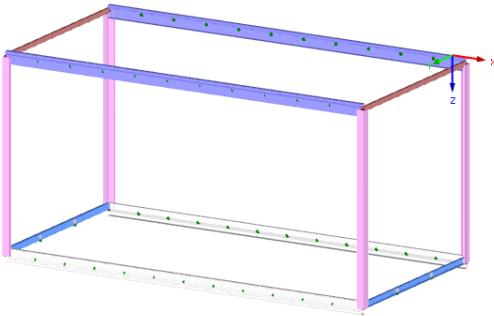
Figure 41: RFEM single unit.

The model used in the RFEM-software is a simplified version of the constructed unit. The twelve main structural elements, forming the skeleton of the model, are recreated in the software. These elements carry the major part of the loads applied onto the model. These elements are bolted together, resulting in a fixed connection between the most important structural elements. The structure of the roof is simplified, to the basic elements, the steel beams. The same simplification is used to reproduce the floor. Only the steel grid of the floor is recreated in to design the structure in the design software. Both the floor and roof profiles can be seen in Figure 43 and Figure 44.

The floor of a unit is constructed with a grid of steel beams. In between the steel elements a layer of 80mm of rock wool insulation is placed. On top of the elements two grids of wooden beams of 60mmx40mm are bolted on top of the steel structure of the floor. Between these wooden beams there is another layer of PUR. On top of the wooden grid a 22mm fibreboard is placed. This is shown in Figure 42. For the designs model in RFEM, the wooden structure is left out.
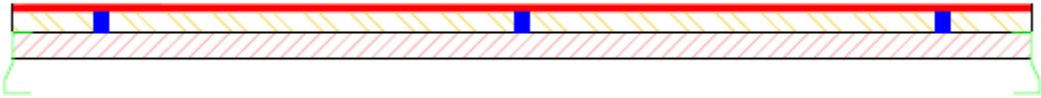
Figure 42: Floor profile of the model.
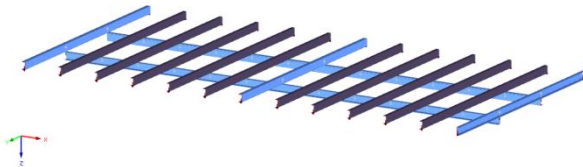
Figure 43: RFEM floor profile.

85

The roof is constructed with steel beams as shown in Figure 44.

Figure 44: RFEM roof profile.

The wall consist of a steel frame as in Figure 44. welded into the steel structure. Onto this frame, wooden beams of 40mmx20mm are attached, this time in three layers. This is shown in Figure 46. In between the beams 160mm of rock wool is placed as insulation. On top of the wooden web, a steel sheet is bolted as facade finishing.
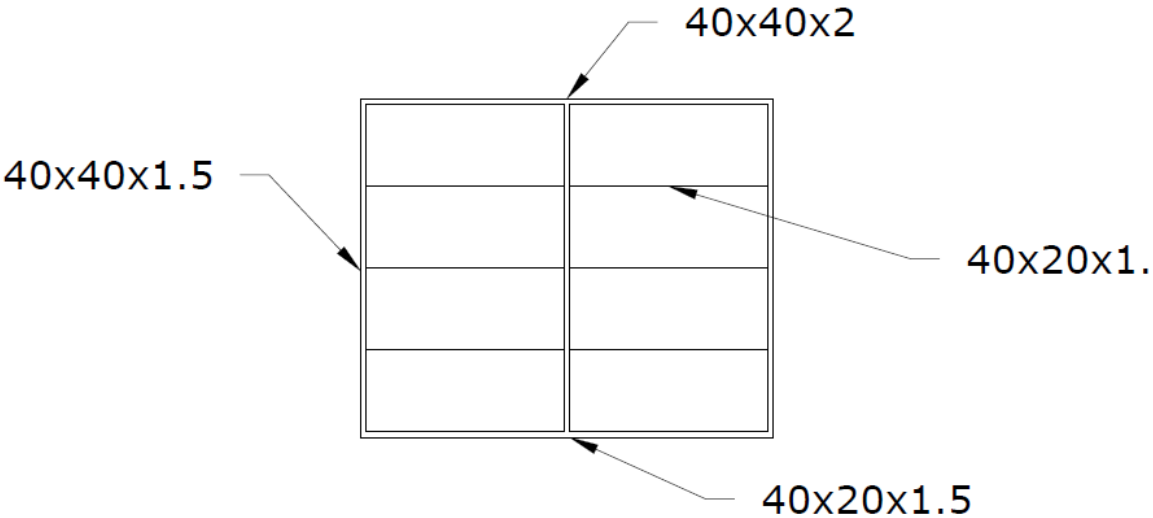
Figure 45: Steel frame welded onto the steel structure.
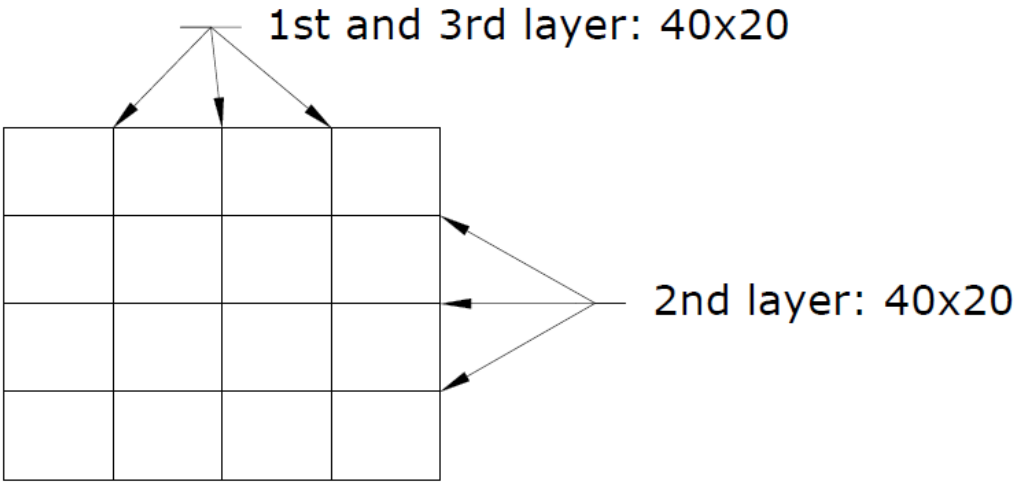
Figure 46: Wooden frame attached on the steel frame.

86

However, in RFEM the walls of the unit are recreated in different ways, as surfaces or as a steel web with the actual elements, in order to realise a representative model as explained earlier.

To analyse the effects of a wall on the stability of a unit, several types of walls are analysed. The calculations are performed on a single, closed unit. The wall build-up is recreated in RFEM with several systems: Rigid walls, orthotropic steel walls and a wall made out of steel profiles, to simulate the situation in real-life.

Finally, the complete structure is created as shown in Figure 47. All different components are shown in Annex C.
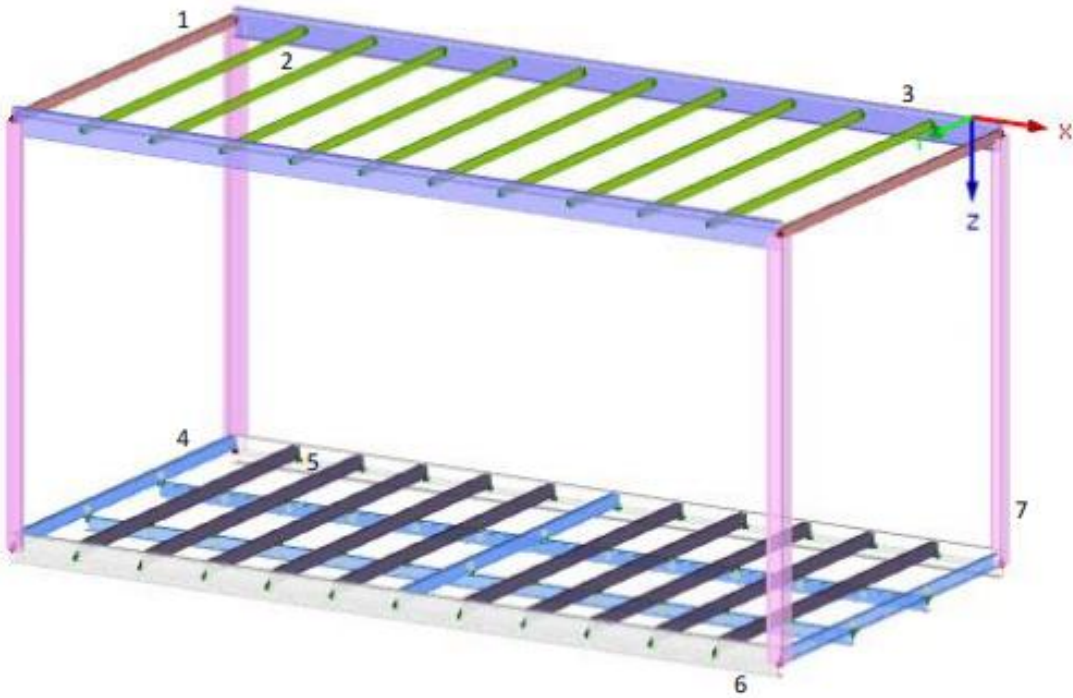
Figure 47: Steel skeleton frame of the model.

3.3.2 Loads

There are three types of loads applied onto the modular units. These load cases are listed in Table 37.

Table 37: Loads applied on the modular units.

Load Case	Loads	Value
LC1	Self-weight	
LC2	Snow	0,40 kN/m²
LC3	Floor Loads	3 kN/m²

The loads are put together in several load combinations as shown in Table 38. These combinations are then used to determine the values for different calculations. The load factors and combination factors, that are highlighted, are used to determine the accidental ULS for the calculations of the fire stability.

Table 38: Load combinations.

Load Combination	Combination factors
CO1	1.35G
CO2	1.35G + 1.5Qs
CO3	1.35G + 1.5Qs + 1.05QiB
CO4	1.35G + 1.5QiB
CO5	1.35G + 0.75Qs + 1.5QiB
CO6	G
CO7	G + Qs
CO8	G + Qs + 0.7QiB
CO9	G + QiB
CO10	G + 0.5Qs + QiB
CO11	G
CO12	G + 0.2Qs
CO13	G + 0.2Qs + 0.3QiB
CO14	G + 0.5QiB
CO15	G
CO16	G + 0.3QiB
CO17	G
CO18	G+0,2Qs
CO19	G + 0.2Qs + 0.3QiB
CO20	G + 0.5QiB
CO21	G
CO22	G + 0.3QiB

4 Fire design of modular units

4.1 Modular building configurations analysed

Four types of units are analysed, based on the different configurations

Case I-III: single modular unit

The closed unit is the most rudimentary case. In this situation, shown in Figure 48, the walls of the modular unit are filled with a type of wall. These walls will divide a portion of the vertical loads, exercised on the structure, to the columns and the bottom horizontal beams.
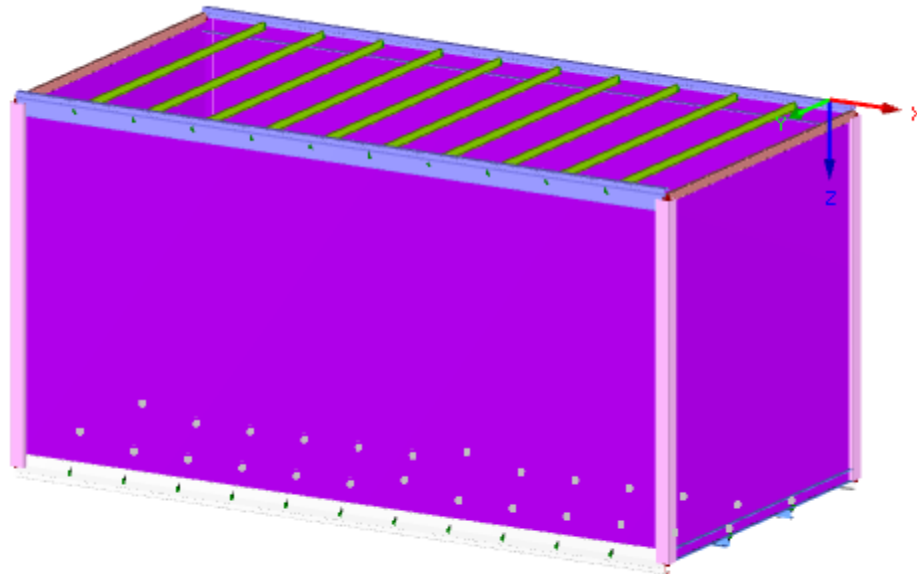
Figure 48: RFEM closed unit.

For multiple modular units in one floor, different build-ups of multiple modular units are tested. Therefore a division is made between the three most common build-ups. It is important to note that the modular units are placed next to each other and connected. This means that the units handle the loads separately. That is why the assumption was made that the modular units can be tested as separated units. The changes in setup is simulated in a simplified way. When units are placed next to each other, the walls are left open to create an open space. This is replicated by leaving the walls open in the different models.

Case II and III are representing an addition of respectively one and two floors.

Case IV-VI: 2x1 short face

To simulate the case shown in Figure 49, one short face of the modular unit was left open as shown in Figure 50. The elements are no longer supported by the wall. This causes an alteration in the division of the loads, causing the unsupported beams to bend.

2 units connected at the short face
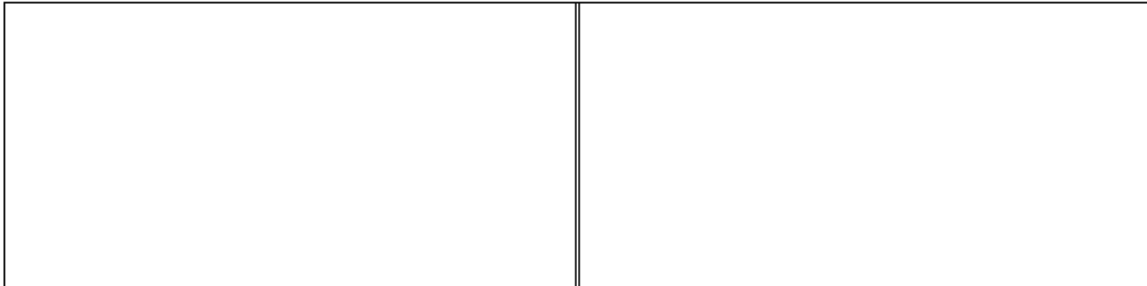
Figure 49: Blueprint of 2 units connected by their short surface.
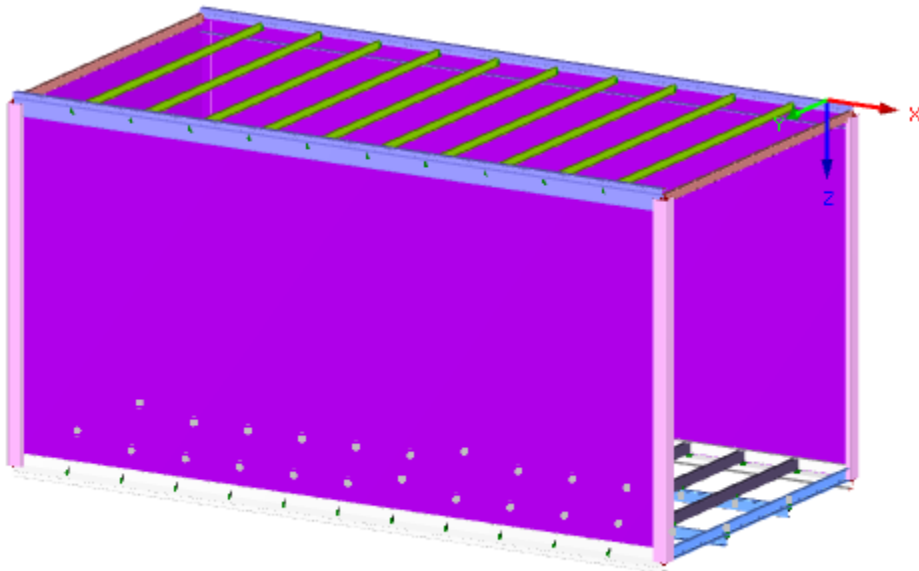
Figure 50: RFEM model of the unit connected by its short surface.

Case V and VII are modelled to simulate the addition of respectively one and two floors.

Case VII-VIII: 2x1 long face

The case shown in Figure 51 is simulated by leaving the long face of the unit open, as shown in Figure 52 . This means that the long roof element is no longer supported by the surface or wall. The structural elements of the open facade are bolted together to combine the units.

Case VIII represents the two story building of this type of set up.

2 units connected by
the long side
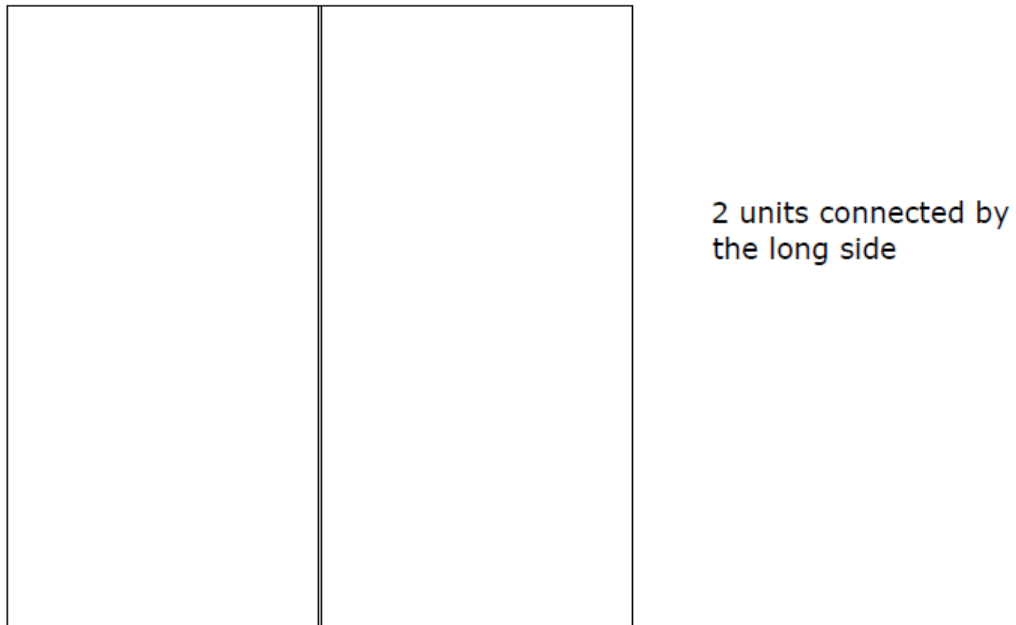
Figure 51: Blueprint of 2 units connected by their long surface.
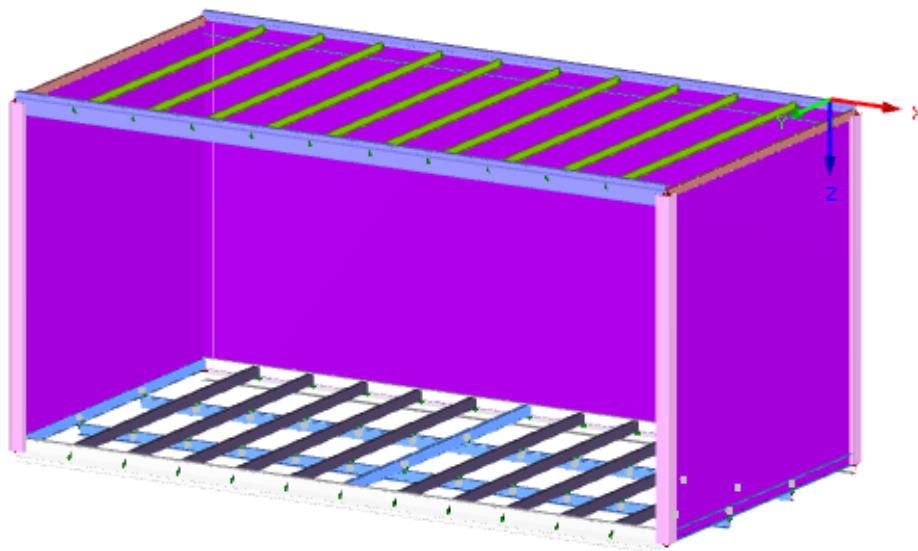
Figure 52: RFEM model of the unit connected by its long surface.

91

Case IX-X: 2x2

To simulate the situation shown in Figure 53, four units are arranged . In this placement there is one column standing completely alone, without the support of the walls. This is represented in Figure 54. The roof structure is only supported by a facade at two sides.
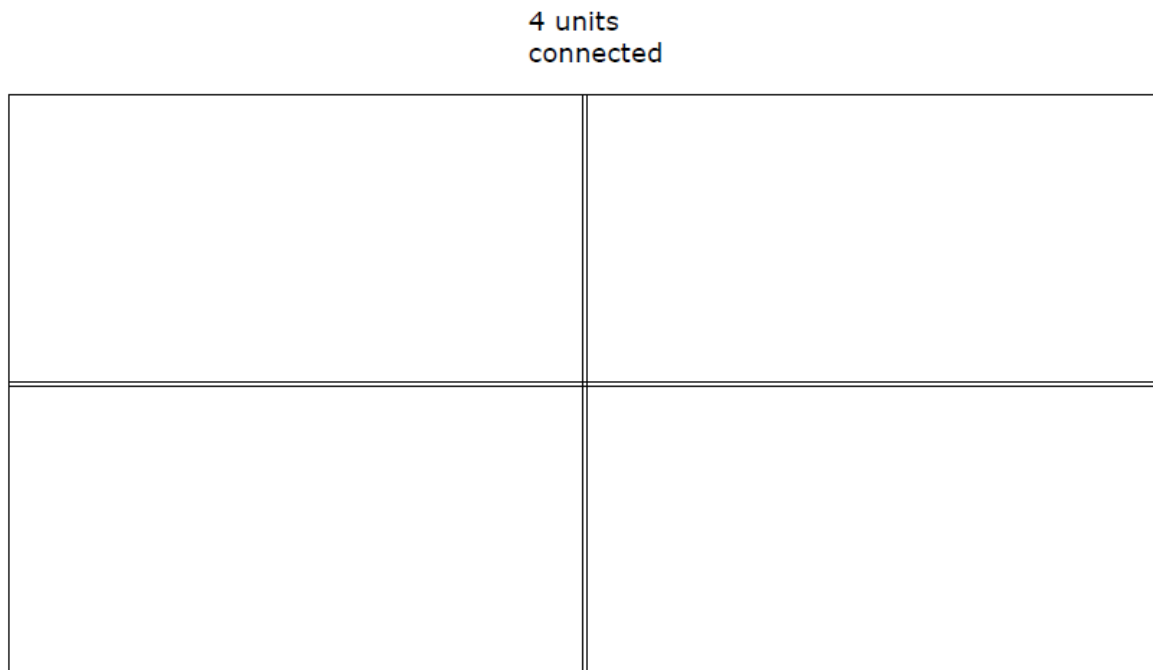
4 units
connected

Figure 53: Blueprint of 4 units connected by both their short and long surfaces.
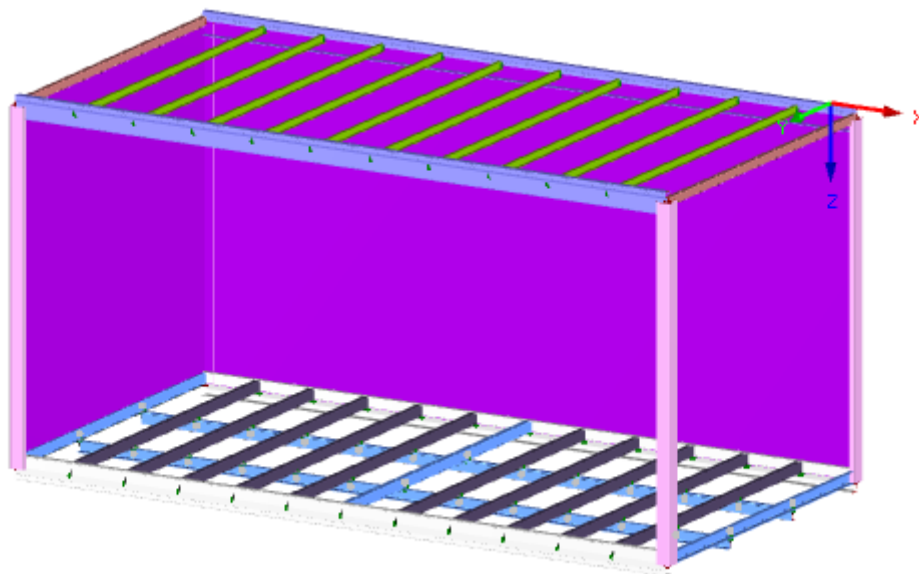
Figure 54: RFEM model of the unit connected by both its short and long surface.

Case X represents an addition of one floor.

For the analysis of modular buildings with more than one floor, the situation can be reduced to a single unit. This can be explained because of the fact that the units are mounted up upon each other. The bottom unit is only carrying the loads of the units stacked upon it. These base units are the critical units in the construction and that is why only the base unit is analysed.

To determine the loads working on the unit, a calculation was made with the RFEM-software as shown in Figure 55. The reaction forces at the bottom are determined by calculating the reaction forces on the supports of the units. The units of the upper floors are supported by the superior structural elements, this is recreated by putting a line load on the bottom of the unit to get a realistic perspective on the loads working on a supporting unit.
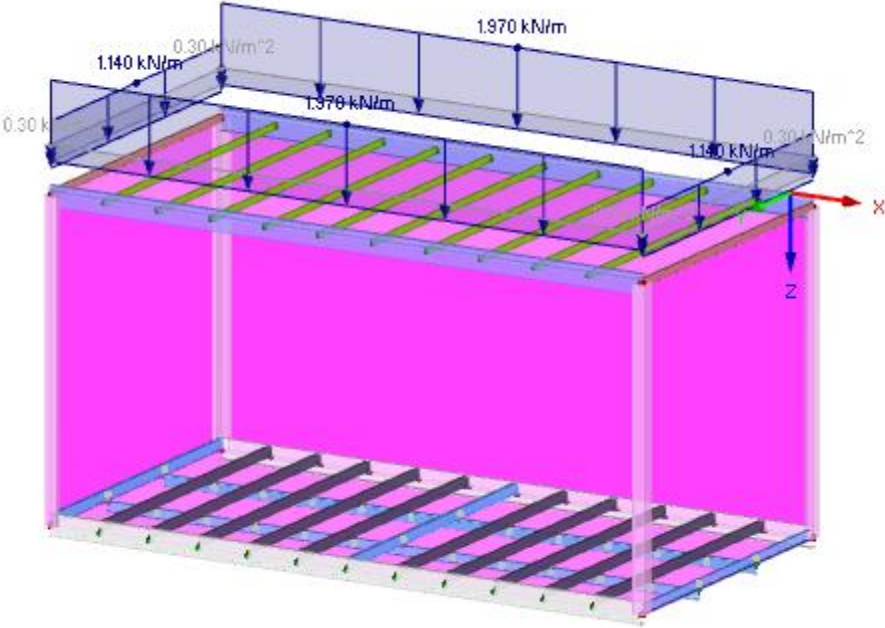
Figure 55: Support line loads for one modular structure.

With this method an analysis of the self-weight and the floor loads of the upper floors is done, in order to obtain the correct values of the support reactions for each setup.

4.2 Results

4.2.1 RFEM design results

For calculations with RFEM, the modular unit shown in Figure 56 is created. The walls are filled with three different structures. For each of these wall build-ups, ten cases are tested.
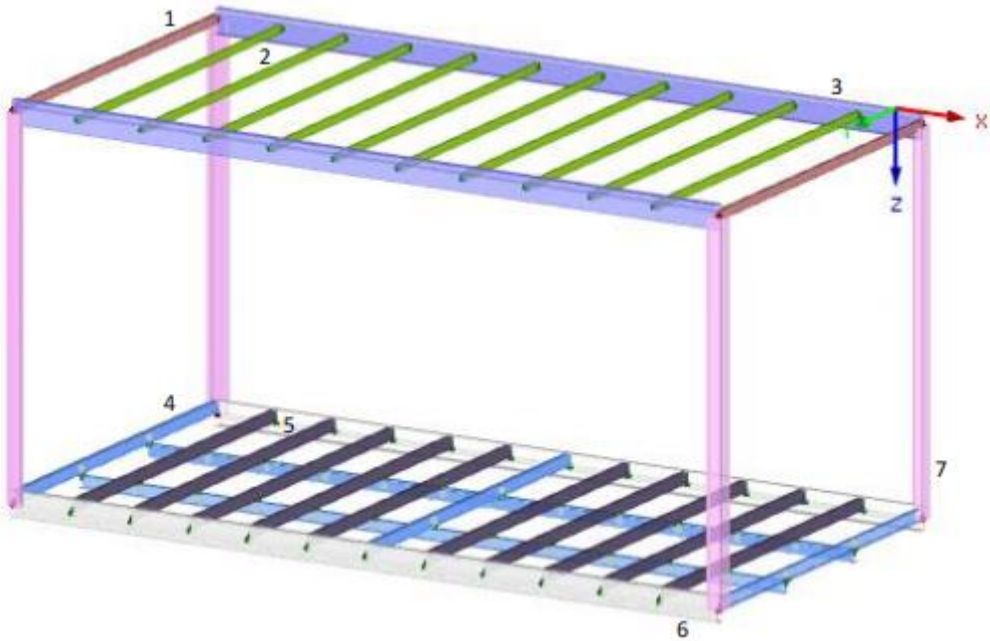
Figure 56: Numeration of the profiles used in the modular unit.

4.2.2 Profiles

For the following ten cases , the wall is made out of the profiles, used by CBZ to produce the actual units. Due to the fact that these walls are welded in the frame, the modelling does not allow to create the real situation. However, the design ratios for this build-up give another indication to compare the different possibilities for the wall modelling.

Cases I-III show the same design ratios as in the previous tests. The non-structural roof elements and floor elements show no increase in design ratio when the loads of extra floors are placed on top of the unit. The profiles will direct a larger amount of the loads towards element 6, therefore the design ratio for these elements are higher. The design ratios are listed in Table 39

In case I the critical element is element 6, with a design resistance to bending is $M_{b,fi,t,Rd} = 1.08$ kNm and the moment on this element is $M_{fi,y,Ed} = 0.52$ kNm. Not a single element of the modular unit fails in a R60 fire situation.

For case II the same element is critical, now with a design ratio of 0.97. Element 7, furthermore all the critical elements shows an increase in their design ratio. Element 3 is supported by several vertical profiles and is therefore less subjected to bending. These profiles direct the loads towards the structural elements of the floor, element 6. For element 6 the resistance moment of the element in a fire situation is $M_{b,fi,t,Rd} = 1.08$ kNm and the moment on this element is $M_{fi,y,Ed} = 1.04$ kNm.

For case III element 6 fails the calculation for stability during a fire situation R60. The design resistance to bending is $M_{b,fi,t,Rd} = 1.08$ kNm and the moment on this element is $M_{fi,y,Ed} = 2.22$ kNm.

Table 39: Design ratios with profiles for case I-III.

Element	Case I		Case II		Case III	
1	0,01	(Eq. 2.6.25)	0,08	(Eq. 2.6.25)	0,16	(Eq. 2.6.25)
2	0,13	(Eq. 2.6.25)	0,13	(Eq. 2.6.25)	0,13	(Eq. 2.6.25)
3	0,04	(Eq. 2.6.12)	0,07	(Eq. 2.6.12)	0,11	(Eq. 2.6.12)
4	0,24	(Eq. 2.6.12)	0,25	(Eq. 2.6.12)	0,26	(Eq. 2.6.12)
5	0,08	(Eq. 2.6.12)	0,06	(Eq. 2.6.12)	0,06	(Eq. 2.6.25)
6	0,48	(Eq. 2.6.12)	0,97	(Eq. 2.6.12)	2,06	(Eq. 2.6.12)
7	0,05	(Eq. 2.6.12)	0,11	(Eq. 2.6.12)	0,16	(Eq. 2.6.12)

The design ratios for case IV to VI are listed in Table 40.

The elements in case IV have the same design ratios as case 1. This is the result of the small loads applied on the structure. The critical element is element 6 with a design resistance to bending of this element, for the fire situation R60, is $M_{b,fi,t,Rd} = 1.08$ kNm and the moment on this element is $M_{fi,y,Ed} = 0.52$ kNm.

Case V demonstrates an increase of the design ratio of element 6, this causes element 6 to be the critical element again. The a design Lateral Torsional Buckling resistance moment of this element is $M_{b,fi,t,Rd} = 1.08$ kNm and the moment on this element is $M_{fi,y,Ed} = 1.04$ kNm, for the fire situation R60.

Case VI shows a big increase in design ratio for element 1 and element 6. Element 6 has a design resistance to buckling $M_{b,fi,t,Rd} = 1.04$ kNm and the moment $M_{fi,y,Ed} = 3.05$ kNm due to the forces in the columns. Element 1 displays a big increase in design ratio and the design ratio is calculated for biaxial bending. The explanation can be found in the deformation of the structure due to the loads applied on top of the structure.

Table 40: Design ratios with profiles for case 4-6.

Element	Case IV		Case V		Case VI	
1	0,04	(Eq. 2.6.25)	0,35	(Eq. 2.6.25)	2,14	(Eq. 2.6.28)
2	0,13	(Eq. 2.6.25)	0,13	(Eq. 2.6.25)	0,48	(Eq. 2.6.28)
3	0,04	(Eq. 2.6.12)	0,07	(Eq. 2.6.12)	0,28	(Eq. 2.6.28)
4	0,24	(Eq. 2.6.12)	0,25	(Eq. 2.6.12)	0,27	(Eq. 2.6.28)
5	0,08	(Eq. 2.6.12)	0,07	(Eq. 2.6.12)	0,11	(Eq. 2.6.28)
6	0,48	(Eq. 2.6.12)	0,95	(Eq. 2.6.12)	2,94	(Eq. 2.6.28)
7	0,05	(Eq. 2.6.12)	0,15	(Eq. 2.6.12)	0,26	(Eq. 2.6.28)

The design ratios for the calculation of the fire stability R60 are presented in Table 41.

Case VII is determined by the most critical element, again element 6. Element 3 shows an increase in design ratio as well. For case 7 the design ratio of element 3 is 0.12. This can be explained by the removal of the profiles. The critical element, element 6, has a design ratio of 0.46. This is because of biaxial bending. $\sigma_{fi,Rd} = 23.50$ kN/cm² and the working stress is $\sigma_{fi,Ed} = 10.95$ kN/cm².

For case VIII, element 6 fails the calculations for fire stability R60. The calculated resistance is $M_{b,fi,t,Rd} = 1.08$ kNm where the moment on the element is $M_{fi,y,Ed} = 1.57$ kNm. Therefore the element has a design ratio of 1.46. None of the other elements fails the calculations.

The floor elements manifest only a small increase in design ratio, due to the deformation of the structure. The same explanation can be given for the small increase of design ratio for the roof elements.

Table 41: Design ratios with profiles for case VII-VIII.

Element	Case VII		Case VIII	
1	0,05	(Eq. 2.6.12)	0,19	(Eq. 2.6.12)
2	0,13	(Eq. 2.6.25)	0,14	(Eq. 2.6.25)
3	0,12	(Eq. 2.6.25)	0,33	(Eq. 2.6.25)
4	0,24	(Eq. 2.6.12)	0,25	(Eq. 2.6.12)
5	0,07	(Eq. 2.6.12)	0,08	(Eq. 2.6.12)
6	0,46	(Eq. 2.6.12)	1,46	(Eq. 2.6.12)
7	0,18	(Eq. 2.6.12)	0,52	(Eq. 2.6.12)

Table 42 gives the design ratios for case 9 and case 10. These are the cases where the units are constructed with two open sides.

Case IX demonstrates the same results as case 7. Because the loads are working on the structure are small and the design loads for the roof and the floor are constant for every case. The critical element is element 6 ,due to instability for biaxial bending. The design ratio is 0.47. The resistance of the element in a fire situation is $\sigma_{fi,Rd}$ = 23.50 kN/cm² and the working stress is $\sigma_{fi,Ed}$ = 10.95 kN/cm².

For case X the explanation of the results interpreted by analysing the build-up of the case. The design results can be found somewhere between case 4 and case 7. The elements without the support of the profiles lose a part of their stability. The increase of force of the columns on element 6 causes the element to fail the calculations. The resistance to bending is $M_{b,fi,t,Rd}$ = 1.08 kNm where the moment on the element is $M_{fi,y,Ed}$ = 1.60kNm. The element fails the calculation of the fire stability R60.

Table 42: Design ratios with profiles for case IX-X.

Element	Case IX		Case X	
1	0,05	(Eq. 2.6.12)	0,29	(Eq. 2.6.28)
2	0,13	(Eq. 2.6.25)	0,13	(Eq. 2.6.28)
3	0,12	(Eq. 2.6.25)	0,34	(Eq. 2.6.28)
4	0,24	(Eq. 2.6.12)	0,25	(Eq. 2.6.28)
5	0,08	(Eq. 2.6.12)	0,08	(Eq. 2.6.28)
6	0,47	(Eq. 2.6.25)	1,49	(Eq. 2.6.28)
7	0,18	(Eq. 2.6.12)	0,51	(Eq. 2.6.28)

4.2.3 Rigid Surface

The elements supported by a rigid surface will not experience any loads. The rigid surface diverts the loads directly to the foundations. Only element 1 on the top of the walls experience a small moment working on it.

The design ratios for case I-III are all results of floor loads working on the elements. The results are shown in Table 43. Except for element 1, no structural element has internal forces working on it due to the rigid surface diverting all the loads away from the elements. Element 2 is loaded with a constant floor load and element 2 has a moment of resistance $M_{b,fi,t,Rd}$ = 0.66 kNm while the moment is $M_{fi,y,Ed}$ = 0.18 kNm. This results in a design ratio of 0.27. None of the element fails the stability calculations for R60.

Table 43: Design ratios with a rigid surface for case I-III.

Element	Case I		Case II		Case III	
1	0		0,01	(Eq. 2.6.29)	0,07	(Eq. 2.6.28)
2	0,27	(Eq. 2.6.28)	0,27	(Eq. 2.6.28)	0,27	(Eq. 2.6.28)
3	0		0,01	(Eq. 2.6.29)	0,02	(Eq. 2.6.29)
4	0,12	(Eq. 2.6.28)	0,12	(Eq. 2.6.28)	0,12	(Eq. 2.6.28)
5	0,17	(Eq. 2.6.28)	0,17	(Eq. 2.6.28)	0,17	(Eq. 2.6.28)
6	0		0		0	
7	0		0		0	

For case IV, V and VI element 1 is no longer supported by the rigid surface. Thus the element can no longer divert the loads to the foundation. The removal of one of the rigid surfaces also causes an increase in the design ratios of the floor elements. The design ratios of these elements, again, do not increase when extra units are stacked on top of the base unit.

For case IV, the non-structural roof element has the highest design ratio. For a fire situation R60, the design Lateral Torsional Buckling resistance moment of element 2 is $M_{b,fi,t,Rd} = 0.66$ kNm and the moment is $M_{fi,y,Ed} = 0.18$ kNm. None of the elements fail during a fire situation R60.

In case V the most critical element is the short structural element: element 1. This can be explained due to the loss of support when the rigid surface was removed. The design LTB resistance moment is $M_{b,fi,t,Rd} = 0.93$ kNm , where the moment on the element is $M_{fi,y,Ed} = 0.80$ kNm. This results in a design ratio of 0.85.

Element 1 fails the calculations for fire stability in fire situation R60 for case VI. The design ratio is 1.51, this means the element does not provide the necessary stability during a fire. The design Lateral Torsional Buckling resistance moment of element 2 is $M_{b,fi,t,Rd} = 0.93$ kNm and the moment is $M_{fi,y,Ed} = 1.41$ kNm for a fire situation R60.

The results are shown in Table 44.

Table 44: Design ratios with a rigid surface for case IV-VI.

Element	Case IV		Case V		Case VI	
1	0,11	(Eq. 2.6.28)	0,85	(Eq. 2.6.28)	1,51	(Eq. 2.6.28)
2	0,27	(Eq. 2.6.28)	0,27	(Eq. 2.6.28)	0,27	(Eq. 2.6.28)
3	0,01	(Eq. 2.6.29)	0,01	(Eq. 2.6.29)	0,02	(Eq. 2.6.29)
4	0,13	(Eq. 2.6.28)	0,13	(Eq. 2.6.28)	0,13	(Eq. 2.6.28)
5	0,20	(Eq. 2.6.28)	0,20	(Eq. 2.6.28)	0,20	(Eq. 2.6.28)
6	0		0		0	
7	0		0		0	

The setup with a long opened face are calculated with the cases VII and VIII. In Table 45 the design ratios for each case is listed.

Case VII is determined by the design of element 6. The design Lateral Torsional Buckling resistance moment of this element, for the fire situation R60, is $M_{b,fi,t,Rd} = 1.04$ kNm and the moment on this element is $M_{fi,y,Ed} = 0.82$ kNm. Therefore the design ratio is 0.79.

The fire design ratio of 0,79 is calculated again for element 6 . This means element 6 fails during a R60 fire design. The resistance moment of the element in a fire situation is $M_{b,fi,t,Rd} = 1.04$ kNm and the moment on this element is $M_{fi,y,Ed} = 0.82$ kNm.

Table 45 displays that the design ratio of the non-structural floor elements again remains constant. The columns are supported by at least one rigid surface and this takes away all the loads.

Table 45: Design ratios with a rigid surface for case VII-VIII.

Element	Case VII		Case VIII	
1	0		0,04	(Eq. 2.6.28)
2	0,41	(Eq. 2.6.28)	0,42	(Eq. 2.6.28)
3	0,11	(Eq. 2.6.28)	0,39	(Eq. 2.6.28)
4	0,19	(Eq. 2.6.28)	0,19	(Eq. 2.6.28)
5	0,19	(Eq. 2.6.28)	0,19	(Eq. 2.6.28)
6	0,79	(Eq. 2.6.28)	0,79	(Eq. 2.6.28)
7	0		0	

Table 46 gives an overview of the design ratio for the structural elements of a modular unit with two open sides.

For case IX, all the structural elements have a design ratio calculated. This is due to the fact that at least one of each profile is no longer supported by a rigid surface. Element 6 is the critical element due to the floor loads working on the elements on the open side of the unit. . The design Lateral Torsional Buckling resistance moment of this element, for the fire situation R60, is $M_{b,fi,t,Rd} = 1.04$ kNm and the moment on this element is $M_{fi,y,Ed} = 0.99$ kNm.

Two elements fail for the setup of case X. Element 6 is again the most critical with a design ratio of 1.12. The design LTB resistance is $M_{b,fi,t,Rd} = 1.04$,kNm and the moment applied on the element is $M_{fi,y,Ed} = 1.17$ kNm. This is because of the extra loads coming from the columns. Therefore the floor element fails the calculations of fire stability R60. This can be explained due to the forces applied on the element by the column, which is no longer supported by a rigid surface. This column also shows a noticeable increase in design ratio.
Element 1 fails the calculations as well due to the loads applied on the beam when an extra floor is added on top. And without the wall supporting the element, the loads are too high, resulting in a design ratio of 1.05.

Table 46: Design ratios with a rigid surface for case IX-X.

Element	Case IX		Case X	
1	0,05	(Eq. 2.6.28)	1,05	(Eq. 2.6.28)
2	0,21	(Eq. 2.6.28)	0,43	(Eq. 2.6.28)
3	0,13	(Eq. 2.6.28)	0,50	(Eq. 2.6.28)
4	0,21	(Eq. 2.6.28)	0,22	(Eq. 2.6.28)
5	0,17	(Eq. 2.6.28)	0,23	(Eq. 2.6.28)
6	0,42	(Eq. 2.6.28)	1,12	(Eq. 2.6.28)
7	0,10	(Eq. 2.6.30)	0,46	(Eq. 2.6.30)

4.2.4 Orthogonal Surface

Table 47 shows us the design ratios of each element for case I-III with the orthogonal surface. The design ratio of the elements carrying only the floor and roof loads (element 2 and 5) do not change when a modular unit is added on top of the case unit.

For case I element 2 is the critical element, with a design ratio of 0.18. The load applied on this element is only the self-weight of the roof. The element has the highest design ratio for Lateral Torsional Buckling. The $M_{b,fi,t,Rd} = 0.95$ kNm and the moment working on element in a fire situation is $M_{fi,y,Ed} = 0.17$ kNm. The design ratios of all the elements are below 0.18 thus no element fails during a fire situation.

For case II the highest design ratio, 0.28, can be found for element 6. This is the longest horizontal floor element. It supports the floor loads and the loads from the upper floor as well. The loads working on this element increases as the amount of floors stacked on top of the base unit . The design Lateral Torsional Buckling resistance moment of this element, for the fire situation R60, is $M_{b,fi,t,Rd} = 0.99$ kNm and the moment is $M_{fi,y,Ed} = 0.28$ kNm. For case 2, again no element is failing in a fire situation R60.

For the analysis of case III, element 6 has a design ratio of 0.45. As said for case 2, this element will take the loads of the units stacked on top of the base units. An extra unit, stacked on top of the base unit, will result in a higher load on the bottom elements. The design Lateral Torsional Buckling resistance moment of this element, for the fire situation R60, is $M_{b,fi,t,Rd} = 0.99$ kNm and the moment on this element is $M_{fi,y,Ed} = 0.45$ kNm. This element does therefore not fail for fire situation R60.

Table 47: Design ratios with an orthogonal surface for case I-III.

Element	Case I		Case II		Case III	
1	0,01	(Eq. 2.6.12)	0,01	(Eq. 2.6.28)	0,03	(Eq. 2.6.28)
2	0,18	(Eq. 2.6.28)	0,18	(Eq. 2.6.28)	0,18	(Eq. 2.6.28)
3	0,01	(Eq. 2.6.29)	0,03	(Eq. 2.6.29)	0,03	(Eq. 2.6.29)
4	0,16	(Eq. 2.6.28)	0,17	(Eq. 2.6.28)	0,17	(Eq. 2.6.28)
5	0,14	(Eq. 2.6.28)	0,14	(Eq. 2.6.28)	0,15	(Eq. 2.6.28)
6	0,03	(Eq. 2.6.28)	0,28	(Eq. 2.6.28)	0,45	(Eq. 2.6.28)
7	0		0,05	(Eq. 2.6.28)	0,08	(Eq. 2.6.28)

Case IV to VI are situations in which the short face of the modular unit is left open. The results of the fire design tests for R60 are listed in Table 48. The open face of the model causes a shift in the division of the forces on the model.

For case IV, element 2 is the most critical, for the same reasons as case I. For a fire situation R60, the design Lateral Torsional Buckling resistance moment of element 2 is $M_{b,fi,t,Rd} = 0.95$ kNm and the moment is $M_{fi,y,Ed} = 0.17$ kNm. No element fails during a fire situation R60.

For case V the critical element is element 1, the structural element of the roof at the open face of the modular unit, with a design ratio of 0.40. The design Lateral Torsional Buckling resistance moment of this element, for the fire situation R60, is $M_{b,fi,t,Rd} = 1.08$ kNm and the moment on this element is $M_{fi,y,Ed} = 0.73$ kNm. The structural elements of the unit does not fail during R60 for a build-up like case V.

In case VI, element 1 has a design ratio of 0.71 for the fire design R60. For a fire situation R60, the design Lateral Torsional Buckling resistance moment of element 2 is $M_{b,fi,t,Rd} = 1.80$ kNm and the moment is $M_{fi,y,Ed} = 1.27$ kNm. None of the elements fail the calculations.

Element VI shows an increasing design ratio because the columns have to bear a bigger load due to the opening in the short face. This causes element 6 to carry a part of the load. The floor elements manifest no augmenting in design ratio due to the constant floor load.

Table 48: Design ratios with an orthogonal surface for case IV-VI.

Element	Case IV		Case V		Case VI	
1	0,05	(Eq. 2.6.28)	0,40	(Eq. 2.6.28)	0,71	(Eq. 2.6.28)
2	0,18	(Eq. 2.6.28)	0,18	(Eq. 2.6.28)	0,18	(Eq. 2.6.28)
3	0,01	(Eq. 2.6.29)	0,01	(Eq. 2.6.29)	0,01	(Eq. 2.6.29)
4	0,17	(Eq. 2.6.28)	0,17	(Eq. 2.6.28)	0,17	(Eq. 2.6.28)
5	0,15	(Eq. 2.6.12)	0,15	(Eq. 2.6.12)	0,15	(Eq. 2.6.28)
6	0,03	(Eq. 2.6.28)	0,07	(Eq. 2.6.28)	0,34	(Eq. 2.6.28)
7	0,01	(Eq. 2.6.12)	0,07	(Eq. 2.6.28)	0,12	(Eq. 2.6.12)

The setup with a long open face is calculated with the cases 7 and 8. Table 49 shows the design ratios of case VII and VIII.

Case VII is be determined by the design of element 6. The removal of the wall causes the moment working on the element to increase. The design Lateral Torsional Buckling resistance moment of this element, for the fire situation R60, is $M_{b,fi,t,Rd} = 1.04$ kNm and the moment on this element is $M_{fi,y,Ed} = 1.02$ kNm. Therefore the design ratio is 0.97. The element does fail during a fire situation R60.

For the fire design of a modular unit like case VIII, the design ratio is 1.41 for element 6. This means element 6 fails during a R60 fire design. The resistance moment of the element in a fire situation is $M_{b,fi,t,Rd} = 1.04$ kNm and the moment on this element is $M_{fi,y,Ed} = 1.48$ kNm.

In Table 49 some other developments can be analysed. The floor elements do not increase in design ratio because the loads applied on these elements do not increase when the units are stacked up upon each other. The roof element on the open face has an increasing design ratio because there is no wall anymore to support the element. This also causes the columns to carry a bigger load.

Table 49: Design ratios with an orthogonal surface for case VII-VIII.

Element	Case VII		Case VIII	
1	0,13	(Eq. 2.6.12)	0,13	(Eq. 2.6.12)
2	0,27	(Eq. 2.6.28)	0,24	(Eq. 2.6.28)
3	0,10	(Eq. 2.6.25)	0,33	(Eq. 2.6.28)
4	0,21	(Eq. 2.6.28)	0,21	(Eq. 2.6.28)
5	0,14	(Eq. 2.6.28)	0,14	(Eq. 2.6.28)
6	0,98	(Eq. 2.6.28)	1,41	(Eq. 2.6.28)
7	0,14	(Eq. 2.6.12)	0,52	(Eq. 2.6.28)

Case IX and X are representing the units with two open faces. The design ratios of the calculations are listed in Table 50.

Element 6 fails the calculations for case IX. The design ratio is 1.03, this is because the design Lateral Torsional Buckling resistance moment of this element, for the fire situation R60, is $M_{b,fi,t,Rd}$ = 1.04 kNm and the moment on this element is $M_{fi,y,Ed}$ = 1.07 kNm, causing the element to fail the calculation.

For case X element 6 fails the calculation as well. The free standing column will carry a larger load and it, again, results in an increase of the moment in element 6. The design resistance moment $M_{b,fi,t,Rd}$ = 1.04 kNm and the moment on this element is $M_{fi,y,Ed}$ = 1.77 kNm. Therefore element 6 does not suffice the fire design calculations.

Because of the deformation of the unit, the moment working on the non-structural roof elements increases. This causes an increase in the design ratio of the elements. The floor elements do not carry a bigger load than 3 kN/m². The floor elements are not affected by the deformation of the other elements because they are supported by the foundations. The free column carries a bigger part of the loads applied on the unsupported elements of the roof.

Table 50: Design ratios with an orthogonal surface for case IX-X.

Element	Case IX		Case X	
1	0,09	(Eq. 2.6.28)	0,40	(Eq. 2.6.25)
2	0,27	(Eq. 2.6.28)	0,31	(Eq. 2.6.28)
3	0,13	(Eq. 2.6.25)	0,40	(Eq. 2.6.28)
4	0,24	(Eq. 2.6.12)	0,24	(Eq. 2.6.12)
5	0,14	(Eq. 2.6.25)	0,14	(Eq. 2.6.28)
6	1,03	(Eq. 2.6.28)	1,68	(Eq. 2.6.28)
7	0,15	(Eq. 2.6.12)	0,72	(Eq. 2.6.25)

4.2.5 Comparison between cases

To compare the differences in the results between the three different types of walls, Table 51 is used. When the different critical elements are analysed, it is remarkable that ,for the wall with the profiles , element 6 is the critical element for each case. This can be explained by looking at the connections between the profiles and the structural elements. The structural elements divert their loads throughout the profiles, causing point loads on element 6. These point loads cause the problems for element 6. They fail due to bending occurring at the connections between the profiles and element 6, where the forces are transferred.

The rigid surface has almost no changes in the design ratio for the critical elements except for case VI and X. This is because a completely rigid surface takes on most of the loads and direct them straight to the foundations. For case 6, element 1 loses its support of the rigid surface and has to take on the loads of the extra unit by itself, causing it to fail the calculations. For case X the instability can be explained by the high forces from the columns working on the unsupported element 6.

The orthogonal surface is the most realistic view of the situation for the division of the forces in the structural elements of a modular unit. Not only does the surface direct a part of the forces to the bottom horizontal elements, a part of the forces is directed towards the columns. The stiffness of the orthogonal surface gives an impression of the stiffness that the wall provides in the real life scenario. The element that is most critical in with this installation is element 6, a structural floor element. Mostly due to the forces applied on it by the columns. When the element is connected to a orthogonal surface, the forces are divided more equally, resulting in a lower design ratio.
In contradiction to the other wall arrangements case IX and case X fail the fire stability calculations. To be more specific, element 6 fails the fire stability calculations due to lateral torsional buckling. This can be explained by the division of the forces to the columns. These transfer the forces to element 6 where they are connected together. This results in the failure of the stability calculation of the element. Furthermore the non-structural roof elements (element 2) are critical when a small load is applied onto the units, this is true for case I and case IV. The biggest surfaces of the unit are stiffened by the wall and the small forces are divided equally. When het rigid surfaces are applied, the other elements are almost unloaded. And in case of the wall made out of profiles the forces are to concentrated on the structural floor elements, element 6.

One thing the three systems do have in common is the failure of element 6 for case X. Again the explanation can be found in the forces of the columns. The column, which is not adjacent to a surface or wall, is loaded with half of the loads on the roof elements. These loads are transferred to element 6 in the connection, causing a moment which is to extensive. In the next chapter a solution is provided for the failure of the walls modelled with an orthogonal surface.

Table 51: Comparison of the results for the three different types of walls.

Summary	Profiles	Rigid	Orthogonal
Case I	0,48 (6)	0,27 (2)	0,18 (2)
Case II	0,97 (6)	0,27 (2)	0,28 (6)
Case III	2,06 (6)	0,27 (2)	0,45 (6)
Case IV	0,48 (6)	0,27 (2)	0,18 (2)
Case V	0,95 (6)	0,85 (1)	0,40 (1)
Case VI	2,94 (6)	1,51 (1)	0,71 (1)
Case VII	0,46 (6)	0,79 (6)	0,98 (6)
Case VIII	1,46 (6)	0,79 (6)	1,41 (6)
Case IX	0,47 (6)	0,42 (6)	1,03 (6)
Case X	1,49 (6)	1,12 (6)	1,68 (6)

4.2.6 Solutions

This research tries to suggest solutions for when the elements do not sustain the loads during a fire situation R60. The solutions are offered for case 8 to 10 of the systems with a orthogonal wall, because these systems are the most realistic.

Case VIII

In case VIII element 6 fails the fire stability calculations for R60 due to lateral torsional buckling. The problem occurs at the beginning and the end of the element, where the columns are attached to the horizontal element. The resistance to buckling can only be improved by increasing the steel quality of the element. The moment that is applied on the element is $M_{fi,y,Ed} = 1.48$ kNm is constant because the loads on the structure do not change. For the original situation the resistance is $M_{b,fi,t,Rd} = 1.05$ kNm.

Table 52 shows the increase of the design lateral torsional buckling resistance with the increase of steel quality. Steel with a quality of S275 does not suffice to increase the design lateral torsional buckling design resistance. The design ratio does decrease to 1.21. The resistance is $M_{b,fi,t,Rd} = 1.23$ kNm.

Increasing the steel quality to S355 improves the design ratio even further, to 0.92. The resistance to lateral torsional buckling is raised to $M_{b,fi,t,Rd} = 1.61$ kNm. With this resistance the element is able to sustain the loads from the column. Therefore realising a fire stability R60 for all the elements of the unit.

Table 52: Solutions for case VIII.

Case VIII	Steel Quality	Design Ratio	Moments
Element 6	S235	1,41	$M_{fi,y,Ed} = 1,48$ kNm $M_{b,fi,t,Rd} = 1,04$ kNm
	S275	1,21	$M_{fi,y,Ed} = 1,48$ kNm $M_{b,fi,t,Rd} = 1,23$ kNm
	S355	0,92	$M_{fi,y,Ed} = 1,48$ kNm $M_{b,fi,t,Rd} = 1,61$ kNm

Case IX

The solution for case IX can be found with two different approaches. The moment $M_{fi,y,Ed} = 1.06$ kNm causes the element to fail due to lateral torsional buckling in the middle. This means that the resistance can be improved by increasing the steel quality, but the moment can also be reduced by placing extra supports and therefore reducing the buckling length. The effects of both these solutions are researched.

First the effects of raising the steel quality is be discussed. The design resistance of the element with a steel quality is $M_{b,fi,t,Rd} = 1.03$ kNm. Improving the quality to S275 results in a design ratio of 0.88. The element no longer fails the calculation for the fire stability R60. The design lateral torsional resistance is $M_{b,fi,t,Rd} = 1.22$ kNm.

When two extra supports are added at 1/4th of the length, the resistance of element 6 does not improve. The moment working onto the element is instead decreased to $M_{fi,y,Ed} = 0.40$ kNm and the design resistance increases slightly to $M_{b,fi,t,Rd} = 1.06$ kNm. Therefore the design ratio reduces to 0.38. This is shown in Table 53.

Table 53: Solutions for case IX.

Case IX	Steel Quality	Design Ratio	Moments
Element 6	S235	1,03	$M_{fi,y,Ed} = 1,06$ kNm $M_{b,fi,t,Rd} = 1,03$ kNm
	S275	0,88	$M_{fi,y,Ed} = 1,06$ kNm $M_{b,fi,t,Rd} = 1,22$ kNm
	Extra Supports		
	2	0,38	$M_{fi,y,Ed} = 0,40$ kNm $M_{b,fi,t,Rd} = 1,06$ kNm

Case X

For case X the lateral torsional buckling is again induced by the loads of the columns being transferred to element 6 resulting in a design ratio of 1.68. The moment is $M_{fi,y,Ed} = 1.77$ kNm and the design resistance is $M_{b,fi,t,Rd} = 1.03$ kNm. The resistance to lateral torsional buckling can be improved by increasing the steel quality.

With a steel quality S275 the design ratio is lowered to 1.43 and the design lateral torsional buckling resistance is $M_{b,fi,t,Rd} = 1.23$ kNm. The element still fails the calculation for fire stability R60. Increasing the quality to S355 decreased the design ratio to 1.10 and the resistance is raised to $M_{b,fi,t,Rd}$ = 1.60 kNm. The element fails the fire stability calculations. The steel quality is raised even further to S450. This does increase the resistance of the element to $M_{b,fi,t,Rd} = 2.06$ kNm, lowering the design ratio to 0.86. Only with a steel quality of S450 this system withstands the loads and is stable during a fire situation of R60. This is shown in Table 54.

Table 54: Solutions for case X.

Case X	Steel Quality	Design Ratio	Moments
Element 6	S235	1,68	$M_{fi,y,Ed} = 1,77$ kNm $M_{b,fi,t,Rd} = 1,04$ kNm
	S275	1,43	$M_{fi,y,Ed} = 1,77$ kNm $M_{b,fi,t,Rd} = 1,23$ kNm
	S355	1,10	$M_{fi,y,Ed} = 1,77$ kNm $M_{b,fi,t,Rd} = 1,60$ kNm
	S450	0,86	$M_{fi,y,Ed} = 1,77$ kNm $M_{b,fi,t,Rd} = 2,06$ kNm

Another possible solution would be to increase the amount of insulation placed in the floor of the modular unit. This can also increase the resistance of the elements against fire. Unfortunately the amount that is modelled, is already the maximum amount of insulation possible in RFEM. Therefore the influence of this solution cannot be explored any further.

Next, a summary for all results is made. First, all critical elements for each case are shown in Table 55 and then all configurations are again shown in Table 56.

<p style="text-align:center">Table 55: Summary for all critical elements for each case.</p>

Profiles	Stable for R60	Failing element	
Case I	Yes	Element 6	(Eq. 2.6.12)
Case II	Yes	Element 6	(Eq. 2.6.12)
Case III	NO	Element 6	(Eq. 2.6.12)
Case IV	Yes	Element 6	(Eq. 2.6.12)
Case V	Yes	Element 6	(Eq. 2.6.12)
Case VI	NO	Element 6	(Eq. 2.6.28)
Case VII	Yes	Element 6	(Eq. 2.6.12)
Case VIII	Yes	Element 6	(Eq. 2.6.12)
Case IX	Yes	Element 6	(Eq. 2.6.25)
Case X	NO	Element 6	(Eq. 2.6.28)
Rigid	**Stable for R60**	**Failing element**	
Case I	Yes	Element 2	(Eq. 2.6.28)
Case II	Yes	Element 2	(Eq. 2.6.28)
Case III	Yes	Element 2	(Eq. 2.6.28)
Case IV	Yes	Element 2	(Eq. 2.6.28)
Case V	Yes	Element 1	(Eq. 2.6.28)
Case VI	NO	Element 1	(Eq. 2.6.28)
Case VII	Yes	Element 6	(Eq. 2.6.28)
Case VIII	Yes	Element 6	(Eq. 2.6.28)
Case IX	Yes	Element 6	(Eq. 2.6.28)
Case X	NO	Element 6	(Eq. 2.6.28)
Orthogonal	**Stable for R60**	**Failing element**	
Case I	Yes	Element 2	(Eq. 2.6.28)
Case II	Yes	Element 6	(Eq. 2.6.28)
Case III	Yes	Element 6	(Eq. 2.6.28)
Case IV	Yes	Element 2	(Eq. 2.6.28)
Case V	Yes	Element 1	(Eq. 2.6.28)
Case VI	Yes	Element 1	(Eq. 2.6.28)
Case VII	Yes	Element 6	(Eq. 2.6.28)
Case VIII	NO	Element 6	(Eq. 2.6.28)
Case IX	NO	Element 6	(Eq. 2.6.28)
Case X	NO	Element 6	(Eq. 2.6.28)

Case	Configuration	Extra floors
Case I	Single modular unit	/
Case II	Single modular unit	+ 1 floor
Case III	Single modular unit	+ 2 floors
Case IV	2x1 Short face	/
Case V	2x1 Short face	+ 1 floor
Case VI	2x1 Short face	+ 2 floors
Case VII	2x1 Long face	/
Case VIII	2x1 Long face	+ 1 floor
Case IX	2x2	/
Case X	2x2	+ 1 floor

Conclusion

This research grants a logical insight into the calculations for a fire situation according to Eurocode 3. An extensive analysis is made of the concept "fire" and the influence of the fire on structural elements and loads.

The calculations for the design of fire stability give a good impression on how these calculations are performed. With these calculations it was also possible to validate the used software, RFEM, with some examples. This was done in order to obtain valid results and to get a better understanding of the background of the software.

The results grant an insight on how the modular units, as constructed by CBZ, behave in a fire situation. Most of the tested configurations have enough fire stability to reach a fire resistance of R60. Only when the long facades of the unit are left open, problems of stability occur.

In order to solve these stability problems, some solutions are presented. With an improvement of the steel quality of one elements, some of the problems are already resolved. In one other specific case, the addition of supports increased the fire resistance.

This research also opens up the opportunity for other researches. The wall configuration for the models of the modular units can be further improved. This has be done with a better analysis of the load dispersion for the actual wall build-up.

Also , it can be useful to explore the influence of the insulation on the fire resistance of some of the elements. This was not possible to do for this research, due to the limitations of the software.

To summarise, this paper grants an insight in the fire resistance calculations according to Eurocode3. The fire resistance of modular units constructed by CBZ is analysed using different setups. This research can therefore be used, by engineers, as a guide to perform similar calculations.

Reference

[1]   "www.sc.edu," [Online]. Available: https://www.sc.edu/ehs/training/Fire/01_triangle.htm.

[2]   D. P. J. F. JF Cadorin, "The Design Fire Tool OZone V2.0 -Theoretical Description and Validation On Experimental Fire Tests," Liège, 2001.

[3]   B. Zhao, "Eurocodes: Background & Applications Structural Fire Design," European Commission, Luxembourg, 2014.

[4]   E. N. E. 1993-1-2. [Online]. Available: https://edu.mynbn.be/nbnframework/index.php/pdfMeta/ro/312537?l=N.

[5]   "Eurocode NBN EN 1990," [Online]. Available: https://edu.mynbn.be/nbnframework/index.php/pdfMeta/ro/116657?l=E.

[6]   E. N. E. 1991-1-2. [Online]. Available: https://edu.mynbn.be/nbnframework/index.php/pdfMeta/ro/119650?l=E.

[7]   E. N. E. 1991-1-1. [Online]. Available: https://edu.mynbn.be/nbnframework/index.php/pdfMeta/ro/116680?l=E.

[8]   K. Poh, "Stress-Strain-Temperature relationship for structural steel," *Journal of matrials in civil engeneering,* pp. 371-379, September/October 2001.

[9]   C. –. A. P. d. C. M. e. Mista, Fire Guideline: Design and Examples, Portugal: Joana Albuquerque, 2015.

[10] "www.nist.gov," [Online]. Available: https://www.nist.gov/<front>/fire-dynamics.

[11] O. a. Mäkeläinen, "Mechanical properties of structural steel at elevated temperatures and after cooling down," Helsinki, 2002.

[12] D. i. L. Pyl, Brandveilig Constructief Ontwerp, Mechelen.

Annex A

$\bar{\lambda}_{\theta,0}$	0,0	0,2	0,4	0,6	0,8	1,0	1,2	1,4	1,6	1,8	2,0
μ_0											
0,04	1000	975	945	906	875	832	783	736	694	677	657
0,06	900	884	863	832	791	751	698	677	654	627	599
0,08	860	837	806	781	743	695	671	644	613	586	561
0,10	820	796	777	747	699	674	645	611	582	554	524
0,12	792	775	752	713	682	653	618	585	555	522	464
0,14	775	755	726	692	665	631	594	563	529	476	357
0,16	758	735	701	678	648	610	576	541	502	394	
0,18	742	714	689	665	631	593	559	520	440		
0,20	725	697	678	651	615	578	541	495	364		
0,22	708	688	667	638	598	564	523	443			
0,24	696	678	655	624	587	549	505	387			
0,26	688	668	644	610	575	535	472				
0,28	679	659	633	598	563	521	432				
0,30	671	649	622	588	552	506	385				
0,32	663	640	610	578	540	483					
0,34	654	630	599	568	528	452					
0,36	646	620	591	559	516	422					
0,38	638	611	583	549	505	382					
0,40	629	601	574	539	486						
0,42	621	593	566	529	464						
0,44	613	586	558	520	441						
0,46	604	579	549	510	418						
0,48	597	571	541	500	387						
0,50	590	564	532	483							
0,52	584	557	524	466							
0,54	577	550	516	449							
0,56	571	542	507	432							
0,58	565	535	498	415							
0,60	558	528	485	391							
0,62	552	520	472								
0,64	545	513	459								
0,66	539	506	445								
0,68	532	497	432								
0,70	526	487	419								

$\bar{\lambda}_{fi,0}$	0,0	0,2	0,4	0,6	0,8	1,0	1,2	1,4	1,6	1,8	2,0
μ_0											
0,04	1000	979	955	922	888	849	794	750	698	681	662
0,06	900	887	870	845	802	764	709	682	660	634	606
0,08	860	841	817	790	757	702	678	651	621	592	568
0,10	820	798	783	758	713	681	653	620	589	562	532
0,12	792	778	759	727	689	661	628	593	564	531	490
0,14	775	759	736	698	673	642	603	572	539	501	395
0,16	758	739	712	685	658	622	585	552	514	426	
0,18	742	720	694	673	642	602	569	531	472		
0,20	725	700	684	660	627	588	552	511	409		
0,22	708	691	673	647	611	575	536	477			
0,24	696	681	662	635	597	561	519	427			
0,26	688	672	652	622	586	548	503	367			
0,28	679	662	641	609	575	535	468				
0,30	671	653	630	598	564	521	430				
0,32	663	644	619	588	553	508	387				
0,34	654	634	609	579	542	489					
0,36	646	625	599	570	531	460					
0,38	638	616	590	561	520	432					
0,40	629	606	582	552	509	403					
0,42	621	598	574	542	497						
0,44	613	590	566	533	476						
0,46	604	583	558	524	455						
0,48	597	576	550	515	434						
0,50	590	569	542	506	413						
0,52	584	562	534	494	376						
0,54	577	555	526	478							
0,56	571	547	518	462							
0,58	565	540	510	447							
0,60	558	533	502	431							
0,62	552	526	491	415							
0,64	545	519	479	396							
0,66	539	512	466								
0,68	532	504	454								
0,70	526	496	441								

$\bar{\lambda}_{\theta,0}$	0,0	0,2	0,4	0,6	0,8	1,0	1,2	1,4	1,6	1,8	2,0
μ_0											
0,04	1000	981	958	928	892	855	799	754	700	683	664
0,06	900	888	873	849	809	769	715	684	662	637	609
0,08	860	843	820	793	762	708	680	654	624	594	570
0,10	820	799	786	762	719	683	656	623	591	564	535
0,12	792	780	762	732	692	664	631	595	567	535	499
0,14	775	760	739	701	676	645	607	575	542	505	407
0,16	758	741	715	688	661	626	589	555	518	437	
0,18	742	721	696	676	646	607	572	535	483	350	
0,20	725	702	686	663	631	592	556	515	422		
0,22	708	692	675	651	616	579	540	489			
0,24	696	682	665	639	601	566	524	441			
0,26	688	673	654	626	590	553	508	388			
0,28	679	664	644	614	579	540	481				
0,30	671	654	633	602	569	527	444				
0,32	663	645	623	592	558	514	407				
0,34	654	636	612	583	547	501					
0,36	646	627	602	574	537	474					
0,38	638	617	593	565	526	446					
0,40	629	608	585	556	515	419					
0,42	621	599	578	547	505	381					
0,44	613	592	570	538	489						
0,46	604	585	562	529	468						
0,48	597	578	554	520	448						
0,50	590	571	546	511	428						
0,52	584	563	538	502	407						
0,54	577	556	530	489	360						
0,56	571	549	522	473							
0,58	565	542	514	458							
0,60	558	535	506	442							
0,62	552	528	498	427							
0,64	545	521	486	412							
0,66	539	514	473	381							
0,68	532	507	461								
0,70	526	499	449								

A.4: Critical temperatures for steel elements, steel grade S420, based on the non-dimensional slenderness and the degree of utilization. [3]

$\overline{\lambda}_{fi,0}$	0,0	0,2	0,4	0,6	0,8	1,0	1,2	1,4	1,6	1,8	2,0
μ_0											
0,04	1000	982	960	931	894	859	802	757	701	683	665
0,06	900	889	874	851	812	772	718	685	663	638	610
0,08	860	844	822	794	764	712	681	655	625	595	571
0,10	820	799	787	764	722	685	657	625	592	566	536
0,12	792	780	764	734	693	666	633	597	568	536	502
0,14	775	761	740	704	678	647	609	577	544	507	412
0,16	758	742	717	689	663	628	590	557	520	443	
0,18	742	722	697	677	648	609	574	537	489	358	
0,20	725	703	687	665	633	594	558	518	428		
0,22	708	692	676	653	618	581	543	495	355		
0,24	696	683	666	641	603	568	527	447			
0,26	688	674	656	628	592	555	511	399			
0,28	679	664	645	616	581	542	488				
0,30	671	655	635	604	571	530	451				
0,32	663	646	624	594	560	517	415				
0,34	654	637	614	585	550	504	363				
0,36	646	627	603	576	539	481					
0,38	638	618	595	567	529	454					
0,40	629	609	587	559	519	426					
0,42	621	600	579	550	508	398					
0,44	613	593	571	541	495						
0,46	604	586	563	532	475						
0,48	597	579	556	523	455						
0,50	590	571	548	514	435						
0,52	584	564	540	505	415						
0,54	577	557	532	494	385						
0,56	571	550	524	479							
0,58	565	543	516	464							
0,60	558	536	509	448							
0,62	552	529	501	433							
0,64	545	522	489	418							
0,66	539	515	477	403							
0,68	532	508	465								
0,70	526	501	453								

A.5: Critical temperatures for steel elements, steel grade S460, based on the non-dimensional slenderness and the degree of utilization. [3]

$\bar\lambda_{\theta,0}$	0,0	0,2	0,4	0,6	0,8	1,0	1,2	1,4	1,6	1,8	2,0
μ_0											
0,04	1000	977	949	913	880	839	787	742	696	678	659
0,06	900	885	866	837	795	756	700	679	656	630	602
0,08	860	839	811	785	749	697	674	647	616	588	564
0,10	820	797	780	752	703	677	648	614	585	557	527
0,12	792	777	755	719	685	656	622	588	559	526	474
0,14	775	757	730	694	668	636	597	567	533	487	373
0,16	758	737	705	681	652	615	580	546	507	408	
0,18	742	717	691	668	636	596	563	524	453		
0,20	725	698	680	655	619	582	545	503	384		
0,22	708	689	669	641	603	568	528	457			
0,24	696	679	658	628	591	554	511	406			
0,26	688	670	647	615	579	540	485				
0,28	679	660	636	602	568	526	446				
0,30	671	651	625	592	557	512	407				
0,32	663	641	614	582	545	496					
0,34	654	632	603	573	534	467					
0,36	646	622	594	563	522	437					
0,38	638	613	586	554	511	408					
0,40	629	603	578	544	499						
0,42	621	595	569	535	477						
0,44	613	588	561	525	455						
0,46	604	581	553	516	433						
0,48	597	573	545	506	411						
0,50	590	566	536	494	367						
0,52	584	559	528	477							
0,54	577	552	520	461							
0,56	571	544	512	444							
0,58	565	537	504	428							
0,60	558	530	493	411							
0,62	552	523	480	375							
0,64	545	515	467								
0,66	539	508	454								
0,68	532	501	441								
0,70	526	490	428								

Annex B

Temperature of unprotected Steel in °C, exposed to the ISO 834 fire curve for different values of $k_{sh}A_m/V$, [m^{-1}] [Franssen and Vila Real, 2010]

Time [min.]	10 m^{-1}	15 m^{-1}	20 m^{-1}	25 m^{-1}	30 m^{-1}	40 m^{-1}	60 m^{-1}	100 m^{-1}	200 m^{-1}	300 m^{-1}	400 m^{-1}
0	20	20	20	20	20	20	20	20	20	20	20
1	21	22	23	24	24	26	29	34	48	61	73
2	25	27	29	31	33	38	46	62	100	133	162
3	29	33	37	41	45	53	68	97	161	214	259
4	33	40	46	52	59	71	94	136	226	296	351
5	39	48	57	65	74	90	122	178	291	373	430
6	45	57	68	79	90	111	151	221	354	441	494
7	51	66	80	94	108	133	181	265	413	498	545
8	58	76	93	110	126	156	213	308	466	545	584
9	65	86	106	126	144	180	245	351	512	583	615
10	73	97	120	142	164	204	277	392	552	614	640
11	80	108	134	159	183	229	309	432	587	640	660
12	88	119	149	177	204	253	340	469	616	662	678
13	97	131	164	195	224	278	372	503	641	680	693
14	105	143	179	213	244	303	402	535	663	695	705
15	114	155	194	231	265	328	432	565	682	708	716
16	122	167	210	249	286	353	460	591	697	718	725
17	131	180	225	268	307	377	487	615	710	727	732
18	140	193	241	286	328	401	513	638	721	733	736
19	150	206	257	305	348	425	538	658	729	737	743
20	159	218	273	323	369	448	561	676	734	743	754
21	168	232	289	342	389	470	583	692	738	754	767
22	178	245	305	360	409	491	604	706	744	767	780
23	188	258	321	378	429	512	623	717	754	780	790
24	197	271	337	396	448	532	641	726	767	791	799
25	207	284	353	414	467	552	658	732	780	801	807
26	217	298	369	432	485	570	674	735	792	809	813
27	227	311	385	449	503	588	688	739	803	816	820
28	237	324	401	466	521	604	701	746	813	823	826
29	247	338	416	482	538	621	712	756	821	829	831
30	257	351	431	498	554	636	721	767	828	835	837
31	267	364	446	514	570	651	728	780	835	840	842

B.2: Evaluation of the temperature of unprotected steel based on the section factor part 2. [9]

Temperature of unprotected Steel in °C, exposed to the ISO 834 fire curve for different values of $k_{sh} A_m / V$, [m⁻¹] [Franssen and Vila Real, 2010] (continued)

Time [min.]	10 m^{-1}	5 m^{-1}	20 m^{-1}	25 m^{-1}	30 m^{-1}	40 m^{-1}	60 m^{-1}	100 m^{-1}	200 m^{-1}	300 m^{-1}	400 m^{-1}
32	277	377	461	530	585	665	733	793	841	845	847
33	288	391	476	545	600	678	736	805	846	850	852
34	298	404	490	559	614	690	740	816	851	855	856
35	308	416	504	574	628	701	745	827	856	860	861
36	318	429	518	587	641	711	753	836	861	864	865
37	329	442	532	601	654	719	763	844	866	868	870
38	339	454	545	614	666	726	774	852	870	873	874
39	349	467	558	626	677	731	786	859	874	877	878
40	359	479	570	638	688	734	798	865	878	881	882
41	369	491	582	650	698	737	810	871	882	884	885
42	379	503	594	661	707	740	822	876	886	888	889
43	389	514	606	672	716	746	832	881	890	892	893
44	399	526	617	683	722	752	842	885	893	895	896
45	409	537	628	692	728	761	852	889	897	899	900
46	419	548	639	701	732	771	860	894	900	902	903
47	429	559	650	709	735	781	868	897	904	906	906
48	439	570	660	717	737	792	875	901	907	909	910
49	449	580	670	723	740	803	882	905	910	912	913
50	458	590	679	728	744	814	888	908	914	915	916
51	468	600	688	732	750	825	894	911	917	918	919
52	477	610	697	734	757	835	899	915	920	921	922
53	487	620	704	736	765	845	904	918	923	924	925
54	496	629	711	739	774	854	908	921	926	927	928
55	505	638	718	743	784	863	913	924	928	930	930
56	514	648	723	747	794	872	917	927	931	932	933
57	523	656	728	753	804	880	920	930	934	935	936
58	532	665	731	760	814	887	924	933	937	938	938
59	541	673	734	768	825	894	927	935	939	940	941
60	549	681	736	777	834	901	931	938	942	943	944
61	558	689	738	786	844	907	934	941	944	946	946
62	566	696	741	796	853	912	937	943	947	948	949

B.3: Evaluation of the temperature of unprotected steel based on the section factor part 3. [9]

Temperature of unprotected Steel in °C, exposed to the ISO 834 fire curve for different values of $k_{sh} A_m/V$, [m⁻¹] [Franssen and Vila Real, 2010] (continued)

Time [min.]	10 m⁻¹	5 m⁻¹	20 m⁻¹	25 m⁻¹	30 m⁻¹	40 m⁻¹	60 m⁻¹	100 m⁻¹	200 m⁻¹	300 m⁻¹	400 m⁻¹
63	574	703	744	805	862	917	940	946	949	950	951
64	583	709	749	815	871	922	942	948	952	953	953
65	591	715	755	824	879	927	945	951	954	955	956
66	598	720	761	834	887	931	948	953	957	958	958
67	606	725	769	843	894	935	950	956	959	960	960
68	614	728	776	852	901	939	953	958	961	962	963
69	622	731	785	861	907	943	955	960	963	964	965
70	629	734	793	869	914	946	958	963	966	967	967
71	636	735	802	877	919	949	960	965	968	969	969
72	644	737	811	885	925	953	963	967	970	971	971
73	651	739	820	893	930	956	965	969	972	973	973
74	658	742	829	900	935	958	967	971	974	975	975
75	665	745	837	906	939	961	969	973	976	977	977
76	671	750	846	913	944	964	972	975	978	979	979
77	678	755	855	919	948	966	974	978	980	981	981
78	684	760	863	925	952	969	976	980	982	983	983
79	690	767	871	930	955	971	978	982	984	985	985
80	696	773	879	935	959	974	980	984	986	987	987
81	702	780	886	940	962	976	982	985	988	989	989
82	707	788	893	945	966	978	984	987	990	991	991
83	712	795	900	949	969	980	986	989	992	992	993
84	716	803	907	954	972	983	988	991	993	994	995
85	720	811	914	958	974	985	990	993	995	996	996
86	724	819	920	961	977	987	992	995	997	998	998
87	727	827	926	965	980	989	993	997	999	1000	1000
88	730	835	931	969	982	991	995	998	1001	1001	1002
89	732	843	937	972	985	993	997	1000	1002	1003	1003
90	734	851	942	975	987	995	999	1002	1004	1005	1005

B.4: Evaluation of the temperature of protected steel based on the modified massivity factor part 1. [9]

Temperature of protected steel in °C, exposed to the ISO 834 fire curve for different values of $\frac{A_p\,\lambda_p}{V\,d_p}$, [W/m³K]
[Franssen and Vila Real, 2010]

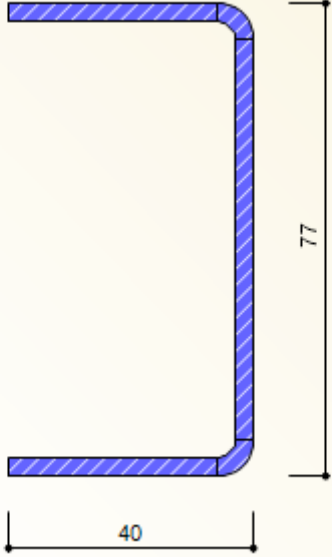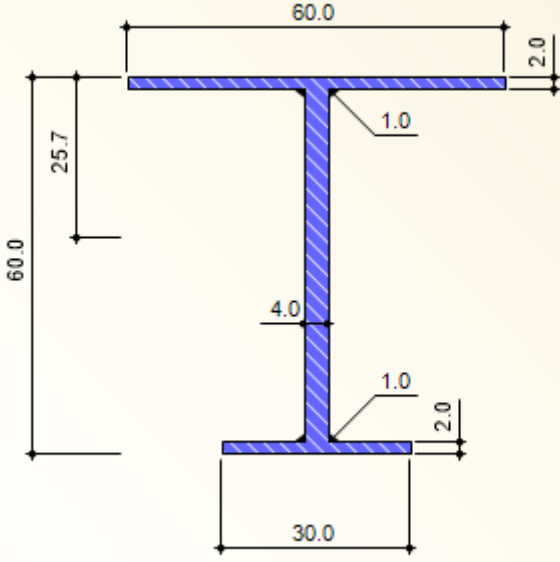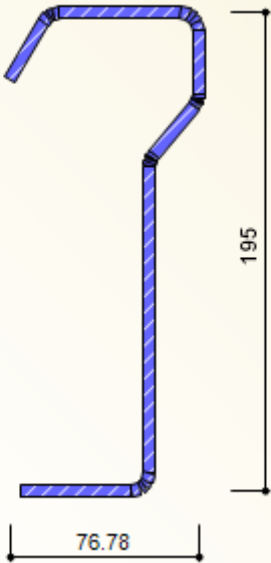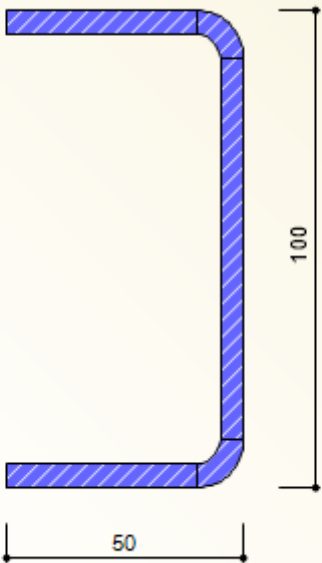| Time [min.]	100 W/m³K	200 W/m³K	300 W/m³K	400 W/m³K	600 W/m³K	800 W/m³K	1000 W/m³K	1500 W/m³K	2000 W/m³K
0	20	20	20	20	20	20	20	20	20
5	24	27	31	35	41	48	55	71	86
10	29	38	46	54	70	85	100	133	164
15	35	49	62	75	100	123	145	194	237
20	41	61	79	97	130	160	189	251	305
25	47	72	96	118	159	197	231	305	366
30	54	84	113	140	188	232	271	354	421
35	60	97	130	161	216	266	309	400	470
40	67	109	147	181	244	298	346	442	514
45	74	121	163	202	270	329	380	481	554
50	80	133	179	222	296	359	413	516	589
55	87	145	196	241	321	387	443	549	621
60	94	156	211	261	345	414	472	578	650
65	100	168	227	279	368	440	499	606	676
70	107	180	242	298	391	465	525	631	699
75	114	191	258	316	412	488	549	655	717
80	120	202	273	333	433	510	571	676	729
85	127	214	287	350	453	531	592	695	735
90	134	225	302	367	472	552	612	712	742
95	140	236	316	383	491	571	631	724	755
100	147	247	330	399	509	589	649	732	773
105	153	258	343	415	526	606	666	736	793
110	160	268	357	430	542	623	682	742	815
115	166	279	370	445	558	638	696	753	838
120	173	289	383	459	573	654	709	767	859
120	173	289	383	459	573	654	709	767	859
125	179	299	395	473	588	668	719	783	880
130	186	310	408	486	602	681	727	801	899

B.5: Evaluation of the temperature of protected steel based on the modified massivity factor part 2. [9]

Temperature of protected steel in °C, exposed to the ISO 834 fire curve for different values of $\frac{A_p}{V} \frac{\lambda_p}{d_p}$. [W/m³K] [Franssen and Vila Real, 2010] (continued)
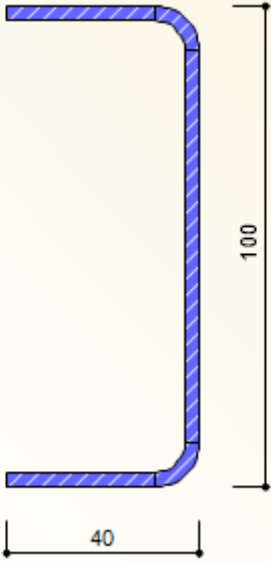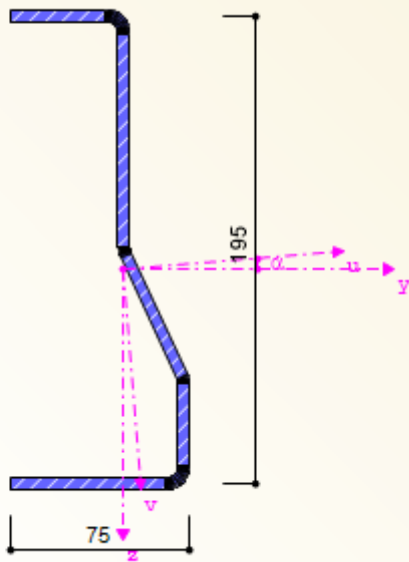
Time [min.]	100 W/m³K	200 W/m³K	300 W/m³K	400 W/m³K	600 W/m³K	800 W/m³K	1000 W/m³K	1500 W/m³K	2000 W/m³K
135	192	320	420	500	616	694	733	820	918
140	198	330	432	512	629	705	736	839	935
145	205	339	444	525	642	715	740	858	950
150	211	349	455	537	654	723	746	876	964
155	217	359	466	549	665	729	755	893	978
160	223	368	477	560	677	733	766	910	990
165	230	377	488	572	687	736	778	925	1002
170	236	387	498	582	697	739	792	940	1013
175	242	396	509	593	706	744	807	954	1023
180	248	404	519	603	714	751	821	967	1032
185	254	413	528	613	721	759	836	979	1041
190	260	422	538	623	727	769	851	991	1049
195	266	431	548	633	731	780	866	1001	1057
200	272	439	557	642	734	792	880	1012	1064
205	277	447	566	651	736	804	894	1021	1071
210	283	455	575	660	738	817	907	1031	1078
215	289	464	583	668	742	830	920	1039	1084
220	295	472	592	677	747	843	933	1048	1090
225	301	479	600	685	753	856	945	1056	1096
230	306	487	608	692	760	869	956	1063	1101
235	312	495	616	699	768	881	967	1070	1107
240	318	502	624	706	777	893	978	1077	1111
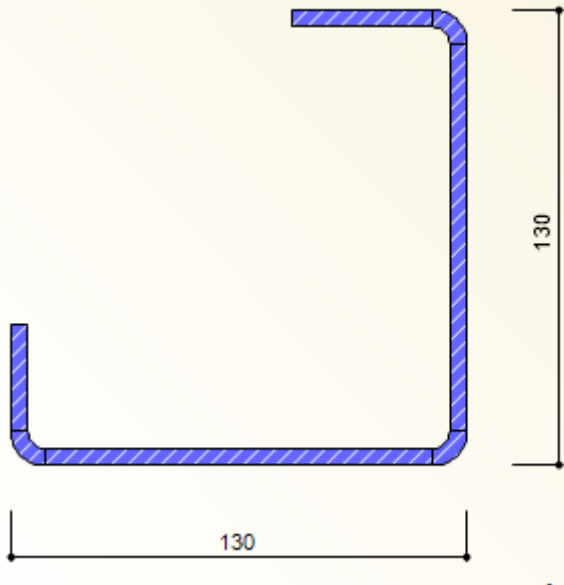
Annex C

Nr.	Profiel	I_1	I_2	A
1.	SHAPE-THIN U80X40X3 77 40 [mm]	40,10	6,93	4,41
2.	IU 60/60/2/4/30/2/1/1 60.0 2.0 1.0 25.7 60.0 4.0 1.0 2.0 30.0 [mm]	20,25	4,08	4,04

129

3.	SHAPE-THIN DAKPROFIEL 195 76.78 [mm]	900,97	71,77	16,80
4.	SHAPE-THIN U100X50X5 100 50 [mm]	135,26	21,85	9,17

5.	SHAPE-THIN U100X40X3	72,34	7,46	5,02
6.	SHAPE-THIN CHASSISRANDPROFIEL	836,76	51,24	15,58

7.	SHAPE-THIN HOEKPROFIEL 130 130 [mm]	530,51	187,33	16,26

Auteursrechtelijke overeenkomst

Ik/wij verlenen het wereldwijde auteursrecht voor de ingediende eindverhandeling:
Research into the fire stability RF60 (according to Eurocode 3) of modular units

Richting: **master in de industriële wetenschappen: bouwkunde**
Jaar: **2017**

in alle mogelijke mediaformaten, - bestaande en in de toekomst te ontwikkelen - , aan de Universiteit Hasselt.

Niet tegenstaand deze toekenning van het auteursrecht aan de Universiteit Hasselt behoud ik als auteur het recht om de eindverhandeling, - in zijn geheel of gedeeltelijk -, vrij te reproduceren, (her)publiceren of distribueren zonder de toelating te moeten verkrijgen van de Universiteit Hasselt.

Ik bevestig dat de eindverhandeling mijn origineel werk is, en dat ik het recht heb om de rechten te verlenen die in deze overeenkomst worden beschreven. Ik verklaar tevens dat de eindverhandeling, naar mijn weten, het auteursrecht van anderen niet overtreedt.

Ik verklaar tevens dat ik voor het materiaal in de eindverhandeling dat beschermd wordt door het auteursrecht, de nodige toelatingen heb verkregen zodat ik deze ook aan de Universiteit Hasselt kan overdragen en dat dit duidelijk in de tekst en inhoud van de eindverhandeling werd genotificeerd.

Universiteit Hasselt zal mij als auteur(s) van de eindverhandeling identificeren en zal geen wijzigingen aanbrengen aan de eindverhandeling, uitgezonderd deze toegelaten door deze overeenkomst.

Voor akkoord,

De Bruycker, Simon   **Vaes, Ruben**

Datum: **6/06/2017**